

# UC Merced

## UC Merced Electronic Theses and Dissertations

### Title

Maternal inflammation directs fetal hematopoiesis

### Permalink

<https://escholarship.org/uc/item/4kv6n3qs>

### Author

Apostol, April

### Publication Date

2022

### Copyright Information

This work is made available under the terms of a Creative Commons Attribution-NonCommercial-NoDerivatives License, available at <https://creativecommons.org/licenses/by-nc-nd/4.0/>

Peer reviewed|Thesis/dissertation

UNIVERSITY OF CALIFORNIA, MERCED

Maternal inflammation directs fetal hematopoiesis

by

April C. Apostol, M.S.

A dissertation submitted in partial satisfaction of the requirements for the  
degree of

Doctor of Philosophy

in

Quantitative and Systems Biology, Molecular and Cell Biology

Committee in charge:

Professor Stephanie Woo, Chair  
Professor Kirk Jensen  
Professor Joel Spencer  
Professor Anna Beaudin, University of Utah

2022

Portions of Chapter 1 © 2020 Apostol AC, et al.  
Training the fetal immune system through maternal inflammation - A  
layered hygiene hypothesis.  
Frontiers of Immunology. Feb 11;11:123.

All other chapters  
© April C. Apostol, 2022

All rights reserved.

The Dissertation of April C. Apostol is approved, and it is acceptable in  
quality and form publication electronically:

---

Anna E. Beaudin

---

Kirk D.C. Jensen

---

Joel A. Spencer

---

Stephanie Woo, Chair

University of California, Merced  
2022



# Table of Contents

0.1 Dedication.....	vii
0.2 List of Abbreviations.....	viii
0.3 List of Symbols.....	x
0.4 List of Tables.....	xi
0.5 List of Figures.....	xii
0.6 Acknowledgements .....	xiv
0.7 Curriculum Vitae.....	xv
0.8 Dissertation Abstract.....	1

## Chapter 1: Introduction

1.1 Maternal microbe exposure shapes early life immune development.....	3
1.2 Possible mechanisms of fetal immune training.....	5
1.3 Hematopoietic stem cells as “sensors” of infection.....	7
1.4 HSC development in early life .....	9
1.6 Conclusions.....	11
1.7 Figures.....	14

## Chapter 2: Prenatal inflammation perturbs fetal hematopoietic development

2.1 Introduction .....	17
<b>2.2 Materials and Methods</b>	
2.2.1 Mouse models and husbandry .....	19
2.2.2 Cell Isolation and Identification by flow cytometry .....	19
2.2.3 Proliferation of HSCs and MPPs.....	20
2.2.4 Transplantation assays.....	21
2.2.5 10x Chromium single-cell sequencing of HSPCs.....	21
<b>2.3 Results</b>	
2.3.1 Prenatal inflammation induced by maternal immune activation (MIA) causes expansion of a developmentally-restricted HSC.....	22
2.3.2 Activation of a developmentally-restricted HSC drives downstream expansion of lymphoid-biased multipotent progenitors.....	24

2.3.3 Single-cell sequencing reveals the response of distinct fetal HSPCs to MIA.....	25
2.3.4 Fetal HSPCs respond distinctly to inflammatory cytokines induced by MIA.....	27
2.3.5 Prenatal inflammation induced by MIA affects self-renewal and hematopoietic output of developing HSCs.....	28
<b>2.4 Discussion</b> .....	29
Table 2-1 List Antibodies.....	34
Table 2-2 Other Reagents and Resources.....	36
2-2.1 Chemicals, Peptides, and Recombinant Proteins.....	36
2-2.2 Critical Commercial Assays.....	36
2-2.3 Experimental Models: Organisms/Strains.....	36
2-2.4 Software and Algorithms.....	36
2-2.5 Deposited Data.....	37
<b>2.5 Figures</b> .....	38

### **Chapter 3: IFN $\gamma$ mediates the response of fetal HSCs to congenital infection with *Toxoplasma***

<b>3.0 Abstract</b> .....	55
<b>3.1 Introduction</b> .....	56
<b>3.2 Materials and Methods</b> .....	59
<b>3.3 Results</b>	
<b>3.3.1 In utero exposure to inflammation from <i>T. gondii</i> impacts fetal hematopoiesis</b> .....	60
<b>3.3.2 In utero exposure to inflammation from <i>T. gondii</i> modulates fetal HSC function</b> .....	62
<b>3.3.3 <i>T. gondii</i> virulence from maternal infection modulates inflammation in the fetal environment</b> .....	64
<b>3.3.4 <i>In utero</i> exposure to IFN<math>\gamma</math> impacts fetal hematopoiesis</b> .....	65
<b>3.3.5 <i>In utero</i> exposure to IFN<math>\gamma</math> directs fetal hematopoietic stem cell differentiation long term multi-lineage reconstitution</b> .....	66

3.3.6 Fetal hematopoietic stem cells (HSCs) respond directly to maternal IFN $\gamma$ through IFN $\gamma$ receptor.....	68
3.4 Discussion.....	70
Table 3-1 <i>Toxoplasma gondii</i> strains.....	75
3.5 Figures.....	76

## Chapter 4: Conclusion

4.1 Contributions to the field.....	98
4.1.2 Experimental models of the effects of prenatal inflammation of fetal hematopoiesis.....	99
4.1.3 Generation of a novel single cell sequencing dataset for fetal HSPCs.....	100
4.1.4 Characterizing cytokines present in the fetal hematopoietic environment.....	101
4.1.5 Fetal Hematopoiesis exhibits a unique response to maternal inflammation.....	103
4.2 Future directions	
4.2.1 Exploring the impact of maternal IFN $\gamma$ exposure on long-term hematopoietic outcomes.....	104
4.2.2 Exploring other infection models.....	105
4.3 Summary .....	106
4.3.1 Figure 1: A summary of fetal HSC responses .....	108
4.3.2 Figure 2: An overview.....	109
<b>References</b> .....	110

## **0.1 Dedication**

I dedicate this work to my family who has always supported me and my ever-changing interests with love and understanding. Thank you, mommy, pops, Ann (and my niece who arrives the same year I receive my PhD), Arielle, grandpa and of course, Loula. I would especially like to thank my partner, Sam Spiegel for all his love and support, and for letting me fill our home with lots of pets. Pepper, Tina, Gene, and Louise. For Reese who we dearly miss.

## 0.2 List of Abbreviations

<b>AF</b>	amniotic fluid
<b>BCG</b>	bacille Calmet-Guérin
<b>BM</b>	bone marrow
<b>C(number)</b>	cluster (number)
<b>CD</b>	cluster of differentiation
<b>CLP</b>	common lymphoid progenitor
<b>CMP</b>	common myeloid progenitor
<b>E(day)</b>	embryonic day
<b>EHT</b>	endothelial to hemogenic transition
<b>EP</b>	erythrocyte progenitor
<b>Fc</b>	fragment crystallizable
<b>FcRN</b>	the neonatal Fc receptor for IgG
<b>FL</b>	fetal liver
<b>flkswitch</b>	flk-2 lineage tracing mouse model
<b>GFP</b>	green fluorescent protein
<b>GM</b>	granulocyte-macrophage
<b>GMP</b>	granulocyte-macrophage progenitor
<b>GSEA</b>	gene set enrichment analysis
<b>het</b>	heterozygous
<b>HIV</b>	human immunodeficiency virus
<b>HLA</b>	human leukocyte antigen
<b>HSC(s)</b>	hematopoietic stem cell(s)
<b>HSPC(s)</b>	hematopoietic stem and progenitor cell(s)
<b>IFNAR</b>	interferon alpha receptor
<b>IFN<math>\alpha</math></b>	interferon alpha
<b>IFN<math>\gamma</math></b>	interferon gamma

<b>IFN<math>\gamma</math>KO</b>	interferon gamma knock out (mouse strain)
<b>IFN<math>\gamma</math>R</b>	interferon gamma receptor
<b>Ig(G)</b>	Immunoglobulin (G)
<b>IL</b>	interleukin
<b>ILC</b>	innate-like lymphocyte
<b>LT-HSC</b>	long-term HSC
<b>LTMR</b>	long term multilineage reconstitution
<b>mCMV</b>	mouse cytomegalovirus
<b>MIA</b>	maternal immune activation
<b>MkP</b>	megakaryocyte progenitor
<b>MPP(s)</b>	multi-potent progenitor(s)
	Nuclear factor kappa-light-chain-enhancer
<b>NF-<math>\kappa</math>B</b>	of activated B cells
<b>PB</b>	peripheral blood
<b>pIC</b>	Polyinosinic:polycytidylic acid
<b>poly(I:C)</b>	Polyinosinic:polycytidylic acid
<b>Pru</b>	Prunigad Type II strain of <i>Toxoplasma gondii</i>
<b>RH</b>	Type I strain of <i>Toxoplasma gondii</i>
<b>ST-HSC</b>	short-term HSC
<b>TGF-<math>\beta</math></b>	tumor growth factor beta
<b>TLR</b>	toll-like receptor
<b>TNF-<math>\alpha</math></b>	tumor necrosis factor alpha
<b>Tom</b>	tomato fluorescent protein
<b>TORCH</b>	toxoplasma other rubella cmv hepatitis
<b>Treg(s)</b>	T-regulatory cells
<b>VSV</b>	vesicular stomatitis virus
<b>WBM</b>	whole bone marrow
<b>WT</b>	wildtype
<b><math>\gamma\delta</math>-T cells</b>	gamma-delta T-cells

### 0.3 List of Symbols

-	negative
-/-	knockout
+	positive
+/-	heterozygous
mg	milligrams
mL	milliliters
$\alpha$	alpha
$\beta$	beta
$\gamma$	gamma
$\delta$	delta
$\mu$	micro

## 0.4 List of Tables

**Table 2-1** List of Antibodies

**Table 2-2** Other Reagents and Resources

**2-2.1** Chemicals, Peptides, and Recombinant Proteins

**2-2.2** Critical Commercial Assays

**2-2.3** Experimental Models: Organisms/Strains

**2-2.4** Software and Algorithms

**2-2.5** Deposited Data

**Table 3-1** *Toxoplasma gondii* strains



## 0.4 List of Figures

### 1.7: Chapter 1 Figures

**Figure 1:** Mechanisms that impact fetal hematopoiesis

**Figure 2:** Bone marrow HSCs respond to inflammation

### 2.5: Chapter 2 Figures

**Figure 1:** Fetal hematopoietic stem and progenitor cells (HSPCs) respond to prenatal inflammation induced by maternal immune activation (MIA)

**Figure 2:** Lymphoid-biased fetal progenitors expand in response to prenatal inflammation induced by MIA.

**Figure 3:** Prenatal inflammation induces distinct molecular changes in fetal HSPCs

**Figure 4:** MIA-induced inflammatory cytokines specifically activate fetal HSPCs

**Figure 5:** Prenatal inflammation induced by MIA causes persistent changes to fetal hematopoietic stem cells upon transplantation.

**Supplementary Figure 1:** The impact of prenatal inflammation induced by MIA on fetal and perinatal development

**Supplementary Figure 2:** Impact of MIA on markers of inflammation in the fetal liver

**Supplementary Figure 3:** Molecular impact of MIA on fetal HSPCs

**Supplementary Figure 4:** Impact of MIA on fetal HSC function through transplantation

### 3.5: Chapter 3 Figures

**Figure 1:** *In utero* exposure to inflammation from *Toxoplasma gondii* directs fetal hematopoiesis.

**Figure 2:** *In utero* exposure to inflammation from *Toxoplasma gondii* modulates fetal HSC long-term multi-lineage reconstitution and differentiation.

**Figure 3:** *Toxoplasma gondii* virulence from maternal infection modulates inflamm

**Figure 4:** *In utero* exposure to IFN $\gamma$  directs fetal hematopoiesis. ation in the fetal environment

**Figure 5:** *In utero* exposure to IFN $\gamma$  direct fetal hematopoietic stem cell differentiation.

Figure 6: Fetal HSCs respond directly to maternal IFN $\gamma$  through IFN $\gamma$  receptor.

**Supplementary Figure 1:** *In utero* exposure to IFN $\gamma$  directly impacts fetal HSPCs

**Supplementary Figure 2:** Maternal infection with *T. gondii* leads to lasting changes in BM reconstitution of fetal HSCs.

**Supplementary Figure 3:** *In utero* exposure to IFN directly impacts fetal HSPCs

**Supplementary Figure 4:** Bone marrow chimerism from IFN $\gamma$  exposed fetal HSCs following transplantation

## Chapter 4 Figures

**4.3.1:** Overview of fetal HSPC responses to maternal inflammation and infection

**4.3.2:** Summary Figure 1: Overview of differences between adult and fetal bone marrow HSC response.

## 0.6 Acknowledgements

I would like to express my gratitude to Dr. Anna Beaudin, not only for her mentorship and guidance throughout the years, but also for her continued support of my interests and career goals, despite the distance between UC Merced and the University of Utah. Dr. Beaudin's mentorship has allowed me to thrive as an independent researcher and has helped me harness my scientific communication skills like no other. I am forever grateful that she took a chance on me as one of her first graduate students and for her unlimited patience as we navigate my next chapter in life.

Next, I would like to thank my co-mentor Dr. Kirk Jensen for his support over the years. Dr. Jensen has always given me excellent guidance, unrestricted access to parasites, and a welcoming place in his lab as an "adopted" graduate student. I would also like to thank the other members of my committee, who began their journey at UC Merced when I first became a graduate student. To Dr. Stephanie Woo and Dr. Joel Spencer, whose expertise and guidance have been instrumental to my growth as a scientist. I would also like to thank Dr. Jennifer Manilay for allowing me to use her lab space, for her invaluable mentorship, and for being a role model for Filipinos in science. It makes a world of difference to see yourself represented and I thank you for paving the way.

I would also like to acknowledge the UC Merced core facilities, The Stem Cell and Instrumentation Foundry and The Department of Animal Research. For Dr. David Gravano for his expertise and guidance in flow cytometry and Emily Slocum for their expertise in the animal facility. Additionally, I would like to thank Dr. Nina Cabezas-Wallsheid and her graduate students Maria Carmen Romero-Mulero and Polina Pavlovich for their excellent guidance and contributions to our single-cell sequencing work. Finally, I would like to thank my colleagues in the Beaudin and Jensen labs, past and present: Diego Lopéz, Kelly Otsuka, Gabriel Leung, Clint Valencia, Dr. Angel Kongsomboonvech and Dr. Scott Souza.

## 0.7 CURRICULUM VITAE

### EDUCATION

- 2022            Doctor of Philosophy, Quantitative and Systems Biology –  
Molecular and Cell Biology  
University of California, Merced
- 2019            Master of Science, Quantitative and Systems Biology;  
University of California, Merced
- 2012            Bachelor of Science, Microbiology; Minor in Chemistry  
San Francisco State University

### RESEARCH AND PROFESSIONAL EXPERIENCE

- 2016-2022    University of California, Merced (2016-2020);  
University of Utah (2020-2022)  
Mentor: Anna E. Beaudin, Ph.D.
- Graduate Student, School of Natural Sciences, Quantitative and Systems Biology (Merced)
  - Fetal hematopoietic stem cells respond to inflammation during maternal infection with toxoplasmosis
- 2016-2022    University of California, Merced  
Co-mentor: Kirk D. C. Jensen, Ph.D.
- 2014-2016    SC Labs, Santa Cruz CA
- Laboratory Technician

### PUBLICATIONS

In preparation	Apostol AC, Otsuka K, Posada J, Jensen KDC, Beaudin AE. "Fetal HSCs respond to inflammation during maternal infection with <i>Toxoplasma gondii</i> ."
Under revision	Apostol AC, Lopez DA, Lebish EJ, Valencia CH, Romero-Mulero MC, Pavlovich P, Hernandez GE, Forseberg EC, Cabezas-Wallsheid N, Beaudin AE. "Prenatal inflammation perturbs fetal hematopoietic development and causes persistent changes to postnatal immunity."
Submitted	Smith FL, Savage HP, Luo Z, Tipton CM, Lee E, Apostol AC, Lopez DA, Jensen I, Keller S, Baumgarth, N. "B-1 plasma cells require CD4 T cell help to generate a unique repertoire of natural IgM."
2020	Apostol AC, Lopez DA, Beaudin AE. "A "switch" in time through genes aligned: unraveling the genomic landscape of HSC development". <i>Cell Stem Cell</i> . 2020 Nov 5;27(5):695-697. doi: 10.1016/j.stem.2020.10.011. PMID: 33157043.
2020	Apostol AC, Jensen KDC, Beaudin AE. "Training the Fetal Immune System Through Maternal Inflammation - A Layered Hygiene Hypothesis." <i>Front Immunol</i> . 2020 Feb 11; 11:123. doi: 10.3389/fimmu.2020.00123. PMID: 32117273; PMCID: PMC7026678.
2018	Apostol AC, Beaudin AE. "Reversing Time: Ezh1 Deficiency Hastens Definitive Hematopoiesis." <i>Cell Stem Cell</i> . 2018 Mar 1;22(3):285-287. doi: 10.1016/j.stem.2018.02.006. PMID: 29499144.

## HONORS, AWARDS, and FUNDING

2016-2022	Graduate Student Research (GSR) Support, University of California Merced
2019	Federation of American Societies for Experimental Biology (FASEB) Mentored Travel Award. Immunology 2019, San Diego, CA.
2018	Graduate Student Association Travel Award, University of California, Merced. Spring and Fall.
2018	International Society for Experimental Hematology conference. First place poster award.
2016-2022	Quantitative and System Biology Summer Research Fellowship, University of California, Merced
2008-2012	Presidential Scholarship, San Francisco State University
2008-2012	Dean's List

## PROFESSIONAL DEVELOPMENT

2020	GRAD-EXCEL mentor, University of California Merced. - Provided mentorship and support for incoming graduate students.
2019	Federation of American Societies for Experimental Biology (FASEB) mentorship. Immunology 2019, San Diego, CA.
2019	Single-cell RNA-seq Workshop, University of California, Davis

2018 International Society for Experimental Hematology student member.

### MENTORSHIP EXPERIENCE

2017-2020 Eric Lebish, University of California, Merced

2018-2020 Jasmine Posada, University of California, Merced

### PRESENTATIONS

#### Oral presentations

2021 Maternal inflammation directs fetal hematopoiesis  
Molecular and Cell Biology Research in Progress,  
University of California, Merced.

2019 The impact of maternal inflammation on fetal hematopoietic stem cells  
Molecular and Cell Biology Seminar Series, University of California, Merced.

#### Poster Presentations

2022 Fetal HSCs respond to inflammation during maternal infection with Toxoplasmosis. Midwinter Conference of Immunologists. Asilomar, CA.

2020 Interferon gamma from acute Toxoplasma gondii infection impacts hematopoietic function in the fetus during pregnancy. Midwinter Conference of Immunologists. Asilomar, CA.

2019 Acute congenital Toxoplasma gondii infection alters fetal hematopoiesis via interferon gamma. Immunology, 2019. San Diego, CA. FASEB mentored poster award recipient.

- 2018 Acute toxoplasmosis during pregnancy impacts fetal hematopoietic development. University of California Immunology Retreat 2018. Honorable mention.
- 2018 Maternal infection with *Toxoplasma gondii* during pregnancy alters the establishment of hematopoietic stem cells and progenitors in the fetus. 47th Annual International Society for Experimental Hematology Conference. First prize award. Los Angeles, CA.
- 2018 Maternal immune perturbation expands developmentally restricted hematopoietic stem cells (HSCs) and innate-like B cells in offspring. QSB annual retreat (Merced, CA) and Midwinter Conference of Immunologists (Asilomar, CA).



# Maternal Inflammation Directs Fetal Hematopoiesis

by

April C. Apostol, M.S.

Doctor of Philosophy in Quantitative and Systems Biology

Concentration in Molecular and Cell Biology

University of California, Merced 2022

Professor Anna E. Beaudin

## 0.8 Disseration Abstract

Infection in the adult organism drives cytokine-mediated inflammation that directly influences hematopoietic stem cell (HSC) function and differentiation within the bone marrow, but much less is known about the fetal hematopoietic response to maternal inflammation and infection during pregnancy. Here, we demonstrate that fetal hematopoietic stem and progenitor cells (HSPCs) respond to prenatal inflammation *in utero*, and that the fetal response drives long-term changes to HSC function after transplantation. First, we modeled maternal immune activation (MIA) with the IFN- $\alpha$  stimulating viral mimetic, poly(I:C), and showed that fetal HSPCs exhibit changes in quiescence, expansion, and lineage-biased output in response to prenatal inflammation. Single cell transcriptomic analysis of fetal HSPCs in response to MIA revealed specific upregulation of inflammatory gene profiles in discrete, transient HSC populations that propagated expansion of lymphoid-biased progenitors in the fetal liver.

Next, we investigated the fetal hematopoietic response to maternal *Toxoplasma gondii* infection. *T. gondii* is an intracellular parasite that elicits Type II, IFN $\gamma$ -mediated maternal immunity to prevent vertical transmission and promote parasite clearance. The production of excessive IFN $\gamma$  during congenital toxoplasmosis has dire consequences for the developing fetus, such as lowered birth weights and premature abortion, but the effects to the developing immune system and the signals that mediate these interactions have not been investigated previously. Our examination revealed that the fetal inflammatory repertoire is distinct from the maternal response and is directly influenced by parasite virulence. We show that maternal IFN $\gamma$  crossed the fetal-maternal interface and was perceived directly by fetal HSCs, and that the response of fetal HSCs was dependent on the fetal IFN $\gamma$  receptor. Functionally, the heterogeneous fetal HSC pool responded to aberrant inflammation with virulence-dependent changes in proliferation, long-term multi-lineage reconstitution, and self-renewal potential. By directly comparing the effect of maternal IFN $\gamma$  injection with congenital *T. gondii* infection of varying virulence, our observations delineate both a direct effect of IFN $\gamma$  on fetal HSCs and illuminate the independent role of additional inflammatory cytokines in driving the expansion of downstream hematopoietic progenitors. Finally, in direct contrast to the adult hematopoietic response to infection and the fetal response to Type I interferon mediated MIA, exposure to Type II interferon-mediated inflammation *in utero* did not impair fetal HSC function, even in response to severe infection. Our findings provide insight into the cues that direct fetal hematopoiesis in response to inflammation and begin to tease apart inflammatory cues that promote a beneficial hematopoietic response versus those that may ultimately be detrimental.

# Chapter 1 Introduction

## 1.1 Maternal microbe exposure shapes early life immune development

A growing body of evidence suggests that maternal exposure - both to non-infectious stimuli and infectious microbes - shapes the fetal and subsequent neonatal immune response (**Figure 1**). The most studied mode of influence of the maternal immune system on fetal and neonatal immunity is the transfer of maternally derived immunoglobulin (Ig) to the offspring, or passive immunity (**Figure 1-i**). This transfer can occur both prenatally through the placenta, or postnatally in breastmilk, mediated by the neonatal Fc receptor, FcRN, (Roopenian and Akilesh 2007) and provides critical protection to the newborn. Importantly, transplacental transport of maternal IgG-antigen complexes by FcRn can also result in direct "priming" of antigen-specific immune responses in fetal cells (Malek, Sager et al. 1997, Malek, Sager et al. 1998, May, Grube et al. 2009) (**Figure 1-i**).

Beyond antigen-specific response driven by maternal-mediated antigen exposure, the maternal immune response also evokes antigen-nonspecific responses in the developing fetal immune system (**Figure 1-ii, iii**). For example, maternal vaccination during pregnancy is broadly associated with reduced mortality to unrelated pathogens in offspring (Wilcox and Jones 2018), suggesting that generalized and protective neonatal immune responses can be elicited. Conversely, prenatal exposure to infection in the context of HIV, malaria, and a cross section of helminth infections correlates with increased susceptibility to diverse infections in neonates and poorer responses to vaccination postnatally (Dauby, Goetghebuer et al. 2012). Whether the outcome of maternal exposure is protective or deleterious may depend on the nature of the maternal immune response, severity of disease, or mechanism of action. As an example, uninfected infants born to

mothers with more advanced HIV disease experience a greater risk of perinatal morbidity and mortality (Kuhn, Kasonde et al. 2005). On the other hand, adverse pregnancy and infant outcomes associated with maternal infection can be attenuated if the maternal inflammatory response is experimentally controlled by administration of a microbial immunomodulatory agent (Scott, Lauzon-Joset et al. 2017). These data suggest that the degree of maternal inflammation can directly influence fetal outcomes.

Mounting evidence suggests that the fetal innate immune system can be 'trained' during pregnancy (Levy and Wynn 2014, Netea, Joosten et al. 2016), by which maternal infection induces generalized and persistent changes to the function of the fetal innate immune system. Some of the best evidence for this comes from studies of infants born exposed to but uninfected with HIV (for review see (Abu-Raya, Smolen et al. 2016)). *In utero* exposure, but not vertical transmission with HIV, results in enhanced neonatal cytokine profiles of monocytes stimulated with various TLR agonists (Reikie, Adams et al. 2014). Similarly, infants exposed prenatally to malaria demonstrated reduced basal levels of innate cytokines in cord blood, but higher responsiveness to stimulation with specific TLR agonists (Gbédandé, Varani et al. 2013, Natama, Moncunill et al. 2018). Human infants exposed to Hepatitis B Virus (HBV) in utero have higher levels of anti-viral cytokines in cord blood and exhibit evidence of greater activation and maturity of monocytes (Hong, Sandalova et al. 2015). Maternal vaccination during pregnancy can also heighten the innate immune response in offspring, as evidenced by an association between maternal Bacille Calmette-Guérin (BCG) scar size and infant pro-inflammatory cytokine production elicited by TLR stimulation (Mawa, Webb et al. 2017). Training of the innate immune system in infants that occurs in the absence of vertical transmission underscores the ability of the fetal immune system

to respond to maternal infection or inflammation in an indirect manner (**Figure 1**). Thus, investigation into the mechanisms that govern the interactions between fetal and maternal immunity warrants investigation.

## **1.2 Possible mechanisms of fetal immune training**

The mechanisms underlying the response of the fetal immune system in the absence of overt fetal infection are unknown, and how indirect 'training' of the fetal immune system by maternal infection or exposure occurs is unclear and understudied (**Figure 1**). One possible explanation for trained fetal immunity could be the direct passage of maternal cytokines or other inflammatory mediators into fetal circulation, which then stimulate the fetal immune system (**Figure 1-III**). Determining whether maternal cytokines cross the placenta in humans during gestation is extremely challenging; *ex vivo* experiments with full-term placenta suggests that transfer of cytokine across the placenta is limited at later developmental stages (Zaretsky, Alexander et al. 2004, Aaltonen, Heikkinen et al. 2005). Nonetheless, evidence from rodent models suggests that some cytokines can cross the placenta earlier in gestation (Medlock, Kaplan et al. 1993, Dahlgren, Samuelsson et al. 2006), and subsequently modulate the neonatal response to infection (Novales, Salva et al. 1993). Dahlgren and colleagues demonstrated that transplacental passage of  $^{125}$ I-labeled IL-6 was considerably higher at mid-gestation (embryonic day (E) 11-13) as compared to late gestation/near term (E17-19), suggesting that a less mature placenta may be more permeable to maternal cytokines (Dahlgren, Samuelsson et al. 2006). TLR ligands for specific pathogens were also recently shown to cross the mouse placenta at mid-gestation (E15) and directly impinge upon fetal cells; however, a direct effect on fetal immune cells was not described (Humann, Mann et al. 2016). Whether other TLR ligands can cross the placenta and directly elicit a fetal immune response

has not been determined. Whether maternal cytokines or inflammatory mediators induce the production or release of different cytokines on the fetal side remains to be understood (**Figure 1-ii, iii**). Finally, vertically transmitted pathogens may directly stimulate fetal immune responses in utero (**Figure 1-IV, iv**). Further investigation of the role of maternal cytokines and other inflammatory mediators in the direct induction of a fetal immune response, and the nature of that response, is warranted.

Another alternative explanation is that the fetus could respond indirectly to inflammation of or impingement on placental function caused by maternal infection (**Figure 1-II**). Chorioamnionitis, an infection of the placenta typically caused by normally non-pathogenic microbes, drives systemic changes to the fetal immune system, including cytokine production and lymphocyte polarization (Kallapur, Presicce et al. 2014). Importantly, fetal cytokine production has been observed in the absence of overt amniotic infection in a macaque model of Group B streptococcal-induced chorioamnionitis (Adams Waldorf, Gravett et al. 2011), suggesting that the fetus can respond directly to other signals outside of the fetal unit. Maternal viral infection of the placenta can also evoke fetal cytokine production in mice in the absence of fetal infection (Cardenas, Means et al. 2010). Recent evidence from studies of cord blood in pre-term human infants suggests that inflammation at the maternal-fetal interface primes fetal lymphocytes to produce more inflammatory cytokines, including TNF- $\alpha$  and IFN- $\gamma$ , in pre-term infants (Frascoli, Coniglio et al. 2018). Genetic dissection of the contribution of the fetal response to placental malaria recently revealed the requirement for fetal innate immune signaling in the control of placental malarial infection (Barboza, Hasenkamp et al. 2019). Thus, the fetal immune system may respond to the consequences of maternal inflammation, as opposed to or in addition to a direct response to maternal inflammatory mediators. Activation of the fetal immune system in the

context of maternal inflammation, infection, or exposure provides evidence that *in utero* exposure can directly evoke a fetal immune response (**Figure 1**).

### **1.3 Hematopoietic stem cells as sensors of infection**

Hematopoietic stem cells (HSCs) are multipotent and self-renewing adult stem cells that reside in the bone marrow of adult mice and humans (**Figure 2**). Adult HSCs are responsible for the production of millions of diverse blood cells daily, including red blood cells, platelets, and all immune cells that encompass the mature innate and adaptive immune systems. In the adult organism, activation of the immune system by infection directly activates hematopoietic stem cells in the bone marrow through inflammatory mediators in the circulation (**Figure 2**). Recent investigation in adult hematopoiesis has illuminated the mechanisms by which adult HSCs can act as both direct sensors and drivers of the immune response during inflammation. In response to infection, the blood system rapidly produces short-lived myeloid cells required to counter infection (**Figure 2**). At the top of the hematopoietic hierarchy, adult HSCs have been documented to respond directly to systemic viral (Hirche, Frenz et al. 2017) and bacterial infections (Matatall, Jeong et al. 2016), as well as to a host of inflammatory cytokines, including Type I and Type II interferons (Essers, Offner et al. 2009, Baldrige, King et al. 2010, Matatall, Shen et al. 2014, Haas, Hansson et al. 2015), IL-1 $\beta$  (Pietras, Mirantes-Barbeito et al. 2016), IL-27 (Furusawa, Mizoguchi et al. 2016), and TNF- $\alpha$  (Haas, Hansson et al. 2015, Yamashita and Passegué 2019), as well as specific TLR ligands (Nagai, Garrett et al. 2006, Esplin, Shimazu et al. 2011). In addition, adult HSCs have been reported to express a multitude of additional cytokine receptors, the functions of which in regulating HSC biology have yet to be investigated (King and Goodell 2011). With progressive exposure, adult HSCs lose self-renewal potential, face oxidative stress, and undergo metabolic changes

that drive reprogramming of myeloid differentiation programs (Schuettpeitz and Link 2013, Pietras 2017). Recent evidence also suggests that specific progenitors within the heterogeneous adult HSC compartment differentially receive and drive the response to inflammation. Work by Essers and colleagues, for example, suggests that specific megakaryocyte-biased progenitors are induced upon acute inflammation to rapidly replenish platelets (Haas, Hansson et al. 2015). How these rapid responses contribute to long-term changes in the adult HSC compartment remains to be determined.

In direct response to broad range of inflammatory stimuli, adult HSCs shift the trajectory of hematopoiesis by adopting a myeloid-biased output (Pietras 2017) (**Figure 2**). Most recently, this myeloid-biased response has been scrutinized in the context of trained immunity. The hematopoietic stem cell is implicated as a driver of 'trained innate immunity'. Whereas immune memory has typically been a distinct and critical feature of adaptive immunity, trained innate immunity refers to the ability of the innate immune cells to evoke a stronger response to a non-specific stimulus following infection (Netea, Joosten et al. 2016). The conundrum of trained innate memory is that most innate immune cells, such as monocytes, are short-lived, with a lifespan shorter than the timespan for which that 'memory' has been observed. Recent work has shed light on one possible mechanism by which trained innate memory is 'stored' by adult HSCs. Two recent publications have revealed that, in response to infection, hematopoietic progenitors specifically produce myeloid cells that have an enhanced response to subsequent infections. These persistent changes are driven by alterations in epigenetic profile and metabolism at the progenitor level (Kaufmann, Sanz et al. 2018, Mitroulis, Ruppova et al. 2018). These data provide additional evidence that the direct sensitivity and responsiveness of



adult HSCs to inflammatory stimuli can redirect the long-term trajectory of the immune system.

## **1.4 HSC development in early life**

The hematopoietic system is one of the first “organs” established during embryonic development. Developmental hematopoiesis is a highly dynamic process that occurs in several waves of hematopoietic cell production across multiple anatomical organs during fetal development. The first wave of hematopoiesis occurs in the extraembryonic yolk sac from so-called “blood islands” derived from endothelial cells that undergo endothelial to hematopoietic transition (EHT) to generate the first blood cells (Moore and Metcalf 1970). This initial “primitive” wave of hematopoiesis generates a limited subset of blood cells, including primitive red blood cells, macrophages, and megakaryocytes that serve the early oxygenation and scavenging needs of the developing embryo. The first “definitive” hematopoietic stem cells (HSCs), capable of generating all mature blood cells arise shortly after primitive hematopoiesis in the developing aorta region (the aorta gonad mesonephros or AGM) around mid-gestation (Muller, Medvinsky et al. 1994, Medvinsky and Dzierzak 1996, de Bruijn, Speck et al. 2000, North, de Bruijn et al. 2002). Definitive HSC, when isolated from the AGM, are also capable of replenishing the blood system after adoptive transfer into an irradiated adult recipient. Following their generation in the AGM, definitive HSCs enter the blood stream where they seed other tissues, primarily the fetal liver (Dzierzak and Speck 2008). Once seeded in the fetal liver, HSCs undergo massive expansion while maintaining repopulation potential (Ema and Nakauchi 2000) that exceeds that of their adult bone marrow counterparts (Rebel, Miller et al. 1996). After expansion in the fetal liver niche, and coincident with the closure of the umbilical inlet (Khan, Mendelson et al. 2016) HSCs then migrate to the bone marrow where they remain for the remainder of the lifespan.

Due to their ability to reconstitute the adult blood system, definitive fetal HSCs have long been considered the precursors of adult HSCs. However, there are several noted differences between fetal HSCs and adult HSCs, and the transition between these two populations is still poorly understood. Fetal HSCs express different surface markers than adult HSCs (Christensen and Weissman 2001, Kim, He et al. 2006) and are more proliferative than their adult counterparts (Bowie, McKnight et al. 2006, Gao, Xu et al. 2018). Fetal HSCs generally include more lymphoid-biased progenitors (Benz, Copley et al. 2012, Beaudin, Boyer et al. 2016) as compared to adult HSCs. Furthermore, fetal HSCs give rise to unique immune progeny that persist across the lifespan and contribute to adult immune function such as B1-a cells (Beaudin and Forsberg 2016),  $\gamma\delta$  T cells (Haas, Ravens et al. 2012, Gentek, Ghigo et al. 2018), ILCs (Schneider, Lee et al. 2019), and Tissue-resident macrophages (Ginhoux and Guilliams 2016). The formation of a “layered” immune system, in which fetal-derived immune cells co-exist alongside adult bone marrow-derived immune cells, contributes to heterogeneity of adult immune cell compartments, particularly within tissues.

A “linear” view of HSC development, in which fetal HSCs mature into adult HSCs in the bone marrow, has been recently challenged by sophisticated lineage tracing and *in vivo* barcoding experiments that have alternately suggested that many fetal HSCs are transient, despite possessing multilineage capability (Sun, Ramos et al. 2014, Busch, Klapproth et al. 2015, Beaudin, Boyer et al. 2016). These same approaches have also yielded critical information on heterogeneity within the adult HSC compartment (Haas, Trumpp et al. 2018). The abundance and diversity of progenitors underlying fetal hematopoiesis has driven an intense interest in defining their function and contribution to both the developing and adult

immune systems. Of particular interest are the functional differences between fetal HSCs and their adult counterparts and how heterogeneity of the fetal compartment influences HSC trajectory following perturbation during development.

## **1.6 Conclusions - Infection and inflammation during pregnancy alters fetal HSC development**

The complexity of the developing hematopoietic system suggests that extrinsic inputs during fetal development could influence phenotypic outcomes for hematopoietic function in a variety of different ways, depending on *when* and *how* these inputs are interpreted. If subsets of transient HSCs are produced *only* during specific windows of fetal development, the nature and timing of those extrinsic inputs will necessarily influence the trajectory of the HSC. It is important to note that in contrast with characterization of adult hematopoietic function, considerably less is known about both the fetal HSC response to inflammation and the specific mechanisms that drive the fetal HSC response to inflammation. In light of growing appreciation that the adult HSC compartment is far more heterogeneous than previously recognized (Haas, Trumpp et al. 2018), the fetal HSC compartment is certain to be even more heterogeneous. For example, numerous progenitors with varying differentiation capacity have been identified within the last decade (Böiers, Carrelha et al. 2013, Frame, McGrath et al. 2013, Beaudin, Boyer et al. 2016, Crisan, Solaimani Kartalaei et al. 2016). As the fetal HSC compartment is composed of heterogeneous, transient progenitors that continuously shift in space and time across development, defining their response to inflammation is a much more complicated feat.

The study of fetal hematopoiesis and inflammation to date has been guided mostly by the concept of 'sterile' inflammatory signaling - the requirement

for transmission of pro-inflammatory signaling during HSC specification, but in the absence of any specifically defined source of inflammatory signal. Indeed, work in mice and zebrafish models has detailed the requirement for TNF receptors, and specific signaling pathways downstream of cytokine receptors, including Myd88 and NFkB, for HSC emergence (for recent review see (Espin-Palazon, Weijts et al. 2018)). While recent work on HSC emergence has revealed the presence of pro-inflammatory macrophages in the developing aorta that may help drive endothelial to hematopoietic transition (Mariani, Li et al. 2019), there has generally been limited investigation of how specific infection or inflammatory signals during pregnancy might impact the fetal HSC compartment. Nonetheless, the capability of fetal HSCs to respond to inflammatory signals, and the responsiveness of the adult HSC compartment to such signals, certainly suggests that fetal hematopoietic progenitors could be responsive to infection and inflammation during gestation.

The direct cellular mechanism driving training of the fetal immune system during early life is underscored by key characteristics unique to the fetal hematopoietic environment. HSCs can sense and respond to extrinsic stimuli by eliciting intrinsic changes to their function and output. While the specific mechanisms driving the fetal HSC response to such stimuli are unknown, distinct features, such as their transient nature and less quiescent state, leave fetal HSCs particularly susceptible to environmental perturbation. The complexity of fetal hematopoietic development is underscored by recent evidence that has identified distinct subsets of functional HSCs that coexist during fetal development and contribute to a layered adult immune system (Beaudin, Boyer et al. 2016). In order to investigate the fetal HSC response to maternal stimuli in the context of a heterogenous fetal HSC compartment, we must take a multi-faceted approach. Using established models of maternal immune activation (Meyer, Feldon et al. 2009) with mouse models that identify distinct subsets of fetal

HSCs (Boyer, Schroeder et al. 2011, Beaudin, Boyer et al. 2016), we can track functional outcomes to fetal HSCs following stimulation of the maternal immune system. Study of the of the fetal hematopoietic response to maternal immune activation is made complicated by the lack of literature examining the potential signaling mechanisms between fetal cells and maternal signals.

To gain insight on the environmental signals that govern the fetal response, in my dissertation I will screen both the maternal and fetal environment for perturbations that may identify potential signals perceived by fetal HSCs, using models of infection and inflammation. In chapter 2, polyIC was used to mimic viral infections and thereby elicit strong Type I IFN responses in the mother during pregnancy. Concurrent analysis of gene expression profiles of the entire fetal hematopoietic stem and progenitor compartment of the fetal liver yielded novel insight of the complexity of the fetal hematopoietic landscape. In chapter 3, maternal infection of the widespread parasite and known TORCH pathogen, *Toxoplasma gondii*, was studied to analyze how maternal infection impacted fetal HSC responses. *T. gondii* infection produces strong Type II IFN $\gamma$  responses, and we noted that the fetal HSC directly responded to maternal IFN $\gamma$  with long term changes to cellular output due to infection. This combinatorial approach of using both Type I and Type II IFN mediated maternal inflammation allowed us to dissect the intricacies of the fetal HSC response and to generate a comprehensive screen of cellular outcomes and extrinsic signals which have yet to be identified prior to my thesis work. In chapter 4, I speculated that both the type of inflammation and timing of this inflammation are important considerations when determining the fetal HSC response to maternal inflammation. I review the foundational knowledge that work done in Chapter 2 and 3 have established to discuss future directions and implications of my dissertation findings.

## 1.7 Figures

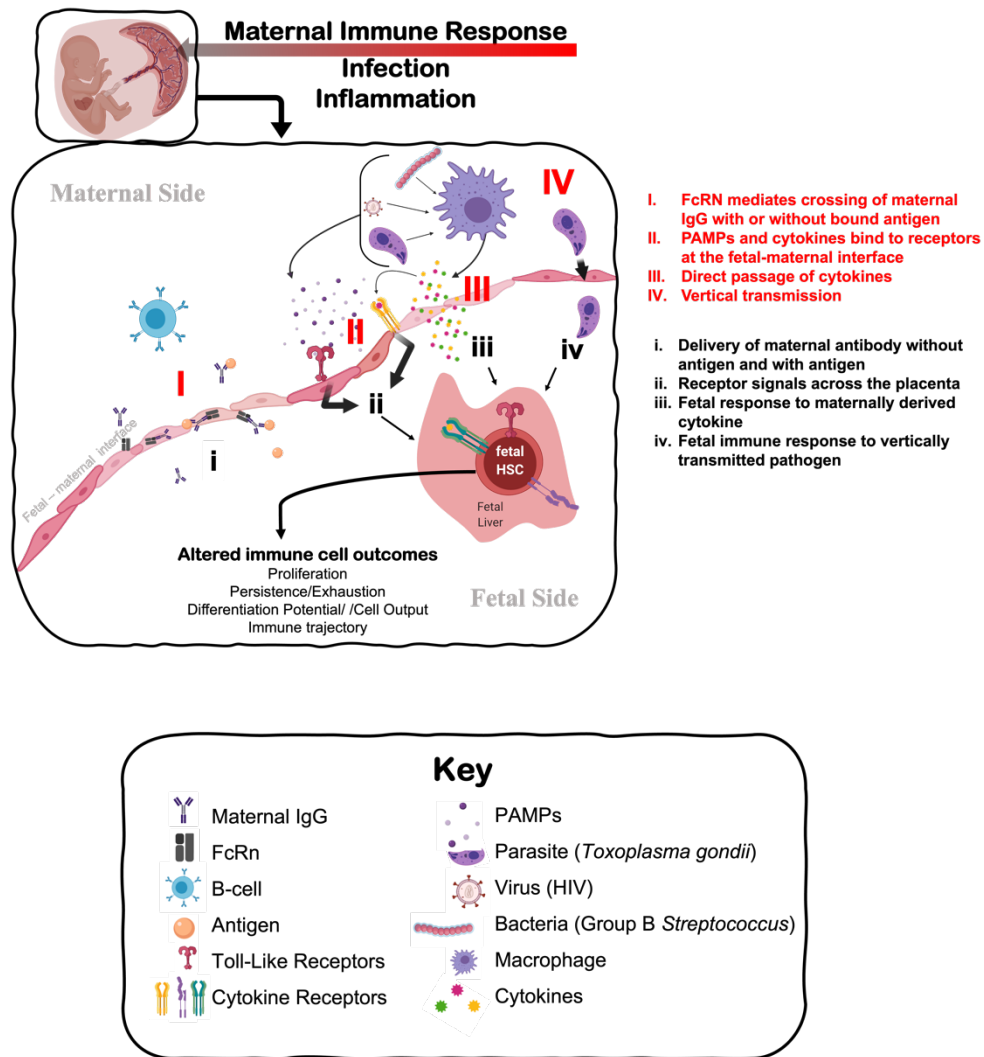


**Figure 1.** Understanding the mechanisms that impact fetal immune development in response to maternal immune perturbation. The maternal immune response to infection and inflammation is necessarily perceived by the fetus at the fetal-maternal interface. The fetus may perceive the maternal immune response through: I. Direct transfer and exposure to maternal antigen (i) via antibody-antigen complexes mediated by neonatal Fc receptor (FcRn); II. Receptors on the maternal side responding to PAMPs (Pathogen-Associated Molecular Patterns) produced by pathogens and maternal cytokines that signal to the fetal side (ii) through TLRs (Toll-Like Receptors) and specific cytokine receptors, respectively; III. Direct passage of cytokines across the fetal-maternal interface interacting directly with

receptors on the fetal side that may evoke a different cellular response on the fetal side (iii); or IV. Vertical transmission of infection from mother to fetus, causing immune cells to directly perceive and respond to infection (iv). Fetal HSCs can respond to these signals of maternal infection and inflammation by direct changes to their function, including changes in cell proliferation or quiescence that alter the persistence of progenitors, and changes to differentiation potential and cellular output.

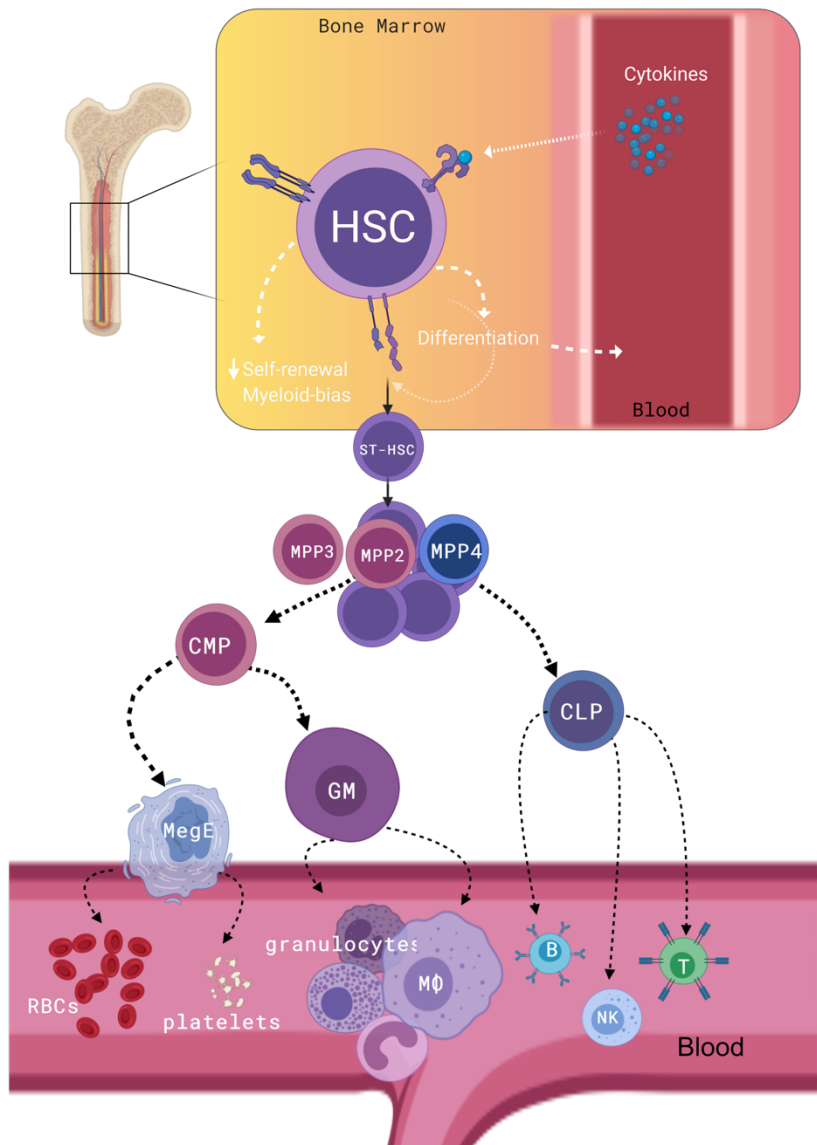


**Figure 2.** Bone Marrow HSCs respond to directly from cytokines produced from infection. When exposed to inflammatory cytokines from the circulation, HSCs become activated and rapidly exit quiescence and consequently, lose self-renewal potential. They exhibit myeloid bias at the progenitor level by differentiating into MPP2/3 at the expensive of lymphoid-biased MPP4. These MPP2 and MPP3 exhibit megakaryocyte and granulocyte/macrophage bias, respectively.



# **Chapter 2: Prenatal inflammation perturbs fetal hematopoietic development**

## **2.1 Introduction**

The adult immune system responds rapidly to infection by increasing the production of immune cells that control infectious microbes (Schultze et al., 2019; Takizawa et al., 2012). This response includes the release of inflammatory cytokines, mobilization and activation of specific immune cells, and increased production of immune cells in the bone marrow (BM) needed to eradicate microbes. The ability of the immune system to initiate a sustained and systemic response to infection has recently been linked to the direct responsiveness of adult BM hematopoietic stem cells (HSCs) to inflammatory signals. Adult HSCs respond to an array of cytokines and TLR ligands in situ (Nagai, Garrett et al. 2006, Essers, Offner et al. 2009, Baldrige, King et al. 2010, Esplin, Shimazu et al. 2011, Schuettpelez and Link 2013, Furusawa, Mizoguchi et al. 2016, Pietras, Mirantes-Barbeito et al. 2016, Takizawa, Fritsch et al. 2017, Yamashita and Passegué 2019), resulting in both acute and long-term changes to HSC function.

In response to inflammation or infection, adult HSCs exit quiescence (Essers, Offner et al. 2009), show accentuated myeloid bias (Matatall, Shen et al. 2014, Pietras, Mirantes-Barbeito et al. 2016), and increased myeloid output, leading to the production of sufficient quantities of myeloid cells required to combat infection. Accumulating evidence suggests that in response to both normal and aging-related inflammation, myeloid-biased output is propagated by the disparate activation of myeloid-biased HSCs (Beerman, Bhattacharya et al. 2010, Matatall, Shen et al. 2014, Haas, Hansson et al. 2015), as well as the downstream expansion of myeloid-

biased multipotent progenitors at the expense of lymphoid progenitors (Pietras, Mirantes-Barbeito et al. 2016).

Prenatal inflammation and infection may shape the fetal HSC trajectory (Apostol, Jensen et al. 2020), but the response of fetal hematopoiesis to inflammation has not been investigated. In the developing embryo, "sterile" inflammatory signaling is required for HSC emergence during early development (Espin-Palazon, Weijts et al. 2018); however, beyond emergence, there is little information regarding whether developing HSCs respond *in utero* to maternal infection and inflammation, how they respond, and the consequences for hematopoiesis. We hypothesize that the fetal HSC response to prenatal inflammation drives lasting changes to hematopoietic output in offspring that help shape the postnatal immune response.

Here, we use a maternal immune activation (MIA) model, wherein we injected pregnant mice with 20mg/kg Polyinosinic:polycytidylic acid (pIC) at E14.5, to decipher the effects of *in utero* inflammation on fetal HSPCs and examine the impact to fetal HSC function. In direct contrast to myeloid bias invoked by inflammation in adult hematopoiesis, our *in vivo* analysis and single-cell transcriptional profiling reveal that prenatal inflammation evokes lymphoid bias by activating transient, lymphoid-biased fetal HSCs and propagating the expansion of lymphoid-biased HSPCs in the fetal liver. By demonstrating that heterogeneity of the fetal HSPC compartment underlies a differential response of prenatal hematopoiesis to inflammation, our findings have important implications for defining developmental origins of immune dysfunction.

## **2.2 Materials and Methods**

### **2.2.1 Mouse models and husbandry**

8-12-week-old female C57BL/6 (RRID: IMSR\_JAX:000664) were mated to male Flkswitch mice (Boyer et al., 2011, 2012; Epelman et al., 2014; Hashimoto et al., 2013, Beaudin, et al., 2016). Flkswitch mice were generated by crossing Flk2-Cre mice (Benz et al., 2008) to mTmG mice (Muzumdar et al., 2007) and gestation day was confirmed by the presence of a sperm plug. Flkswitch males were used because the Flk-Cre transgene is only transmitted through the Y chromosome. At gestation day 14.5, pregnant dams were weighed and injected with 20mg/kg Polyinosinic:polycytidylic acid (pIC). For fetal timepoints, pregnant dams were euthanized, and fetuses were dissected from the uterine horn. Fetal liver GFP+ (Flkswitch) expression was confirmed by microscopy in fetuses or by peripheral blood analysis at postnatal timepoints, Postnatal day (P)14 and 8-week-old adult. For transplantation assays, FlkSwitch mice were used as donors for cell isolation and 8- to 12-week-old WT C57BL/6 were used as recipients. Sex of recipients was random and split evenly between male and female. All mice were maintained in the University of California, Merced vivarium according to Institutional Animal Care and Use Committee (IACUC)-approved protocols.

### **2.2.2 Cell isolation and identification by flow cytometry**

Fetal livers were dissected and pipetted gently in staining media to form a single cell suspension. Adult and P14 BM cells isolated by dissecting long bones and using a mortar and pestle to gently crush bones in “staining media” (1XPBS, 2%FBS, .5mM EDTA) and bone marrow was extracted by

gently pipetting. Cells were filtered through a 70µM filter. Cell populations were analyzed using a four-laser FACS Aria III (BD Biosciences). Cells were sorted on The FACS Aria II (BD Biosciences) or III. All flow cytometric analysis was done using FlowJo™. Hematopoietic and mature blood cell populations were identified as follows: Lineage dump or “Lin” for all fetal liver populations (CD3, CD4, CD5, CD8, CD19, Ter-119, Nk1.1, Gr-1, F4/80), Lin for adult bone marrow populations (CD3, CD4, CD5, CD8, Cd11b, CD19, Ter-119, Nk1.1, Gr-1, F4/80); LT-HSCs (Lin<sup>-</sup>, CD45<sup>+</sup>, cKit<sup>+</sup>, Sca1<sup>+</sup>, Flk2<sup>-</sup>, CD48<sup>-</sup>, CD150<sup>+</sup>), ST-HSCs (Lin<sup>-</sup>, CD45<sup>+</sup>, cKit<sup>+</sup>, Sca1<sup>+</sup>, Flk2<sup>-</sup>, CD48<sup>-</sup>, CD150<sup>-</sup>), Tom<sup>+</sup> aHSCs, (Lin<sup>-</sup>, CD45<sup>+</sup>, cKit<sup>+</sup>, Sca1<sup>+</sup>, CD150<sup>+</sup>, Tom<sup>+</sup>), GFP<sup>+</sup> drHSCs (Lin<sup>-</sup>, CD45<sup>+</sup>, cKit<sup>+</sup>, Sca1<sup>+</sup>, CD150<sup>+</sup>, GFP<sup>+</sup>), MPP2 (Lin<sup>-</sup>, CD45<sup>+</sup>, cKit<sup>+</sup>, Sca1<sup>+</sup>, Flk2<sup>-</sup>, CD48<sup>+</sup>, CD150<sup>+</sup>), MPP3 (Lin<sup>-</sup>, CD45<sup>+</sup>, cKit<sup>+</sup>, Sca1<sup>+</sup>, Flk2<sup>-</sup>, CD48<sup>+</sup>, CD150<sup>-</sup>), MPP4 (Lin<sup>-</sup>, CD45<sup>+</sup>, cKit<sup>+</sup>, Sca1<sup>+</sup>, Flk2<sup>+</sup>, CD48<sup>+</sup>, CD150<sup>-</sup>), Granulocyte-Macrophage Progenitor (GMP: Ckit<sup>+</sup>, CD150<sup>+</sup>, CD41<sup>-</sup> FcGR2/3<sup>+</sup>) Megakaryocyte Progenitor (MP: Ckit<sup>+</sup>, CD150<sup>+</sup>, CD41<sup>+</sup>), Erythrocyte progenitor (EP: Ckit<sup>+</sup>, CD150<sup>+</sup>, FcGR2/3<sup>-</sup>, Endoglin<sup>+</sup>).

### **2.2.3 Proliferation of HSCs and MPPs**

Fetal liver cells were processed into a single cell suspension and cKit-enriched using CD117 MicroBeads (Miltenyi Biotec, San Diego, CA, USA). The cKit-enriched population was stained with an antibody cocktail for surface markers of hematopoietic stem and progenitor cells. Cells were then fixed and permeabilized with the True-Nuclear Transcription buffer set (Biolegend) and then stained with Ki67-APC (Invitrogen, Carlsbad, CA, USA) and Hoescht 33342 (Invitrogen).

## **2.2.4 Transplantation assays**

Transplantations were performed by sorting GFP<sup>+</sup> drHSCs and Tom<sup>+</sup> HSCs from fetal liver. Recipient C57BL/6 mice (8-12 weeks) were lethally irradiated using 1000 cGy (split dose, Precision X-Rad 320). 5x10<sup>6</sup> whole bone marrow cells from untreated age matched C57BL/6 and 200 sorted GFP<sup>+</sup> drHSCs or Tom<sup>+</sup> HSCs wells were diluted in PBS and transplanted via retroorbital injection using a 1mL tuberculin syringe in a volume of 100-200  $\mu$ L. Peripheral blood chimerism was determined in recipients by blood collection via cheek bleeds every 4 weeks for 16 weeks and cells were analyzed by flow cytometry using the LSRII (BD Biosciences). Long-term multilineage reconstitution (LTMR) was defined as chimerism >1% in all mature blood lineages. At 18 weeks, recipients were euthanized, and BM populations were assessed for chimerism by flow cytometry.

## **2.2.5 10x Chromium single-cell sequencing of HSPCs**

Pregnant dams from C57BL/6 Flkswitch crosses were exposed to pIC or saline at E14.5. E15.5 fetal liver cells were pooled, cKit-enriched, and sorted for HSPCs (CD45<sup>+</sup>, Lin<sup>-</sup>, cKit<sup>+</sup> Sca1<sup>+</sup>). In order to get adequate cell numbers for analysis, at least 9 litters/condition (with 3-8 fetal livers/litter) were used for sorts. Sorted HSPCs were frozen at -80°C in FBS and 15% DMSO in cryovials until all samples were collected. Frozen cells were thawed in a 37°C water bath for 2-3 minutes and washed and resuspended in 10% FBS and assessed for 60-70% viability before processing. A sample library was generated using Chromium 10x V3 and run using NovaSeq.

## 2.3 Results

### 2.3.1 Prenatal inflammation induced by maternal immune activation (MIA) causes expansion of a developmentally-restricted HSC

To investigate how fetal hematopoietic progenitors respond to maternal inflammation, we employed a mouse model of maternal immune activation (MIA) (Meyer, Feldon et al. 2009), where we mimicked a mild viral infection in pregnant mice with a single injection of the toll-like receptor 3 (TLR3) agonist Polyinosinic:polycytidylic acid, or pIC. We performed these experiments using the FlkSwitch mouse model (Boyer, Schroeder et al. 2011), which we previously used to identify a developmentally-restricted, lymphoid-biased hematopoietic stem cell (drHSC) with specific potential to produce fetal-restricted immune cells, including B1-B cells (Beaudin et al., 2016). In the FlkSwitch model, Flk2-driven expression of Cre results in a permanent genetic switch from Tomato (Tom) to GFP expression (Boyer et al., 2011). Both Tom<sup>+</sup> and GFP<sup>+</sup> HSCs are present during perinatal development (Fig. 1A), but only Tom<sup>+</sup> HSCs persist and contribute to the adult HSC compartment (Boyer, Schroeder et al. 2011, Boyer, Beaudin et al. 2012). We therefore denote Tom<sup>+</sup> HSCs in the fetal liver (FL) as “conventional” HSCs, and GFP<sup>+</sup> HSCs in the FL as “developmentally-restricted” HSCs, or GFP<sup>+</sup> drHSCs (Beaudin et al., 2016).

To induce MIA, we injected pregnant C57BL/6J (WT) females crossed to FlkSwitch males with 20mg/kg pIC or saline control at embryonic day (E)14.5, when hematopoietic progenitors in the FL undergo massive expansion. We examined hematopoietic stem and progenitor cells (HSPCs) in offspring 1-3 days later, postnatally, and into adulthood (Fig. 1A). The dose of pIC used produced no obvious signs of illness in the mom. Crown-rump length (CRL) of E15.5 fetuses was lower in MIA litters compared to saline-treated litters (SFig. 1A) and onset of birth was delayed by one day

in 35% of litters born (SFig. 1B). After birth, by postnatal day (P)14, there was a slight reduction in surviving pups from MIA (SFig. 1C) although those pups were on average, larger than controls (SFig. 1D), most likely due to longer gestation time (SFig. 1B).

Clear changes to the fetal hematopoietic compartment were observed one day after MIA induction. HSPCs (CD45+, Lineage-, cKit+ Sca1+) showed a marked increase in frequency one day after injection (Fig. 1B, C), that was normalized by E17.5 (Fig. 1D). Despite increased HSPC frequency, HSPC cellularity at E15.5 was not significantly increased (SFig. 1E), likely reflecting an overall decrease in CD45+ cells in the FL (SFig. 1F). Importantly, as compared to adult BM HSPCs (SFig. 2A-B), MIA did not induce Sca1 upregulation in the FL (SFig. 2C), including CD45+ cells (SFig. 2D) or long-term (LT)-HSCs (SFig. 2E-F), suggesting that increased fetal HSPC frequency was not caused by interferon-induced Sca1 upregulation. We also observed a significant increase in frequency of GFP-labeled cells across all HSPCs (Fig. 1E), consistent with expanded progenitors. Cellularity of LT-HSCs (CD45+ Lin-, cKit+, Sca1+ CD150+ CD48-; Fig. 1F), including Tom+ HSCs (CD45+, Lin-, cKit+, Sca1+, CD150+, Tom+; Fig. 1G) was unchanged from E15.5-E17.5 in response to MIA. In contrast, we observed a significant spike in the number of GFP+ drHSCs (CD45+, Lin-, cKit+, Sca1+, CD150+, GFP+) one day following MIA, after which cellularity returned to control levels by E16.5 (Fig. 1H).

To examine the mechanism underlying the specific expansion of the GFP+ drHSCs in response to MIA, we assessed proliferation at E15.5. MIA drove increased proliferation of both Tom+ HSCs and GFP+ drHSCs (Fig. 1I-J), but proliferation of GFP+ drHSCs was significantly greater in comparison to Tom+ HSCs in both saline- and MIA-treated conditions (Fig. 1I-J).

Importantly, only proliferation of GFP<sup>+</sup> drHSCs corresponded to a significant increase in cellularity one day later (Fig. 1H).

### **2.3.2 Activation of a developmentally-restricted HSC drives downstream expansion of lymphoid-biased multipotent progenitors**

As MIA induced a rapid response by HSCs that coincided with an increase in overall GFP expression across all HSPCs (Fig. 1E), we next examined how downstream hematopoietic progenitors responded to MIA, including short-term (ST)-HSCs and multipotent progenitor (MPP) subsets as defined phenotypically by Pietras et al (2015) (Fig. 2A). Cellularity of myeloid-biased ST-HSCs, MPP2, and MPP3 cells were unaffected by MIA (Fig. 2B-D), an observation that deviates from previously reported dynamics in the adult hematopoietic response to inflammation (Pietras 2017). Similarly, committed myeloid progenitors were not expanded in response to MIA (SFig. 1G, I). In contrast, lymphoid-biased Flk2<sup>+</sup> MPP4s were significantly expanded two-days post-MIA compared to saline treated controls (Fig. 2E.) Expansion of Flk2<sup>+</sup> MPP4s did not immediately translate into expansion of downstream committed lymphoid progenitors or mature lymphoid cells (SFig. 1 H), as expected based on differentiation dynamics of lymphoid lineages (Busch, Klapproth et al. 2015). Investigation of proliferation across all CD150<sup>-</sup> MPPs revealed increased proliferation at E15.5 and E16.5 (Fig. 2F-G), likely driving the significant increase in cellularity of MPP4s at E16.5. Expansion of both lymphoid-biased GFP<sup>+</sup> drHSCs and lymphoid-biased Flk2<sup>+</sup> MPP4s in response to MIA raised the possibility that prenatal inflammation specifically evoked a lymphoid-biased response in fetal progenitors.



### **2.3.3 Single-cell sequencing reveals the response of distinct fetal HSPCs to MIA**

To further understand how MIA remodels hematopoietic development at the molecular level, we sorted E15.5 FL HSPCs from MIA or saline-treated dams and analyzed the transcriptional profiles of 23,505 cells using single-cell RNA sequencing (scRNA-seq). Unsupervised clustering analysis identified 14 distinct clusters (C0-C13) (Fig. 3A, SFig. 3A). Clusters segregated based on differential gene expression profiles and cell-cycle states (SFig. 3B). MIA altered the distribution of cells across clusters (Fig. 3B,C). Differential response to MIA was observed among clusters: C1, C3, C5, C6, C9, and C10 were robustly expanded in response to MIA, whereas C2, C4, C7, and C8 were significantly reduced in response to MIA (Fig. 3D).

We utilized our previously published data set (Beaudin et al., 2016) to determine overlap of the phenotypical FL GFP+ drHSCs and Tom+ HSCs with our identified clusters. This resulted in the emergence of two divergent regions encompassing multiple clusters enriched for Tom+ HSC (Fig. 3E, G) or GFP+ drHSC signature (Fig. 3F, H). Surprisingly, several clusters that expanded in response to MIA significantly overlapped with the GFP+ drHSC signature (C1, C3, C5, C9, and C10), whereas clusters decreasing in response to MIA overlapped with the Tom+ HSC signature (C2, C4, C7, and C8). TdTomato and eGFP transcript expression was also enriched in clusters overlapping with Tom+ HSC and GFP+ drHSC signatures, respectively (SFig. 3C), although overlap was not precise due to broad GFP expression across MPPs within the FlkSwitch model (Boyer, Schroeder et al. 2011).

To annotate clusters responding to MIA, we determined HSC and MPP identity based on adult transcriptional profiles from previously published datasets (Cabezas-Wallscheid, Klimmeck et al. 2014). Clusters segregated

into either HSC- (Fig. 3I, K) or MPP-like populations (Fig. 3J, L). Two clusters, C2 and C9, were the most enriched for HSC identity and showed no significant enrichment for MPP genes. Gene set enrichment analysis (GSEA) of HSC-like C2 revealed best concordance with Tom+ HSC identity (Fig. 3M) and was defined by expression of canonical HSC genes, including *Mecom* (SFig. 3A), *Hlf* (SFig 3A), *Mllt3* (SFig. 3D), and *Meis1* (SFig 3E) (Gazit, Garrison et al. 2013). C2 was quiescent, and expressed low levels of mKi67, even after MIA (SFig. 3F). The remaining Tom+ HSC clusters -- C0, C4, C7, C8 and C13 (Fig. 3G) -- overlapped with both HSC and MPP signatures (Fig. 3I-L) and showed significant enrichment of megakaryocyte-associated genes (SFig. 3G) and no enrichment for lymphoid- (Fig. 3O) or myeloid-associated genes (SFig. 3H). The identification of HSC-like C2 within the clusters most enriched for Tom+ HSC identity is consistent with HSC activity within the Tom+ HSC fraction.

Clusters enriched for the GFP+ drHSC signature -- C1, C3, C5, C9, C10, C11, and C12 (Fig. 3H) -- exhibited varying degrees of stemness (Fig. 3I-L), lymphoid- (Fig. 3O) and myeloid-priming (SFig. 3H). Uniquely, C9 was specifically enriched for both GFP+ drHSC signature (Fig. 3F, H) and adult HSC signature (Fig. 3K). Additionally, C9 was the only cluster to be significantly enriched for lymphoid-, myeloid-, and megakaryocyte-associated genes (Fig. 3O, SFig 3G-H). Although C9 did not express the same set of canonical HSC genes expressed by C2, C9 expressed other canonical and non-canonical HSC markers, including HLA genes (SFig. 3A), *Spi1* (Staber, Zhang et al. 2013) (SFig. 3I), *Pbx1* (Ficara, Murphy et al. 2008)(SFig. 3J), *Cd74* (Luckey, Bhattacharya et al. 2006) (SFig. 3A, K), and *Tet2* (Moran-Crusio, Reavie et al. 2011) (SFig. 3L). C9 was heterogenous for cell cycle markers (SFig. 3B, F), with a subset of cells appearing highly quiescent. C5, C9, C10, C11, and C12 were all highly enriched for lymphoid gene signature (Fig. 3O) while C1, C5, C9, C11, and C12 were all enriched

for myeloid gene signature (SFig 3H). Importantly, overlap of multiple stem cell-, lymphoid-, and myeloid-associated clusters with the phenotypically-defined GFP<sup>+</sup> drHSC reflects both multipotency and lymphoid bias of the GFP<sup>+</sup> drHSC *in vivo*.

### **2.3.4 Fetal HSPCs respond distinctly to inflammatory cytokines induced by MIA**

Our data indicate a molecular basis for the observed changes to the fetal HSPC compartment following MIA. *In utero*, the fetus may be passively exposed to maternal cytokines or other inflammatory mediators through the placental barrier or alternatively, the response of placental or fetal cells to maternal inflammation may translate into a discrete fetal immune response (Apostol, Jensen et al. 2020). To interrogate potential signaling mechanisms that drive the specific response of lymphoid-biased FL HSPCs, we examined and compared inflammatory cytokine profiles in maternal serum, amniotic fluid (AF) and FL supernatant one day post MIA, at E15.5. IFN- $\alpha$  and IL-23 were significantly increased in maternal serum (Fig. 4A, SFig. 2G). In AF, we observed an increase in levels of IFN- $\alpha$ , IFN- $\beta$ , IL-27, and GM-CSF in response to MIA (Fig. 4B, C). In contrast, the FL only exhibited upregulation of two cytokines: IL-1 $\alpha$  and IFN- $\alpha$  (Fig. 4D, E). The increase in Type I interferons in the maternal serum, AF, and FL suggest that Type I interferon-mediated inflammation is evoked from either maternal sources of cytokine (Fig. 4A, SFig. 2G), or non-HSPC populations in FL, as IFN- $\alpha$ , IFN- $\beta$ , and IL-1 $\alpha$  cytokine was not produced directly from HSPCs (data not shown).

To gain additional insight into possible interactions between fetal HSPCs and cytokines observed in the fetal microenvironment, we scored the enrichment of immune-related cytokine signaling gene signatures in our single-cell sequencing data. Only C9, a stem cell-like cluster that

overlapped significantly with a GFP<sup>+</sup> drHSC expression signature, was significantly enriched for expression of genes associated with immune cytokine signaling, as compared to all other clusters (Fig. 4F). Further examination of IL-1 $\alpha$  and IFN- $\alpha$  signaling -- cytokines upregulated in the FL following MIA (Fig. 4D, E) -- revealed significant enrichment for interferon signaling pathways within C9 (Fig. 4G). Interferon- $\alpha/\beta$  receptor (IFNAR) pathway genes *Stat1*, *Isg15*, and *Irf2712a* were highly expressed within C9 and increased expression following MIA (Fig. 4H). In contrast, overall interleukin-1 signaling expression was unchanged or decreased across clusters following MIA (SFig. 2H), suggesting that IFN- $\alpha$  signaling is likely a major driver of the inflammatory response within fetal HSPCs. Together, these data suggest that the fetal response to maternal poly (IC) is driven by an immediate HSC response to Type-1 interferons.

### **2.3.5 Prenatal inflammation induced by MIA affects self-renewal and hematopoietic output of developing HSCs**

Single-cell transcriptional profiling suggested Tom<sup>+</sup> HSCs and GFP<sup>+</sup> drHSCs respond differently to prenatal inflammation in situ. To investigate how MIA impacted function and output of Tom<sup>+</sup> HSCs and GFP<sup>+</sup> drHSCs, we performed transplantation assays and investigated long-term multi-lineage reconstitution (LTMR). We isolated Tom<sup>+</sup> HSCs or GFP<sup>+</sup> drHSCs from E15.5 FL one day post MIA or saline treatment, and competitively transplanted sorted cells with 5x10<sup>5</sup> adult whole bone marrow (WBM) cells into lethally irradiated adult recipients (Fig. 5A). Recipient mice were monitored every 4 weeks for 16 weeks post-transplantation to assess mature blood lineage reconstitution in both primary and secondary transplants (Fig. 5A). Under control conditions, fewer recipients of GFP<sup>+</sup> drHSCs were reconstituted as compared to recipients of Tom<sup>+</sup> HSCs (Fig. 5B), and GFP<sup>+</sup> drHSC recipients demonstrated lymphoid-biased

contribution to peripheral blood (PB) output as compared to Tom<sup>+</sup> HSC recipients (SFig. 4A), as previously reported (Beaudin, 2016). In primary transplantation, MIA did not impact LTMR frequency in recipients of either Tom<sup>+</sup> HSCs or GFP<sup>+</sup> drHSCs (Fig. 5B). MIA induced significantly increased granulocyte-monocyte (GM) output in PB (Fig. 5C) of primary Tom<sup>+</sup> HSC recipients, although there were no differences in BM chimerism of HSPCs (SFig. 4B-C), myeloid progenitors, lymphoid progenitors, or mature cells after 18 weeks (SFig. 4D, E). MIA did not affect PB (Fig. 5C) or BM progenitor output (SFig. 4B-E) in primary recipients of GFP<sup>+</sup> drHSCs. In sharp contrast, secondary transplantation revealed a significant reduction in the number of Tom<sup>+</sup> HSC recipients that exhibited LTMR (Fig. 5D), whereas the effect of MIA in secondary recipients of GFP<sup>+</sup> drHSCs was less severe. Tom<sup>+</sup> HSC exhaustion was evident in both PB output (Fig. 5E) and BM progenitor chimerism in MIA-treated Tom<sup>+</sup> HSC recipients (SFig. 4G-J). In contrast, secondary recipients of GFP<sup>+</sup> drHSCs did not exhibit any functional differences in response to MIA: both PB and BM chimerism was unaffected by MIA, and lymphoid-biased output was sustained (Fig. 5E; SFig. 4F). Together, serial transplantation assays revealed a disparate response of two fetal HSC populations, with an initial myeloid bias followed by subsequent loss of self-renewal potential in Tom<sup>+</sup> HSCs, but not GFP<sup>+</sup> drHSCs, following MIA.

## 2.4 Discussion

Adult HSCs respond directly to inflammation, resulting in both acute and sustained changes to HSC function that drive the systemic immune response to infection (Pietras 2017). Whereas in the adult BM, HSCs are directly exposed to pathogens, cytokines, and other inflammatory mediators through circulation, exposure of the fetus to prenatal inflammation is necessarily limited by the maternal-fetal barrier (Ander, Diamond et al. 2019). Maternal infection and microbial exposure during pregnancy has

been linked to altered immune outcomes in infants (Apostol, Jensen et al. 2020), but any causal relationship has not been clearly established, and there is little information regarding how *in utero* inflammation might be interpreted by the developing fetal HSCs. “Sterile” inflammatory signaling is required for HSC emergence and specification during early development (He, Zhang et al. 2015, Espin-Palazon, Weijts et al. 2018), but to our knowledge there has been no direct investigation of how *in utero* inflammation directly influences fetal hematopoiesis. Here we demonstrate, for the first time, that developing fetal HSCs respond directly to *in utero* inflammation. To test the fetal HSC response to inflammation, we used a mouse model of maternal immune activation (MIA), in which injection of pIC at mid-gestation mimics an immune response to viral infection during pregnancy (Meyer, Feldon et al. 2009). Importantly, the use of MIA allows us to distill the effect of *in utero* inflammation in the absence of overt fetal infection. We also performed these experiments using our “FlkSwitch” model (Boyer, Schroeder et al. 2011, Beaudin, Boyer et al. 2016) in which we have previously described two distinct fetal HSC progenitors: a Tom+ HSC that persists into adult BM, and a lymphoid-biased, GFP+ developmentally-restricted hematopoietic stem cell (drHSC) that is transient and exists only in the perinatal period. This platform allowed us to test the response of a dynamic and heterogeneous fetal hematopoietic compartment to inflammation *in utero*. Our investigation reveals that prenatal inflammation drives both an immediate and sustained response in otherwise transient fetal progenitors.

In order to respond appropriately to injury and inflammation, adult hematopoietic progenitors exhibit myeloid bias and increased myeloid output in response to a range of inflammatory cues (Matatall, Shen et al. 2014, Haas, Hansson et al. 2015, Pietras, Mirantes-Barbeito et al. 2016). Myeloid bias is propagated both by the specific activation of myeloid-biased

HSCs to inflammatory cues (Beerman, Bhattacharya et al. 2010, Gekas and Graf 2013, Haas, Hansson et al. 2015, Mann, Mehta et al. 2018), as well as through downstream expansion of myeloid-biased progenitors, including MPP2 and MPP3, at the expense of lymphoid-biased MPP4s (Pietras, Mirantes-Barbeito et al. 2016). In sharp contrast, our analysis of the response of fetal hematopoiesis to prenatal inflammation reveals that inflammation during the fetal period invokes a lymphoid-biased response. Using the FlkSwitch model, our analysis reveals that prenatal inflammation activates lymphoid-biased fetal GFP<sup>+</sup> drHSCs and drives the downstream expansion of lymphoid-biased MPPs, including Flk2<sup>+</sup> MPP4s. Expansion of GFP<sup>+</sup> drHSCs one day post MIA is therefore likely responsible for subsequent expansion of Flk2<sup>+</sup> MPP4s one day later. Together, our data indicate that inflammation during the fetal period invokes a lymphoid-biased response by activating lymphoid-biased HSCs that subsequently drive the downstream expansion of lymphoid-biased progenitors.

Consistent with expanded lymphoid-biased progenitors *in situ*, our single-cell analysis of over 23,000 fetal single HSPCs confirmed the expansion of both HSC-like progenitors and lymphoid-primed progenitors in response to prenatal inflammation. At least two clusters, Cluster (C) 2 and C9, resembled HSCs in both transcriptional profile and proliferative state, but only one of these populations, C9, overlapped transcriptionally with the GFP<sup>+</sup> drHSC and was expanded in response to MIA. C9 also stood out as the only cluster to exhibit a strong cytokine-responsive transcriptional profile and increased inflammatory gene expression in response to MIA. Cytokine analysis revealed upregulation of IFN- $\alpha$  in the FL, and C9 exhibited a robust transcriptional response to interferon. Surprisingly, upregulation of Type I interferons did not increase non-specific Sca1 expression in the fetus, as observed in adult hematopoiesis (King and Goodell 2011). In contrast, C2, which overlaps transcriptionally with the Tom<sup>+</sup> HSC, exhibited a more

"adult-like" HSC profile, as revealed by expression of more canonical HSC genes including *Mllt3* and *Meis1*, among others. Furthermore, C2 contracted in response to MIA, and expressed little to no inflammatory gene signature. Our transcriptional analysis mirrors our *in vivo* data, whereby we identified an HSC-like cluster, overlapping with the GFP+ drHSC, that both expands and exhibits a robust transcriptional response to cytokines that are upregulated within the fetal microenvironment in response to prenatal inflammation.

Tom+ HSCs exhibited higher GM chimerism upon transplantation, suggesting the possibility that MIA also activated Tom+ HSCs and induced myeloid bias, although Tom+ HSCs were not expanded, and myeloid bias was not observed *in situ*. In contrast, MIA did not exaggerate lymphoid bias in GFP+ drHSCs upon transplantation. Furthermore, serial transplantation resulted in rapid exhaustion of Tom+ HSCs, but not GFP+ drHSCs. This observation is consistent with prenatal inflammation inducing abnormal persistence of the GFP+ drHSC, potentially at the expense of persistence of some fraction of the Tom+ HSCs. Susceptibility of adult HSC precursors, and the long-term effects of prenatal inflammation on their self-renewal capability, output, and response to infection, will need to be investigated in the future.

The MIA model was used previously to examine how prenatal inflammation affects brain development during a "critical window" of synapse formation (Meyer, Feldon et al. 2009). A critical window is defined as a developmental window during which extrinsic or intrinsic inputs can shape the phenotype of the adult organism. Here, we use the same approach to establish a framework for a critical window for hematopoietic development wherein extrinsic input, in the form of *in utero* inflammation, shapes the establishment and output of hematopoietic stem cells. We previously



demonstrated that under homeostatic conditions, the GFP+ drHSC fails to persist into adulthood, yet contributes to adult immunity by generating specialized immune cells that persist postnatally (Beaudin, Boyer et al. 2016, Beaudin and Forsberg 2016). Our data reveal that MIA drives proliferation and sustained output of GFP+ drHSCs. Together, our results illuminate how *in utero* inflammation can influence immune trajectories by reshaping hematopoiesis during a critical developmental window. Our discovery has significant implications for understanding the ontogeny of many hematopoietic-related disorders with poorly understood etiology, including diseases of tolerance, autoimmunity, and clonal hematopoiesis. Future studies should directly address the long-term consequences of perturbed fetal hematopoietic development.

## Table 2-1 List of Antibodies

<b>B220-BV605</b>	Biologend	RRID AB_2563312 (BioLegend Cat. No. 103244)
<b>CD105-PE-Cy7</b>	eBioscience	RRID AB_2573380 (Thermo Fisher Scientific Cat. No. 25-1051-82)
<b>CD11b-Biotin</b>	Biologend	RRID AB_312787 (BioLegend Cat. No. 101204)
<b>Cd11b-PB</b>	Tonbo Biosciences	RRID AB_2621936 (Tonbo Biosciences Cat. No. 72-0112)
<b>Cd11b-PE-Cy7</b>	Tonbo Biosciences	RRID AB_2621836 (Tonbo Biosciences Cat. No. 60-0112)
<b>CD150-BV785</b>	Biologend	RRID AB_2565962 (BioLegend Cat. No. 115937)
<b>CD150-PE-Cy7</b>	Biologend	RRID AB_756199 (BioLegend Cat. No. 122514)
<b>CD16/32</b>	Biologend	RRID AB_312801 (BioLegend Cat. No. 101302)
<b>CD16/32-APC</b>	Biologend	RRID AB_1953273 (BioLegend Cat. No. 101326)
<b>CD19-APC-Cy7</b>	Biologend	RRID AB_830707 (BioLegend Cat. No. 115530)
<b>CD19-Biotin</b>	Biologend	RRID AB_313639 (BioLegend Cat. No. 115504)
<b>CD1d-BV605</b>	BD Biosciences	RRID AB_2740098 (BD Biosciences Cat. No. 740366)
<b>CD21-PE-Cy7</b>	eBioscience	RRID AB_1518766 (Thermo Fisher Scientific Cat. No. 25-0211-82)
<b>CD23-e450</b>	Biologend	RRID AB_2571987 (BioLegend Cat. No. 101630)
<b>CD3-APC</b>	Biologend	RRID AB_312677 (BioLegend Cat. No. 100312)
<b>CD3-Biotin</b>	Biologend	RRID AB_312669 (BioLegend Cat. No. 100304)
<b>CD4-Biotin</b>	Biologend	RRID AB_312689 (BioLegend Cat. No. 100404)
<b>CD41-BV421</b>	Biologend	RRID AB_2650893 (BioLegend Cat. No. 133912)
<b>CD45.2-BV605</b>	Biologend	RRID AB_2563485 (BioLegend Cat. No. 109841)
<b>CD45.2-BV785</b>	Biologend	RRID AB_2562604 (BioLegend Cat. No. 109839)
<b>CD48-APC</b>	Biologend	RRID AB_571997 (BioLegend Cat. No. 103412)
<b>CD48-BV605</b>	Biologend	RRID AB_2650825 (BioLegend Cat. No. 103441)
<b>CD5-AlexaFluor647</b>	Biologend	RRID AB_2075301 (BioLegend Cat. No. 100614)
<b>CD5-Biotin</b>	eBioscience	RRID AB_466340 (Thermo Fisher Scientific Cat. No. 13-0051-85)
<b>CD61-APC</b>	Biologend	RRID AB_2234024 (BioLegend Cat. No. 104314)
<b>CD8<math>\alpha</math>-Biotin</b>	Biologend	RRID AB_312743 (BioLegend Cat. No. 100704)
<b>cKit-APC-Cy7</b>	Biologend	RRID AB_1626278 (BioLegend Cat. No. 105826)

<b>cKit-BV605</b>	Biolegend	RRID AB_2562042 (BioLegend Cat. No. 135122)
<b>F4/80-Biotin</b>	Biolegend	RRID AB_893501 (BioLegend Cat. No. 123106)
<b>Fik2-APC</b>	Biolegend	RRID AB_2107050 (BioLegend Cat. No. 135310)
<b>Gr-1-Biotin</b>	Tonbo Biosciences	RRID AB_2621652 (Tonbo Biosciences Cat. No. 30-5931)
<b>Gr-1violetFluor450</b>	Tonbo Biosciences	RRID AB 2621968 (Tonbo Biosciences Cat. No. 75-5931)
<b>IL7R<math>\alpha</math>-PE-Cy7</b>	Biolegend	RRID AB_2621859 (Tonbo Biosciences Cat. No. 60-1271)
<b>Ki67-APC</b>	eBioscience	RRID AB_2688057 (Thermo Fisher Scientific, Cat. No. 17-5698-82)
<b>Nk1.1-Biotin</b>	Biolegend	RRID AB_313391 (BioLegend Cat. No. 108704)
<b>Sca1-APC-Cy7</b>	Biolegend	RRID AB_756199 (BioLegend Cat. No. 122514)
<b>Sca1-PB</b>	Biolegend	RRID AB_2143237 (BioLegend Cat. No. 122520)
<b>Sca1-PECy7</b>	Biolegend	RRID AB_756199 (BioLegend Cat. No. 122514)
<b>Ter-119-Biotin</b>	Biolegend	RRID AB_313705 (BioLegend Cat. No. 116204)
<b>Ter-119-PE-Cy5</b>	eBioscience	RRID AB_468811 (Thermo Fisher Scientific Cat. No. 15-5921-83)

## Table 2-2 Other Reagents and Resources

### 2-2.1 Chemicals, Peptides, and Recombinant Proteins

<b>ACK Lysing Buffer</b>	Thermo Fisher	Thermo Fisher Scientific Cat. No. A1049201
<b>Calibrite Beads - APC</b>	BD Biosciences	BD Biosciences Cat. No. 340487
<b>CD117 Microbeads, Mouse</b>	Miltenyi Biotec	Miltenyi Biotec Cat. No. 130-091-224
<b>DMSO</b>	Sigma	Sigma Cat. No D2650
<b>FBS</b>	Gibco	Thermo Fisher Scientific Cat. No. 26140079
<b>Hoescht 33342</b>	<b>Invitrogen</b>	Thermo Fisher Scientific Cat. No. H3570
<b>Propidium Iodide</b>	VWR	VWR Cat. No. 89139-064
<b>Polyinosinic:polycytidylic acid</b>	Millipore Sigma	Millipore Sigma Cat. No. P1530
<b>Streptavidin-PE-Cy5</b>	Biolegend	Biolegend Cat. No. 405205

### 2-2.2 Critical Commercial Assays

<b>True Nuclear Transcription Factor Buffer Set</b>	Biolegend Cat. No. 424401
<b>LEGENDPLEX Custom Mouse 13plex panel</b>	Biolegend

### 2.2.3 Experimental Models: Organisms/Strains

<b>Mouse: C57BL/6J</b>	The Jackson LaboratoryRRID:IMSR_JAX:006965
<b>Mouse: mT/mG</b>	The Jackson LaboratoryRRID:IMSR_JAX:007576
<b>Mouse: Flk2-Cre (Flt3-Cre)</b>	T. Boehm and C. Bleul (Max Planck, Freiburg, Germany)

### 2-2.4 Software and Algorithms

<b>Rstudio</b>	RStudio RRID SCR_000432
<b>Flowjo v.10</b>	Treestar RRID SCR_000410
<b>Graphpad Prism v.8</b>	Graphpad RRID SCR_015807
<b>BD FACS Diva</b>	BD Biosciences RRID SCR_001456
<b>snakePipes</b>	Bhardwaj et al., 2019 <a href="https://github.com/maxplanck-ie/snakepipes">https://github.com/maxplanck-ie/snakepipes</a>

**STARsolo** Dobin et al., 2013

<https://github.com/alexdobin/STAR/blob/master/docs/STARsolo.md>

**Deeptools QC** Ramírez et al., 2016 <https://deeptools.readthedocs.io/en/develop/>

**Seurat Satija et al., 2015** RRID SCR\_007322

**DEseq2** Love, et. al., 2014 RRID:SCR\_015687

## 2-2.5 Deposited Data

scRNA-seq	Accession Number	GSE161927
-----------	------------------	-----------

## 2.5 Figures

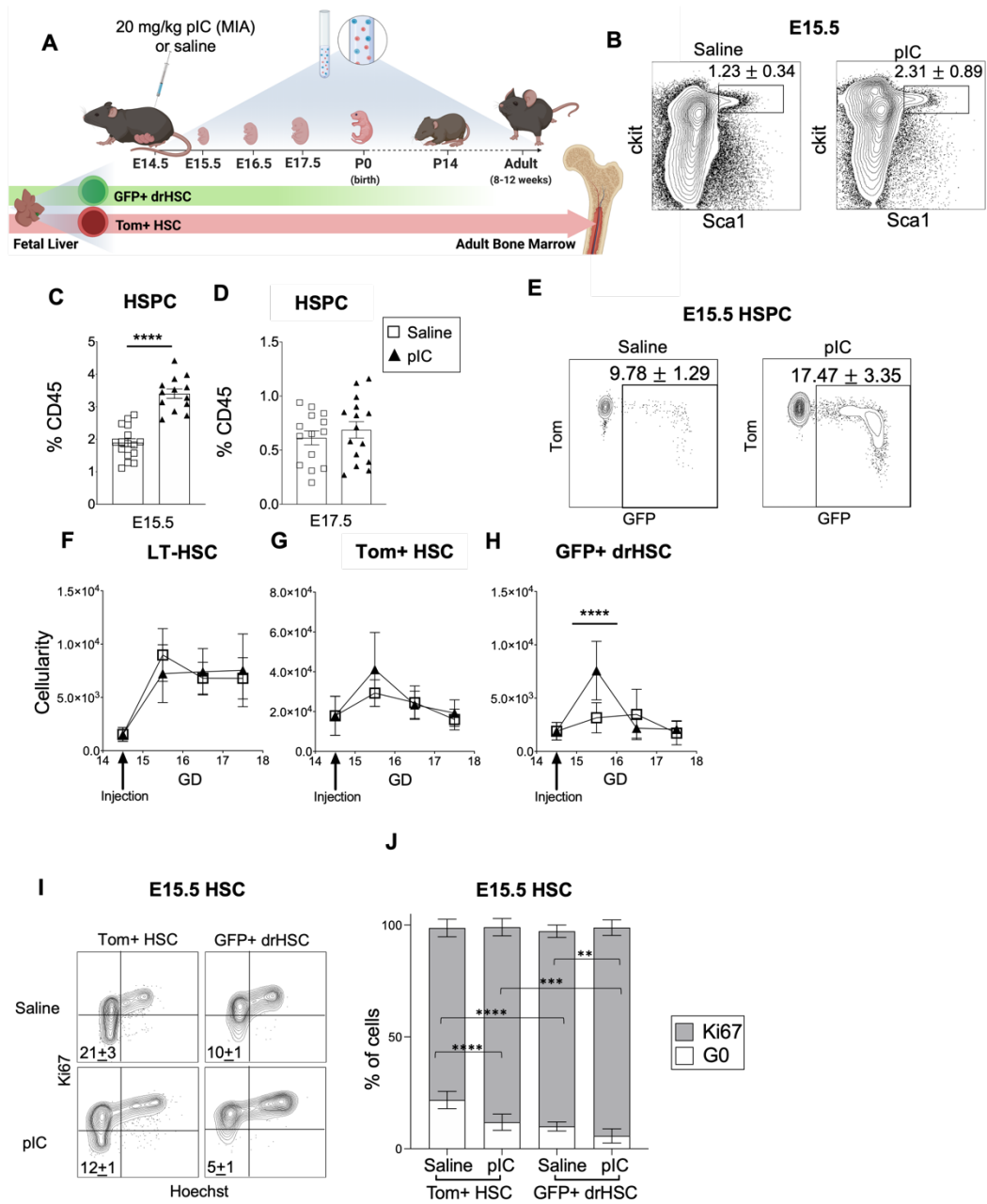


**Figure 1. Fetal hematopoietic stem and progenitor cells (HSPCs) respond to prenatal inflammation induced by maternal immune activation (MIA)**

**A** Timeline of MIA induction and analysis of fetal liver (FL) hematopoiesis. Pregnant WT dams mated to FlkSwitch males were intraperitoneal (i.p.) injected with 20 mg/kg

Polyinosinic-polycytidylic acid (pIC) at embryonic day (E) 14.5. Both Tom+ HSCs and GFP+ drHSCs are present in the fetal liver (FL) during development, but only Tom+ HSCs persist into the adult bone marrow (BM). Image created with Biorender.com.

**B)** Representative FACS plots of the hematopoietic stem and progenitor compartment “HSPC” (Live, Lin-, CD45+, cKit+, Sca1+) at E15.5, one day after pIC or saline induction. Numbers indicate average frequency  $\pm$  SD.

**C, D)** Frequency of HSPCs (as %CD45+ cells) in FL at E15.5 (C) and E17.5 (D).

**E)** Representative FACS plots showing frequency of GFP+ cells within the HSPC compartment at E15.5 in mice described in Fig.1B. Data represent frequency  $\pm$  SD.

**F-H)** Quantification of long-term HSCs (**F**) (LT-HSCs; LSK Flk2- CD150+ CD48-), Tom+ HSCs (**G**; LSK CD150+ Tom+), and GFP+ drHSCs (**H**; LSK CD150+ GFP+) across gestation days (GD) following maternal injection of pIC or saline. For all above experiments, N=3-6 pups/litter representing at least 3 litters/condition. Data represent average  $\pm$  SEM. \* $p \leq 0.05$ ; \*\* $p \leq 0.01$ ; \*\*\* $p \leq 0.001$ ; \*\*\*\* $p \leq 0.0001$ .

**I)** Representative FACS plots measuring proliferation by Ki67 expression and Hoechst staining of Tom+ HSC and GFP+ drHSCs after saline or pIC. N=3 litters/condition, 2-3 pups/litter. Data represent frequency  $\pm$  SD.

**J)** Quantification of Ki67 expression at E15.5 in both Tom+ HSCs and GFP+ drHSCs following pIC or saline in mice described in Fig. 1L. \* $p \leq 0.05$ ; \*\*\* $p \leq 0.001$ . Bars represent average  $\pm$  SD.

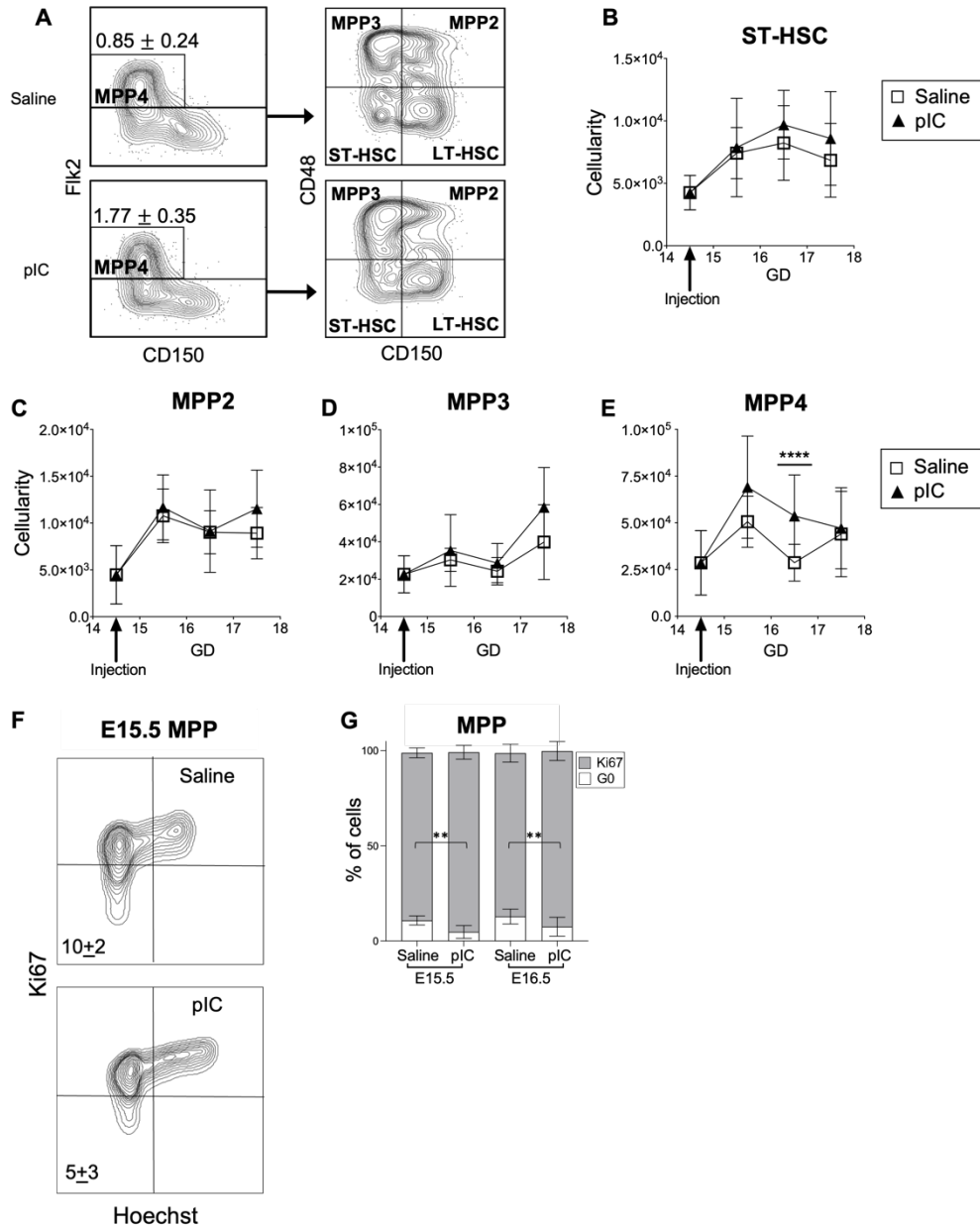


**Figure 2. Lymphoid-biased fetal progenitors expand in response to prenatal inflammation induced by MIA.**

A) Representative FACS plots of the HSPC compartment (Live, Lin<sup>-</sup>, CD45<sup>+</sup>, cKit<sup>+</sup>, Sca1<sup>+</sup>) at E15.5. Numbers indicate average frequency + SD of MPP4s in MIA and saline conditions. Data represent at least 3-6 pups/litter and 3 litters/condition.

B-E) Cellularity of short-term HSCs (ST-HSC) (B), MPP2s (C), MPP3s (D), and MPP4s (E) across gestation days (GD) 15-17 following MIA or saline. Data represent average + SEM for at least 3-6 pups/litter and 3 litters/condition. \*\*\*\*p ≤ 0.0001.



F) Representative flow cytometric plots of Ki67 expression and Hoechst staining in MPP (CD150- HSPC) populations after MIA or saline. Data represent average + SD. N ≥ 3 litters/condition, 3-6 pups/litter.

G) Quantification of Ki67 expression in MPPs (CD150- HSPC) from GD 15-17 after MIA or saline treatment. Data represents average + SD for at least 3-6 pups/litter for 3 litters/condition at each timepoint. \*\*p ≤ 0.01; \*\*\*\*p ≤ 0.0001.

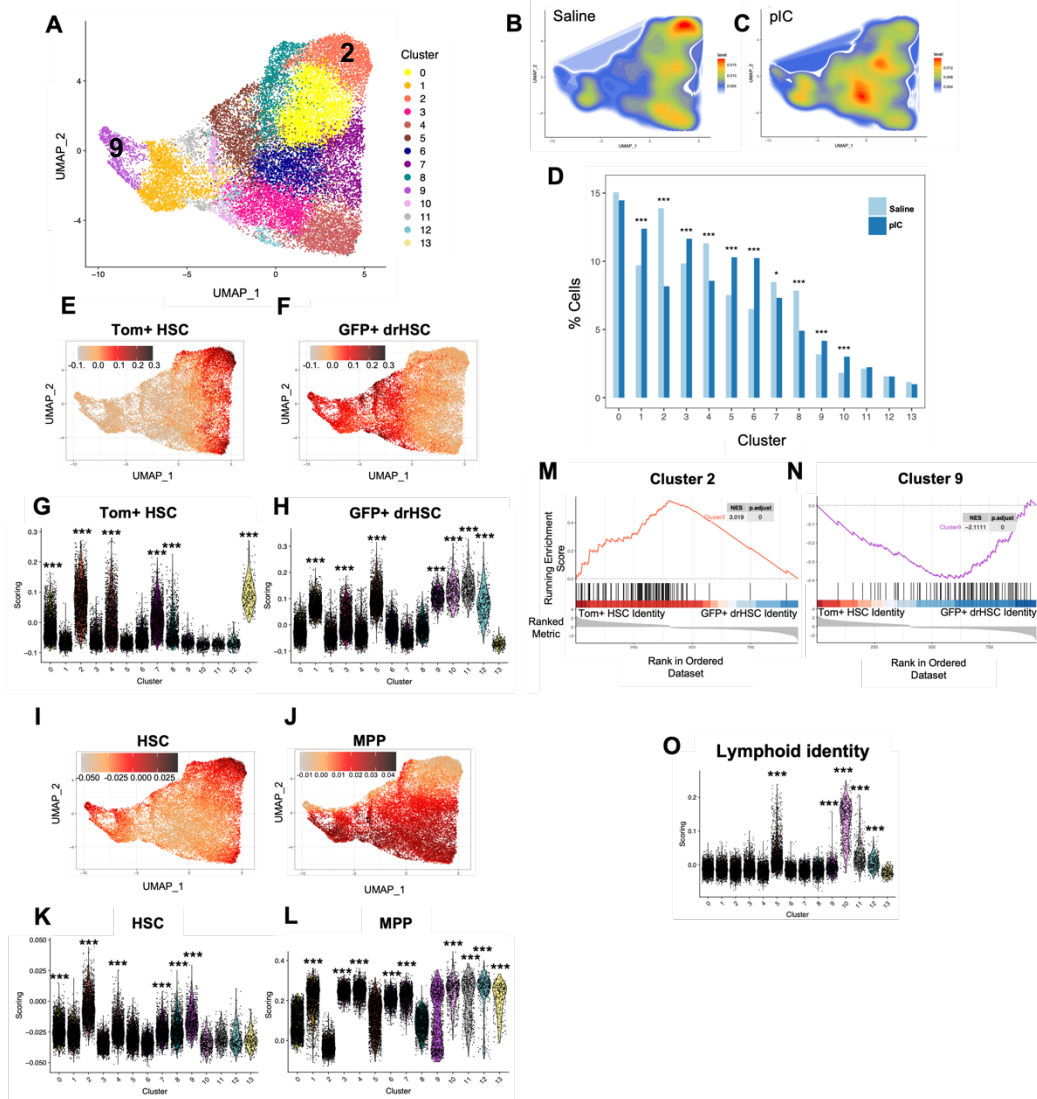


**Figure 3. Prenatal inflammation induces distinct molecular changes in fetal HSPCs.**

A) UMAP plot of single cell RNA-sequencing showing 14 identified clusters from sorted E15.5 FL Tom+ or GFP+ HSPCs (Lin-CD45+cKit+Sca1+) following pIC or saline treatment at E14.5.

B-C) Representative density plots of clusters shown in (A) under saline (B) or pIC (C) conditions.

D) Changes in percent of cells in each cluster, visualized in a barplot, in response to pIC or saline. Significance determined using Fisher tests. \* $p \leq 0.05$ ; \*\*\* $p \leq 0.001$ .

E, F) UMAP plots showing enrichment scoring for Tom+ HSC (E) or GFP+ drHSC (F) signatures across clusters using reference bulk data set (Beaudin et al., 2016). Color bar indicates the enrichment scoring assessed by the AddModuleScore function.

G, H) Violin plots showing enrichment scoring for Tom+ HSC (G) or GFP+ drHSC (H) signatures across clusters using a reference population data set (Beaudin et al., 2016). Wilcoxon signed rank test with respect to background. \*\*\* $p \leq 0.001$ .

I, J) UMAP plots showing enrichment scoring for HSC (I) or MPP (J) signatures across clusters using reference bulk data set (Cabezas-Wallscheid et al., 2014). Color bar indicates the enrichment scoring assessed by the AddModuleScore function.

K, L) Violin plots showing enrichment scoring for adult HSC (K) or MPP (L) signatures across clusters using a reference population data set (Cabezas-Wallscheid et al., 2014). Wilcoxon signed rank test with respect to background. \*\*\* $p \leq 0.001$ .

M, N) Gene set enrichment analysis (GSEA) of Cluster C2 (M) and C9 (N) markers identified by FindMarkers function in a ranked set of differentially expressed genes between Tom+ HSC and GFP+ drHSCs (Beaudin et al., 2016).

(O) Violin plots showing enrichment scoring for lymphoid gene signature across all clusters using a reference population data set (Cabezas-Wallscheid et al., 2014). Wilcoxon signed rank test with respect to background. \*\*\* $p \leq 0.001$ .

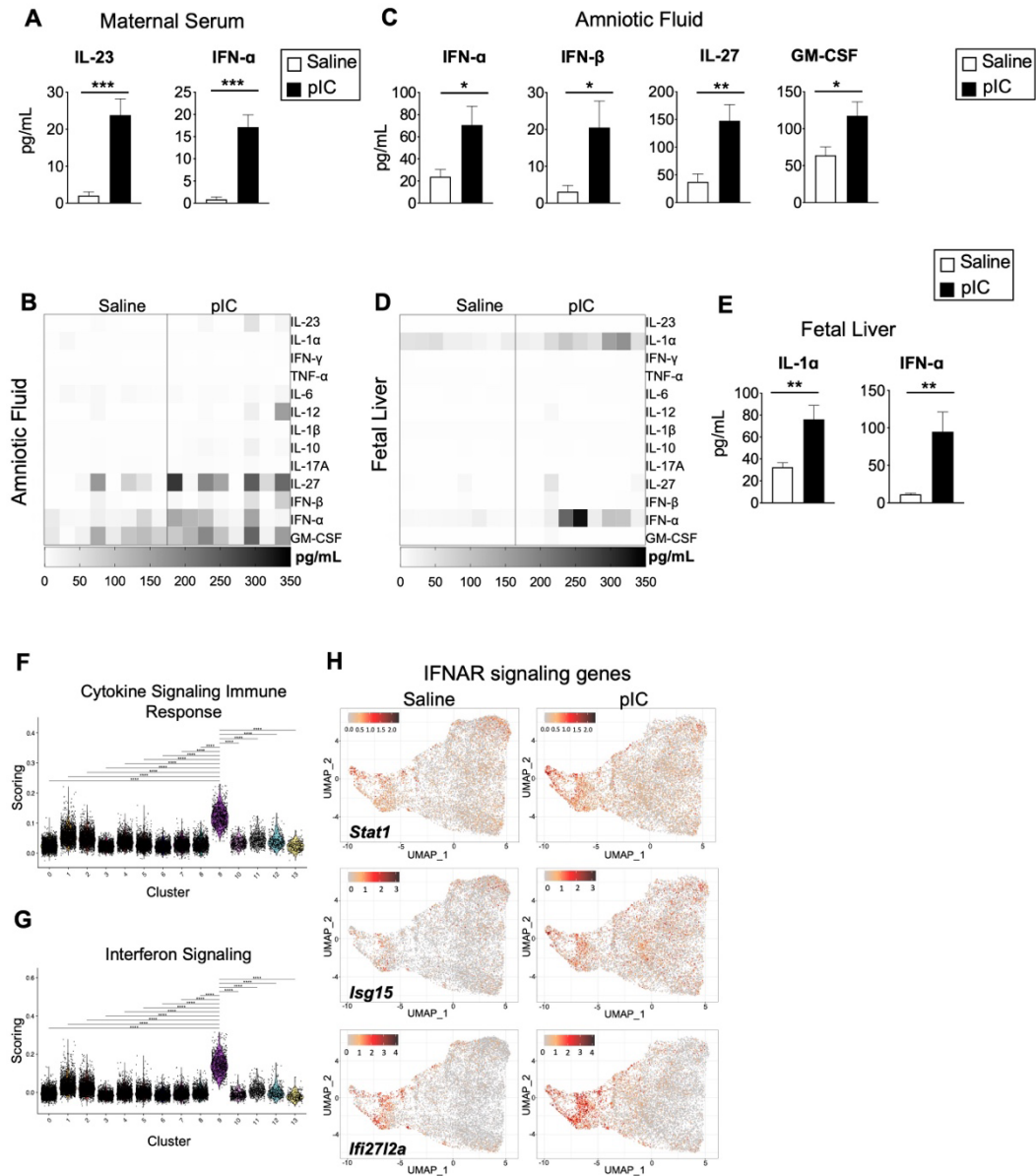


**Figure 4. MIA-induced inflammatory cytokines specifically activate fetal HSPCs**

A) Absolute quantification of cytokines in maternal serum at E15.5 as measured by LegendPlex assay. Data represents average + SD. \*\*\* $p \leq 0.001$ .

B) Heatmap displaying cytokines measured in amniotic fluid collected from E15.5 fetuses in litters following pIC or saline.

C) Absolute quantification of significantly upregulated cytokines in amniotic fluid at E15.5. Data represents average + SD. \* $p \leq 0.05$ ; \*\* $p \leq 0.01$ .

- D) Heatmap displaying cytokines in fetal liver supernatant at E15.5 following pIC or saline.
- E) Absolute quantification of significantly upregulated cytokines in fetal liver supernatant at E15.5. For all experiments, N= 3 litters/condition with 3 pups/litter. Data represents average + SD. \*\* $p \leq 0.01$ .
- F) Single cell RNA-sequencing clusters scored against database of pathways (reactome.org) integral to cytokine signaling in the immune system. Scoring indicates enrichment assessed by the AddModuleScore function within individual clusters. Wilcoxon signed rank test. \*\*\*\* $p < 0.0001$ .
- G) Single cell RNA-sequencing clusters scored against (reactome.org) database of pathways integral to interferon signaling in the immune system. Scoring indicates enrichment assessed by the AddModuleScore function within individual clusters. Wilcoxon signed rank test. \*\*\*\* $p < 0.0001$ .
- H) UMAP plots showing expression levels of genes associated with interferon alpha receptor (IFNAR) signaling following treatment with pIC or saline. Color bar indicates the relative expression level.

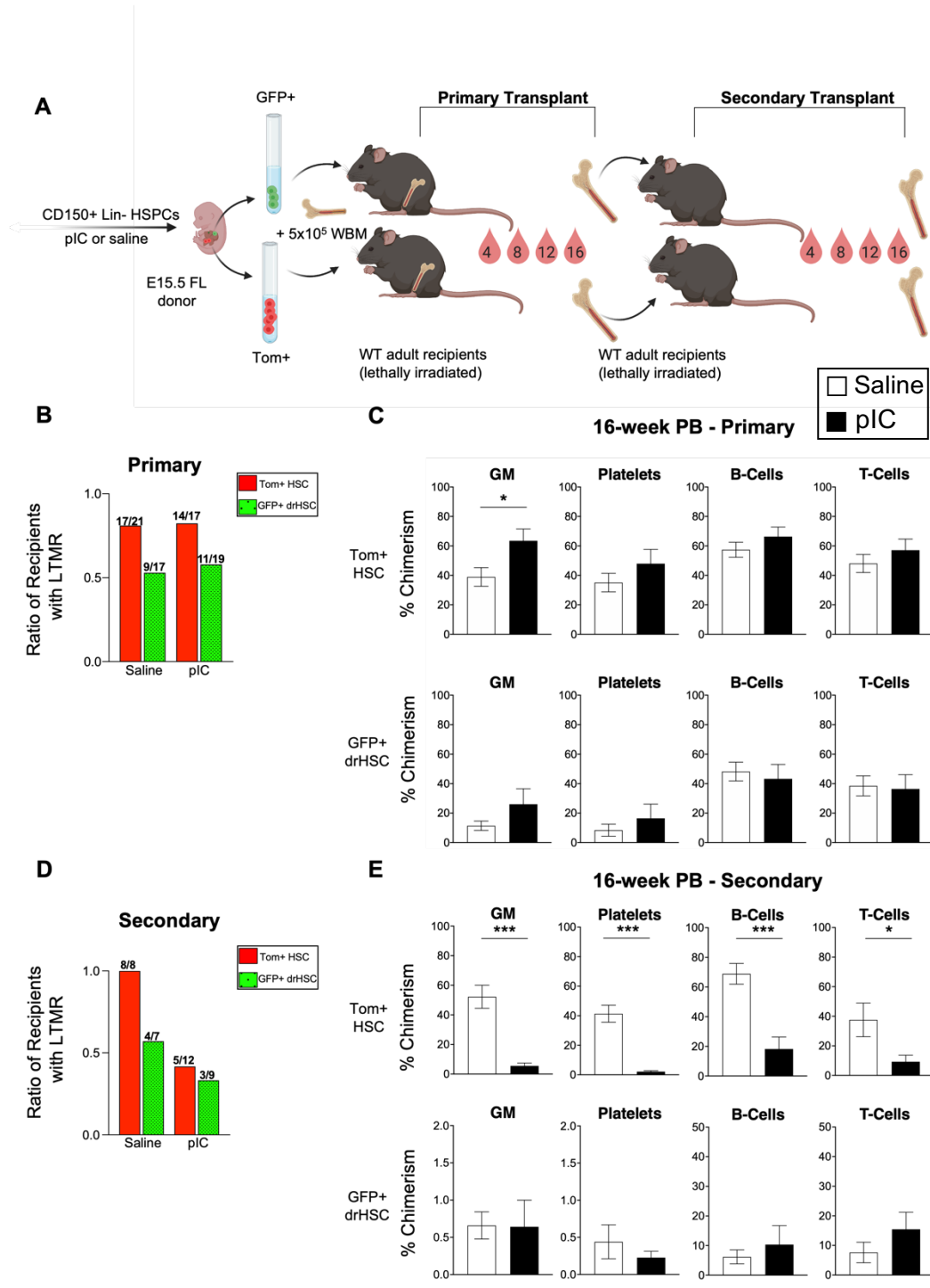


**Figure 5. Prenatal inflammation induced by MIA causes persistent changes to fetal hematopoietic stem cells upon transplantation.**

A) Schematic of transplantation approach. After MIA at E14.5, E15.5 Tom+ HSCs or GFP+ drHSCs were sorted and transplanted into lethally irradiated C57BL/6 hosts

(200 HSCs/host) along with  $5 \times 10^5$  whole bone marrow (WBM) cells. Peripheral blood (PB) was analyzed every 4 weeks until week 16. Image created with Biorender.com.

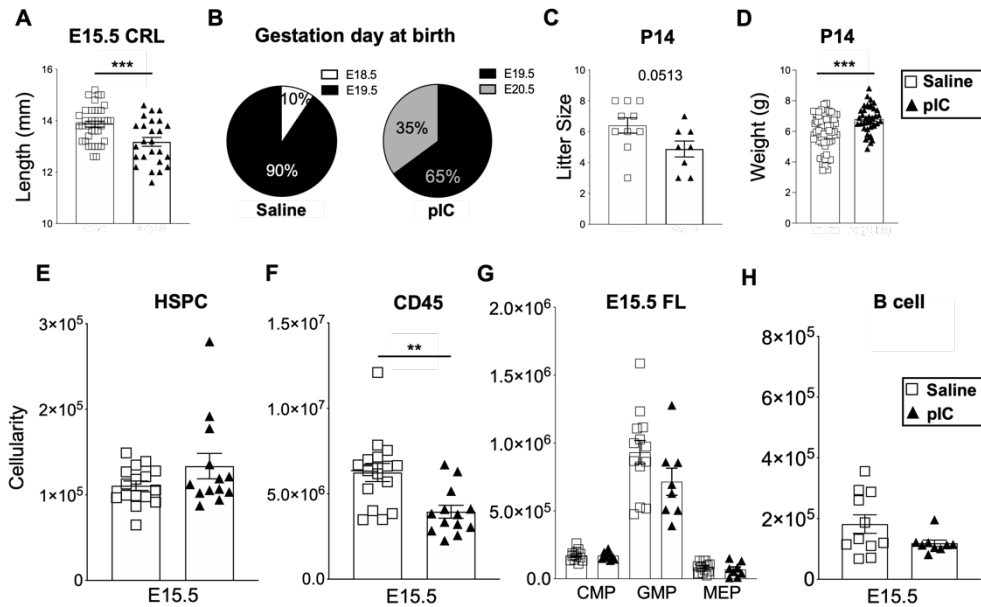
B) The ratio of recipients with long-term multilineage reconstitution (LTMR) from transplants of Tom+ HSCs (red bar) and GFP+ drHSCs (patterned green bar) from pIC and saline-treated litters. N as indicated by numbers above bars, 13-19 recipients/condition.

C) PB chimerism at 16-weeks of GM (granulocyte/macrophage), platelets (Plt), B-cells, and T-cells in recipients of Tom+ HSCs or GFP+ drHSCs, from same mice indicated in B. Data represent average + SEM. \* $p \leq 0.05$ .

D) The ratio of recipients with long-term multilineage reconstitution (LTMR) from secondary transplants of  $5 \times 10^6$  WBM cells from primary recipients of Tom+ HSCs (red bar) and GFP+ drHSCs (patterned green bar) from mice indicated in B. N as indicated by numbers above bars, 7-12 recipients/condition.

E) PB chimerism at 16-weeks of GM (granulocyte/macrophage), platelets (Plt), B-cells, and T-cells in secondary recipients described in D. Data represent average + SEM. \* $p \leq 0.05$ ; \*\*\* $p \leq 0.001$ .

## Supplemental Figures



**Supplemental Figure 1. The impact of prenatal inflammation induced by MIA on fetal and perinatal development**

**A)** Crown-rump length (CRL) of E15.5 fetuses following pIC or saline treatment. N=4-8 pups/litter representing at least 4 litters/condition.

**B)** Occurrence of gestation day at birth in pIC or saline treated litters. N=8-10 litters/condition.

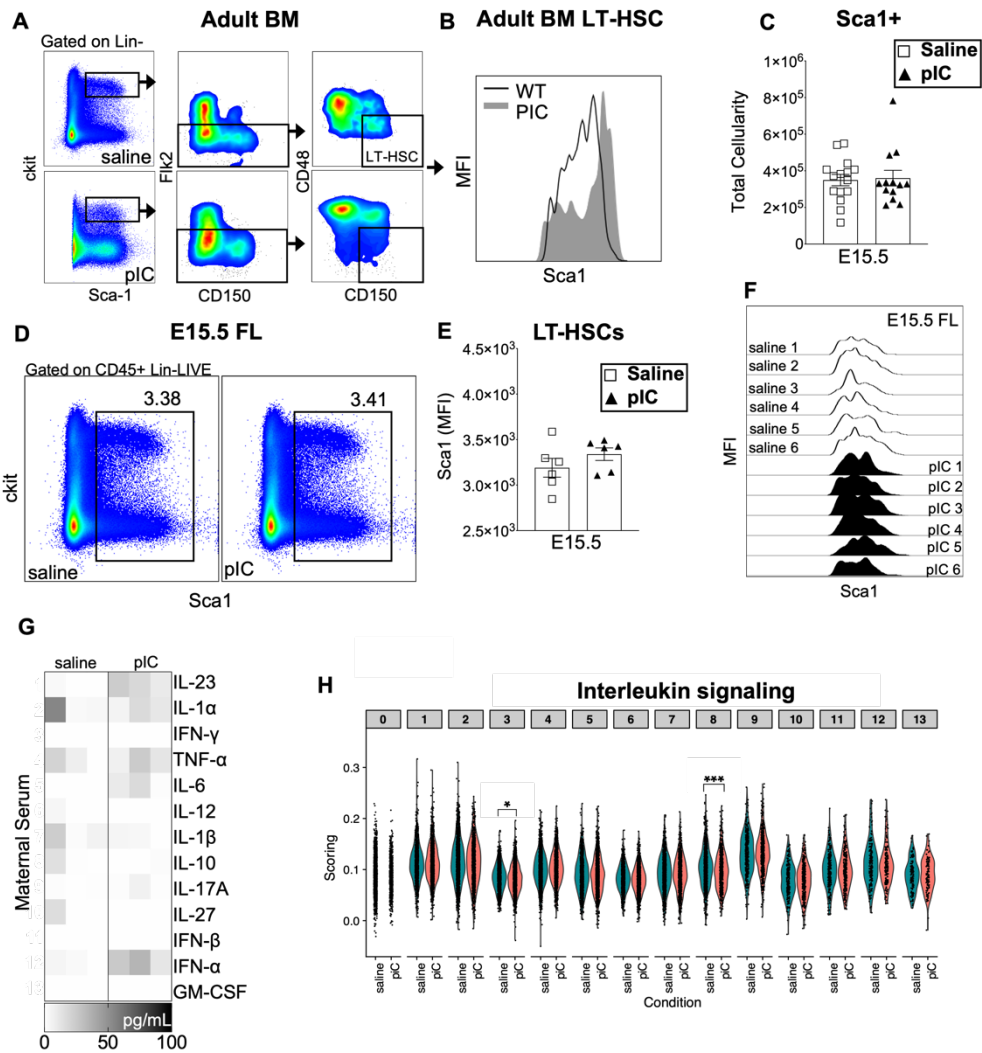
**C-D)** Litter size (**C**) and weight (**D**) of mice shown in **B** on postnatal day (P)14.

**E-F)** Absolute cellularity of HSPCs (**E**) and CD45+ cells (**F**) at E15.5 in the fetal liver (FL) from pIC or saline treated mice shown in **Fig. 1C-D**.

**G)** Absolute cellularity of myeloid progenitors (GMPs, FcrlII/II+CD34+; CMPs, FcrlII/II, CD34+; MEPs, FcrlII/II-CD34-) in the FL at E15.5 in the same mice described in **Fig. 1C-D**.

**H)** Absolute cellularity of B-cells (CD45+CD19+B220+) in the FL at E15.5 in the same mice described in **Fig. 1C-D**.

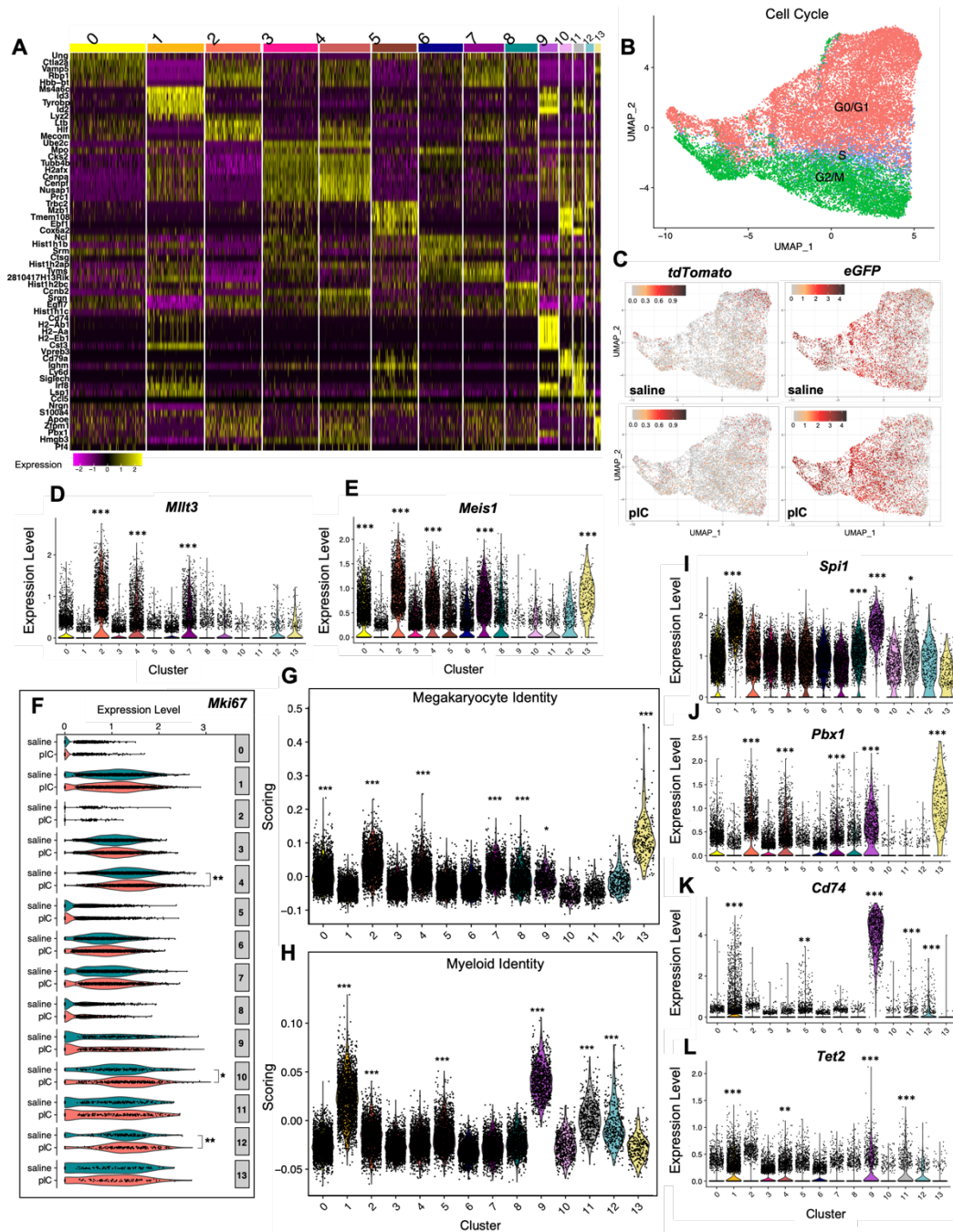




**Supplemental Figure 2. Impact of MIA on markers of inflammation in the fetal liver**

- A)** Representative FACS plots of Sca-1 expression in adult BM HSPCs one day after pIC or saline treatment.
- B)** Representative histogram of Sca-1 expression in adult LT-HSCs as shown in A.
- C)** Absolute quantification of FL Sca+1 cells in the same mice as described in **Fig. 1C-D**.
- D)** Representative FACS plots of Sca-1 expression in E15.5 FL CD45+ Lin- cells one day after pIC or saline treatment. Relative frequency of Sca-1+ cells is indicated.

- E)** Quantification of Sca1 MFI in FL LT-HSCs one day following treatment with pIC or saline.
- F)** Representative histograms of Sca-1 expression of LT-HSCs in FL one day following treatment with pIC or saline.
- G)** Heatmap displaying cytokines measured in maternal serum by LegendPlex multiplex assay at E15.5. N = 3 per condition.
- H)** Single cell RNA-sequencing clusters scored against database of pathways (reactome.org) integral to interleukin signaling in the immune system. Scoring indicates enrichment assessed by the AddModuleScore function within individual clusters in each condition. Wilcoxon signed rank test. \* $p < 0.05$ ; \*\*\* $p < 0.001$ ; ns, not significant.



**Supplemental Figure 3. Molecular impact of MIA on fetal HSPCs**

**A)** Heat map of top seven most differentially expressed genes per cluster following pIC or saline treatment. Legend represents normalized gene expression. Plot generated using DoHeatmap.

**B)** UMAP plot depicting cell-cycle states (G0/G1, S, G2/M) of every cell across all 14 clusters based on Cyclone scoring.

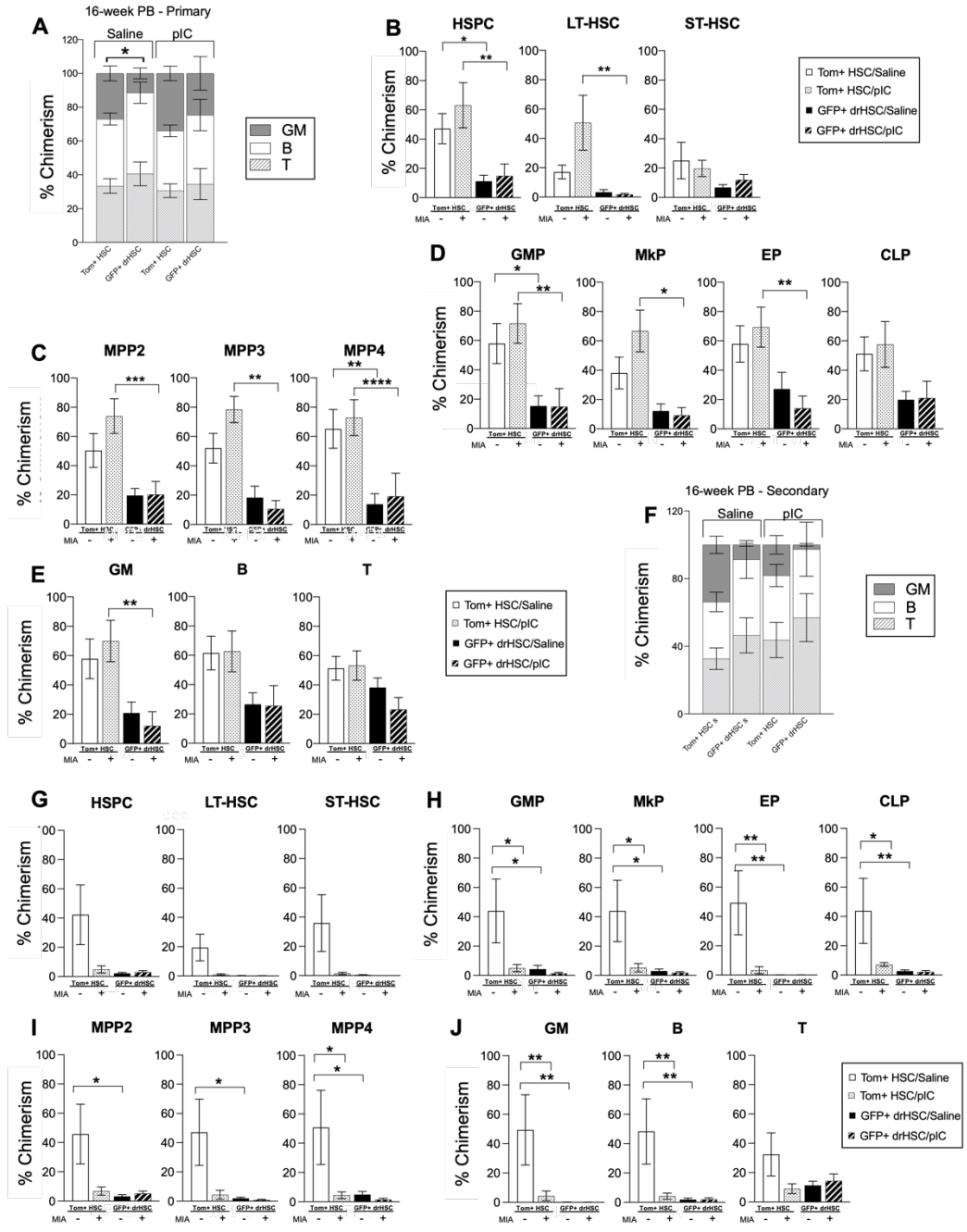
**C)** UMAP plots depicting enrichment of eGFP or tdTomato transcripts across all 14 clusters in response to pIC or saline. Color bar indicates the enrichment scoring.

**D-E)** Violin plot showing relative expression of marker genes associated with C2 across all clusters, including *Mitf3* (**D**) and *Meis1* (**E**). Wilcoxon signed rank test with respect to background. \*\*\* $p \leq 0.001$ .

**F)** Violin plot indicating gene expression of *Mki67* across all clusters, between pIC or saline conditions. Wilcoxon signed rank test. \* $p \leq 0.05$ ; \*\* $p \leq 0.01$ .

**G-H)** Violin plots showing scoring of megakaryocyte (**G**) and myeloid (**H**) identity across all clusters (Cabezas-Wallscheid et al., 2014). Wilcoxon signed rank test with respect to background. \* $p \leq 0.05$ ; \*\*\* $p \leq 0.001$ .

**I-L)** Violin plot showing relative expression of marker genes associated with C9 across all clusters including *Spi1* (**I**), *Pbx1* (**J**), *Cd74* (**K**) and *Tet2* (**L**). Wilcoxon signed rank test with respect to background. \* $p \leq 0.05$ ; \*\* $p \leq 0.01$ ; \*\*\* $p \leq 0.001$ .



**Supplemental Figure 4. Impact of MIA on fetal HSC function through transplantation**

**A)** Frequency of GM, B-cells, and T-cells within the reconstituted PB of recipients shown in **Fig. 5B-C**.

**B-E)** 18-week bone marrow (BM) chimerism in recipients of Tom+ HSCs or GFP+ drHSCs following saline or pIC as described in **Fig. 5B-C**. Chimerism in HSPCs,

LT-HSCs, and ST-HSCs **(B)**; MPP2, MPP3, and MPP4 **(C)**; granulocyte/macrophage progenitors (GMP), megakaryocyte progenitors (MkP), erythrocyte progenitors (EPs) and common lymphoid progenitors (CLP) **(D)**; and granulocytes/macrophages (GM; CD11b+, Gr1+), B-cells (CD19+) and T-cells (CD3+) **(E)**. Data represents average  $\pm$  SEM. \* $p \leq 0.05$ ; \*\* $p \leq 0.01$ ; \*\*\* $p \leq 0.001$ ; \*\*\*\* $p \leq 0.0001$ .

**F)** Frequency of GM, B-cells, and T-cells within the reconstituted PB of secondary recipients shown in **Fig. 5D-E**.

**G-J)** 18-week bone marrow (BM) chimerism in secondary recipients of WBM from primary transplants of Tom+ HSCs or GFP+ drHSCs following saline or pIC described in **Fig. 5D-E**. Chimerism in HSPCs, LT-HSCs, and ST-HSCs **(G)**; MPP2, MPP3, and MPP4

**(H)** granulocyte/macrophage progenitors (GMP), megakaryocyte progenitors (MkP), erythrocyte progenitors (EPs) and common lymphoid progenitors (CLP) **(I)**; and granulocytes/macrophages (GM; CD11b+, Gr1+), B-cells (CD19+) and T-cells (CD3+) **(J)**. Data represents average  $\pm$  SEM. \* $p \leq 0.05$ ; \*\* $p \leq 0.01$ ; \*\*\* $p \leq 0.001$ ; \*\*\*\* $p \leq 0.0001$ .

## Chapter 3. IFN $\gamma$ mediates the response of fetal HSCs to maternal infection with *Toxoplasma*

### Abstract

Infection in the adult organism drives cytokine-mediated inflammation that directly influences hematopoietic stem cell (HSC) function and differentiation within the bone marrow, but much less is known about the fetal hematopoietic response to maternal infection during pregnancy. Here, we investigated the fetal hematopoietic response to maternal *Toxoplasma gondii* (*T. gondii*) infection. *T. gondii* is an intracellular parasite that elicits Type II IFN $\gamma$ -mediated maternal immunity to prevent vertical transmission and promote parasite clearance. The production of excessive IFN $\gamma$  during congenital toxoplasmosis has dire consequences for the developing fetus, such as reduced birth weights and premature abortion, but the effects on developing hematopoietic cells and the signals that mediate these interactions have not been investigated. Our investigation reveals that the fetal inflammatory repertoire is distinct from the maternal response and is directly influenced by parasite virulence. We show that maternal IFN $\gamma$  crosses the fetal-maternal interface and is perceived directly by fetal HSCs, and the response of fetal HSCs is dependent on the fetal IFN $\gamma$  receptor. Functionally, the heterogeneous fetal HSC pool responds to aberrant inflammation with virulence-dependent changes in proliferation, long-term multi-lineage reconstitution, and self-renewal potential. However, in direct contrast to the adult hematopoietic response to infection, exposure to inflammation *in utero* did not diminish fetal HSC function in response to mild infection. By directly comparing the effects of maternal IFN $\gamma$  injection with maternal *T. gondii* infection of varying virulence, our observations delineate both a direct effect of IFN $\gamma$  on fetal HSCs and illuminate the independent role of additional inflammatory cytokines in driving the expansion of downstream hematopoietic progenitors.

### 3.1 Introduction

Congenital infection can have dire outcomes for fetal health and development. Several pathogens are implicated in vertical transmission or infection of the fetus from the maternal host. These so called “TORCH” pathogens include *Toxoplasma gondii*, “Other” (syphilis, varicella-zoster, parvovirus B19) (Stegmann and Carey 2002), Rubella virus, Cytomegalovirus, and Herpes simplex virus (Megli and Coyne 2021), and have recently been extended to include Zika virus (Kovacs and Maternal 2022). Even in the absence of vertical transmission, prenatal inflammation during infection can cause systemic changes to fetal immunity, including cytokine production and lymphocyte polarization (Adams Waldorf, Gravett et al. 2011). These changes to fetal immunity translate into alterations in neonatal functional immune outcomes, including response to vaccine and susceptibility to infection. Several proposed mechanisms may underlie this phenomenon, including the transplacental transport of maternal antibody-antigen complexes that directly prime fetal immune cells, or the active/passive transplacental transport of maternal inflammatory mediators or metabolites that directly stimulate an immune response in the fetus (Apostol, Jensen et al. 2020). However, very little is known about how these signals are “seen” and “translated” by the fetus.

Accumulating evidence from studies on the effects of inflammation and infection on the adult hematopoietic system indicate that inflammation modulates hematopoietic output by directly influencing hematopoietic stem cell (HSC) function (Essers, Offner et al. 2009, Baldrige, King et al. 2010, Matatall, Shen et al. 2014, Haas, Hansson et al. 2015, Matatall, Jeong et al. 2016). Inflammation can directly activate HSCs residing in the bone marrow (BM) due to their capacity to respond to inflammatory stimuli, either from circulation (Baldrige, King et al. 2011) or from the BM niche (Mitroulis, Kalafati et al. 2020). HSCs have the capacity to respond directly to a variety



of inflammatory cytokines including TNF- $\alpha$  (Yamashita and Passegué 2019), IL1- $\beta$  (Pietras, Mirantes-Barbeito et al. 2016), IL-27 (Furusawa, Mizoguchi et al. 2016), and interferons (Essers, Offner et al. 2009, Baldrige, King et al. 2010, Matatall, Shen et al. 2014, Haas, Hansson et al. 2015). In addition to direct “sensing” of cytokines, adult HSCs also respond directly to signals from bacterial (Matatall, Jeong et al. 2016) and viral (Hirche, Frenz et al. 2017) infections. Across a wide variety of inflammatory stimuli, BM HSCs stereotypically respond by restricting lymphoid cell production in favor of myeloid expansion, mediated by activation of myeloid-biased HSCs and expansion of myeloid-primed progenitors (Haas, Hansson et al. 2015, Pietras, Reynaud et al. 2015, Pietras, Mirantes-Barbeito et al. 2016). Inflammation also causes adult HSCs to rapidly exit quiescence, which has negative consequences for their ability to self-renew and persist following transplantation (Essers, Offner et al. 2009, Baldrige, King et al. 2010)

There is very little information about the impact of prenatal inflammation on developmental hematopoiesis during early life. Proinflammatory cytokine signaling is required for normal pregnancy and fetal development, but is also detrimental to fetal health during maternal infection (Yockey and Iwasaki 2018). In early development, “sterile” inflammatory cytokine signaling is necessary for proper HSC specification in the ventral aortic endothelium (Espin-Palazon, Weijts et al. 2018). Importantly, HSC profiling from the AGM (aorta/gonad/mesonephros) region at mid-gestation indicates that both Type I and II interferon signaling regulate HSC specification (Li, Esain et al. 2014, Sawamiphak, Kontarakis et al. 2014), as the lack of signaling contributes to fewer hematopoietic stem and progenitor cells (HSPCs) overall. Emerging evidence suggests that fetal HSPCs, including HSCs, may also be amenable to inflammatory signals perceived from maternal sources (Apostol, Jensen et al. 2020). However,

in comparison to the direct exposure of HSCs to inflammation within the BM, the physical barrier imposed by the maternal-fetal interface complicates characterizing the response of fetal HSCs to prenatal inflammation. Using a Flk2-mediated fate mapping model referred to as the “FlkSwitch model” (Boyer, Schroeder et al. 2011, Beaudin and Forsberg 2016), in which Flk2-Cre drives an irreversible reporter switch from Tomato to GFP expression, we demonstrated that Type I interferons activate transient, lymphoid-biased hematopoietic progenitors, driving a lymphoid-biased response during fetal hematopoiesis (Apostol, López et al. 2022). Therefore, we postulate that fetal hematopoietic progenitors could be responsive to infection and inflammation during gestation (Apostol, Jensen et al. 2020).

To gain further insight into the mechanism by which prenatal infection and inflammation affects fetal HSC development, we utilized a novel model of maternal infection using *Toxoplasma gondii* (*T. gondii*). As a vertically-transmitted pathogen (Megli and Coyne 2021), *T. gondii* is a ubiquitous (Bigna, Tochie et al. 2020) intracellular parasite that elicits a Type II IFN $\gamma$ -mediated maternal immunity to simultaneously promote parasite clearance and prevent vertical transmission; however, the production of excessive IFN $\gamma$  from *T. gondii* infection can also have dire consequences for the developing fetus, such as stillbirth and spontaneous abortion (Abou-Bacar, Pfaff et al. 2004, Shiono, Mun et al. 2007, Georgios, Nikos et al. 2009, Senegas, Villard et al. 2009). We performed experiments using the FlkSwitch model which identifies two functionally-distinct fetal HSC populations: a lymphoid-biased, developmentally restricted GFP $^+$  HSC (drHSC) marked by Flk2 expression that specifically generates innate-like B1-B and  $\gamma\delta$  T-cells, and a “canonical” Tom $^+$  HSC that persists into the adult bone marrow (Beaudin, Boyer et al. 2016). Additionally, to investigate how IFN $\gamma$  directly mediates the fetal hematopoietic response within the

complex framework of infection, we compared the effects of congenital *T. gondii* infection of varying degrees of virulence to the effects of a single cytokine injection of IFN $\gamma$ . We also utilized both IFN $\gamma$  receptor and IFN $\gamma$  cytokine knockout crosses to dissect the specific responses of fetal hematopoietic cells to IFN $\gamma$ -mediated inflammation. Our results demonstrate for the first time in both an infection and Type II interferon model, that fetal HSCs are responsive to maternally-derived cytokines, and that maternal cytokines drive an independent inflammatory response within the fetus. This study presents a novel and multifaceted approach to study the intricacies of fetal hematopoiesis in response to maternal inflammation and infection.

## **3.2 MATERIALS AND METHODS**

### **3.2.1 Mouse models and husbandry**

8-12-week-old female C57BL/6 (RRID: IMSR\_JAX:000664) were mated to male Flkswitch mice (Boyer et al., 2011, 2012; Epelman et al., 2014; Hashimoto et al., 2013, Beaudin, et al., 2016). At gestation day 14.5, pregnant dams were injected with 20 ug recombinant IFN $\gamma$ ., IFN $\gamma$  knock out mice (JAX 002287) were used to assess IFN $\gamma$  transfer across the fetal maternal interface. To investigate the fetal HSC response via the IFN $\gamma$  receptor, IFN $\gamma$  receptor knock out (IFN $\gamma$ RKO) mice (JAX 003288) were bred with wildtype C57BL/6J (WT) mice to generate mice with one copy of IFN $\gamma$ R (+/- mice). Pregnant dams were euthanized, and fetuses were dissected from the uterine horn. Fetal liver GFP+ (Flkswitch) expression was confirmed by microscopy.

### **3.2.2 Parasite strains and peritoneal injections**

*Toxoplasma gondii* (Table 3-1) strains were cultured and passaged as described in Kongsomboonvech, et al., 2020 (Kongsomboonvech, Rodriguez et al. 2020), and administered into pregnant dams via intraperitoneal injection of  $2 \times 10^4$  tachyzoites in a volume of 100  $\mu$ L in 1x PBS.

All other methods for this chapter are shown in **Chapter 2**

List of antibodies used are shown in **Table 2-1**

## 3.3 Results

### 3.3.1 *In utero* exposure to inflammation from *T. gondii* impacts fetal hematopoiesis

To determine the direct effects of congenital infection on fetal hematopoiesis, we employed a mouse model of maternal infection using the “TORCH” or congenitally transmitted pathogen (Megli and Coyne 2021) *Toxoplasma gondii*, a ubiquitous parasite that elicits a well-characterized IFN $\gamma$ -mediated immune response during pregnancy (Shiono, Mun et al. 2007, Senegas, Villard et al. 2009). At embryonic day (E)10.5, we injected pregnant dams with  $2 \times 10^4$  tachyzoites (**Fig. 1A**) of either the Pru or RH strains (Saeij, Boyle et al. 2005, Robbins, Zeldovich et al. 2012) of *T. gondii*. While the Pru strain is of “intermediate” virulence with a LD<sub>50</sub> of  $2 \times 10^3$  parasites, RH is considered highly virulent with an LD<sub>100</sub> of one parasite. This dichotomy in virulence is evident in fetal size at E16.5, as increased inflammation is correlated with lowered crown-rump length (**Fig. 1B, SFig. 1C**) and increased fetal resorption (**SFig. 1F**).

Using our previously characterized FlkSwitch lineage tracing model, we have recently shown that heterogenous fetal HSCs show distinct responses to prenatal inflammation induced by maternal immune activation (MIA) via poly(I:C) (**Chapter 2**). Specifically, lymphoid-biased GFP<sup>+</sup> developmentally restricted HSCs, or drHSCs, exhibit increased responsiveness to Type I interferons that translates into specific activation and downstream expansion of lymphoid-biased progenitors in response to prenatal inflammation.

In order to investigate how specific populations within the fetal liver (FL) HSPC compartment respond to maternal *T. gondii* infection, we used previously described (Yilmaz, Kiel et al. 2006) surface markers to demarcate long-term (LT-) and short-term (ST-) HSCs along with multipotent progenitor (MPP) 2, 3, and 4 (**SFig. 1A-B**). Congenital toxoplasmosis significantly affected fetal HSPCs at E16.5. While total number of FL cells remained consistent between saline and Pru infections (**SFig. 1D**), there was a significant reduction in total FL cellularity after maternal infection with RH (**SFig. 1D**). Despite a virulence-dependent reduction in total CD45<sup>+</sup> cells (**SFig. 1E**) in fetuses following congenital infection, the frequency (**Fig. 1C-E**) and total number (**Fig. 1F**) of HSPCs remained constant in the Pru condition relative to saline controls but increased significantly in the RH condition, indicating specific maintenance (Pru) or expansion (RH) of fetal HSPCs in response to congenital infection. Exposure to Pru infection did not affect frequency of LT-HSCs, ST-HSCs, or MPP2, -3, and -4 compared to controls (**Fig. 1D**), whereas frequency of all RH-exposed HSPC subsets was increased (**Fig. 1E**). Meanwhile, total cellularity of LT-HSCs (**Fig. 1G**), ST-HSCs (**Fig. 1H**), Tom<sup>+</sup> HSCs (**Fig. 1I**), GFP<sup>+</sup> drHSCs (**Fig. 1J**), and MPP2s (**Fig. 1K**) decreased in a virulence-dependent manner. Cellularity of MPP3 were comparable to controls for both infections (**Fig. 1L**). Surprisingly, MPP4 cellularity increased

significantly in the RH condition (**Fig. 1M**), driving the relative increase in HSPC cellularity (**Fig. 1F**). As HSPC numbers were maintained despite an overall decrease in cellularity, we next examined how congenital infection impacted HSPC proliferation. A virulence-dependent increase in Ki67 expression in both GFP<sup>+</sup> drHSCs (**Fig. 1N**) and Tom<sup>+</sup> HSCs (**Fig. 1O**) indicated exit from quiescence due to infection. MPP proliferation as determined by Ki67 expression increased significantly only in the RH condition (**Fig. 1P**), supporting observations of an expanded MPP compartment (**Fig. 1E, K-M**). Thus, severity of maternal infection appeared to drive immediate virulence-dependent changes to proliferation and differentiation of FL HSPCs.

### **3.3.2 *In utero* exposure to inflammation from *T. gondii* modulates fetal HSC function**

As fetal HSPCs responded rapidly to infection by exiting quiescence, we directly investigated the impact of congenital infection on HSC self-renewal and function by performing transplantation assays and investigating long-term multi-lineage reconstitution (LTMR). We isolated and sorted Tom<sup>+</sup> HSCs or GFP<sup>+</sup> drHSCs from E15.5 FL following congenital infection and competitively transplanted them with 5x10<sup>5</sup> adult whole bone marrow (WBM) cells into lethally irradiated adult recipients (**Fig. 2A**). Recipient mice were monitored every 4 weeks for 16 weeks post-transplantation to assess mature blood lineage reconstitution in both primary and secondary transplants.

Congenital toxoplasmosis influenced the long-term function of both Tom<sup>+</sup> HSCs and GFP<sup>+</sup> drHSCs upon transplantation. While the ratio of Tom<sup>+</sup> recipients with sustained long-term multi-lineage reconstitution after primary transplantation remained equivalent across all conditions (**Fig. 2B**), there

was a reduction in the LTMR ratio among GFP<sup>+</sup> drHSCs in response to RH infection (**Fig. 2B**). Among reconstituted recipients of Tom<sup>+</sup> HSCs, congenital infection resulted in increased myeloid output: peripheral blood (PB) granulocyte-macrophage (GM) chimerism was higher in response to both Pru and RH infections (**Fig. 2C**), while platelet (Plt) chimerism was also increased in response to Pru infection (**Fig. 2D**). Congenital infection did not significantly affect GM or Plt chimerism in primary recipients of GFP<sup>+</sup> drHSCs in either condition (**Fig. 2G-H**). B- and T-cell chimerism in recipients of both Tom<sup>+</sup> HSCs (**Fig. 2E-F**) or GFP<sup>+</sup> drHSCs (**Fig. 2I-J**) was also unchanged in response to infection.

Increased BM chimerism across most HSPC subsets was evident in recipients of Pru-exposed Tom<sup>+</sup> HSCs, whereas HSPC chimerism in recipients of RH-exposed Tom<sup>+</sup> HSCs was comparable to controls (**SFig. 2A-F**). We observed myeloid bias in BM progenitors of Tom<sup>+</sup> HSC recipients following Pru exposure, as evidenced by increase chimerism of progenitors of granulocytes, macrophages, and megakaryocytes (**SFig. 2G-H**), but not erythrocytes (**SFig. 2I**). In contrast to Tom<sup>+</sup> HSC recipients, BM chimerism of GFP<sup>+</sup> drHSC remained comparable to controls in response to Pru exposure but was generally decreased but only significantly in MPP2s in the RH-exposed recipients across all BM progenitor populations (**SFig. 2A-M**) indicating early exhaustion in RH, but not Pru, recipients. All Tom<sup>+</sup> HSCs recipients retained robust LTMR upon secondary transplantation (**Fig. 2K**) that was equivalent across all subsets regardless of virulence (**Fig. 2L-O**). In contrast, GFP<sup>+</sup> drHSC LTMR was abolished with 0/8 GFP<sup>+</sup> drHSC recipients exhibiting LTMR in the RH condition (**Fig. 2K**), further attesting to an exhaustion of GFP<sup>+</sup> drHSCs following exposure to maternal RH infection. Surprisingly, chimerism among reconstituted recipients of Pru-exposed GFP<sup>+</sup> drHSCs was significantly higher than controls for both GM (**Fig. 2P**) and B-cell (**Fig. 2R**) lineages, with no differences in Plt (**Fig. 2Q**)

or T-cell lineages (**Fig. 2T**). Analysis of BM chimerism in secondary recipients confirmed that only GFP<sup>+</sup> drHSC recipients in the Pru condition exhibited any progenitor chimerism, whereas recipients of RH-exposed GFP<sup>+</sup> drHSCs had no detectable BM chimerism, consistent with the absence of LTMR. Tom<sup>+</sup> HSC recipients therefore maintained LTMR without loss of self-renewal potential in response to congenital toxoplasmosis infection, regardless of virulence, while GFP<sup>+</sup> drHSCs succumbed to exhaustion in a virulence-dependent manner evident by decreased LTMR in recipients (**SFig. 2 N-Z**).

### **3.3.3 *T. gondii* virulence from maternal infection modulates inflammation in the fetal environment.**

To decipher the mechanism underlying the effects of congenital infection on fetal hematopoiesis, we characterized inflammation across the maternal-fetal interface by collecting and analyzing samples of maternal serum, fetal amniotic fluid (AF), and FL for levels of inflammatory cytokines (**Fig. 3A**). Increases in maternal serum levels of IFN $\gamma$ , TNF $\alpha$ , and IL-6 (**Fig. 3B-D**), were observed following infection, with Pru eliciting a much greater IFN $\gamma$  and TNF $\alpha$  response compared to RH. In contrast, maternal serum levels of IL-1 $\alpha$  remained unchanged between infected and uninfected conditions and IL-6 increased in RH infection only (**Fig. 3E**). In the fetal AF, infection with either Pru or RH induced high levels of IFN $\gamma$  and IFN $\beta$  compared to saline controls (**Fig 3F, I**). Other upregulated cytokines in fetal amniotic fluid mimicked the virulence patterns of Pru and RH infections, including significant increases in IL-6 (**Fig. 3G**) and IL-1 $\alpha$  (**Fig. 3H**) in RH only. While there were measurable but not statistically significantly elevated levels of IFN $\gamma$  present in FL supernatant (**Fig. 3M**), we observed a significant virulence-dependent upregulation of IL-1 $\alpha$  in FL (**Fig. 3J**) and an equally



significantly increase in IL-1 $\beta$  for both *T. gondii* strains (**Fig 3K**). In contrast, IL-1 $\alpha$  was not increased in maternal serum (**Fig. 3D**), indicating that increased IL-1 $\alpha$  is unique to the fetal *T. gondii* response. While IFN $\gamma$  is a significant component of cytokine activity in the fetus, *T. gondii* infection upregulates several other cytokines into the fetal environment which may drive further changes to hematopoiesis.

### 3.3.4 *In utero* exposure to IFN $\gamma$ impacts fetal hematopoiesis

As congenital infection elicited a broad and diverse cytokine proinflammatory response in the fetus (**Figure 3**), we sought to disentangle the immediate fetal hematopoietic response to toxoplasmosis by focusing on the impact of a single cytokine, IFN $\gamma$ . At E15.5, single cell sequencing of fetal liver HSPCs revealed that clusters previously associated with the GFP<sup>+</sup> developmentally restricted hematopoietic stem cell (drHSC) (**Chapter 2**) expressed high levels of *Ifngr1* relative to other hematopoietic stem and progenitor cells (HSPCs), including Tom<sup>+</sup> HSCs (**SFig. 3A**). The maternal response to *T. gondii* infection is a robust IFN $\gamma$  response (**Fig. 3C**) and IFN $\gamma$  was also present in the fetus during maternal infection (**Fig. 3F**); we therefore surmised that fetal HSCs may be directly responsive to IFN $\gamma$ . To test the immediate response of fetal HSPCs to IFN $\gamma$ , we injected 20  $\mu$ g of IFN $\gamma$  into pregnant (E14.5) WT dams mated to FlkSwitch mice (**Fig. 4A**). A single injection of maternal IFN $\gamma$  did not have overt physical effects on fetal development, as crown-rump length was unaffected in E16.5 fetuses (**SFig. 3B**). One day following maternal injection with IFN $\gamma$  (E15.5), the overall frequency of CD45<sup>+</sup> cells was increased (**SFig. 3C**). As there were no overt changes to phenotypic HSPCs by frequency (**SFig. 3D-E**), we assessed changes to total cellularity of specific HSPC populations. Although E15.5 LT-HSCs were not significantly affected (**SFig. 3F**), GFP<sup>+</sup> drHSCs but not the Tom<sup>+</sup> HSCs were significantly increased (**Fig. 4B-C**),

concomitant with increased proliferation of the GFP+ drHSC only (**Fig. 4D-E**). Overall HSPC cellularity was also unaffected by IFN $\gamma$  exposure (**Fig. 4G**), consistent with no overall increase in proliferation of MPPs (**Fig. 4F**) and a decrease (**Fig. 4H**) or maintenance (**Fig. 4 I-K**) of cellularity in downstream populations 24 hours post IFN $\gamma$  administration. Two days following injection at E16.5, HSPC numbers increased significantly (**Fig. 4L**) due to increases in cellularity of MPP2, MPP3, and MPP4 (**Fig. 4N-P**). Cellularity of Tom+ HSC and GFP+ drHSCs was not significantly different between IFN $\gamma$  and saline conditions (**SFig. 3G-H**). However, both LT-HSC (**SFig. 3I**) and ST-HSCs (**Fig. 4M**) exhibited a sharp decrease in cellularity at E16.5, suggesting mobilization and differentiation of LT- and ST- HSCs at the top of the hierarchy in response to IFN $\gamma$ . As ST-HSCs are a metabolically active precursor to MPPs (Cabezas-Wallscheid, Klimmeck et al. 2014, Pietras, Reynaud et al. 2015), the observed decrease in ST-HSCs concomitant with increases in all MPP subsets suggests that these changes may be mediated at the HSC-level. Our observation of expansion and increased proliferation of E15.5 GFP+ drHSCs, and not Tom+ HSCs, that normalizes by E16.5 (**SFig. 3G-H**) is in agreement with GFP+ drHSCs being the initial “responders” to maternal IFN $\gamma$  injection that then drive a subsequent increase in MPPs one day later at E16.5.

### **3.3.5 *In utero* exposure to IFN $\gamma$ directs fetal hematopoietic stem cell differentiation and long-term multi-lineage reconstitution**

As an immediate HSC-mediated response to inflammation was present one day after maternal injection with IFN $\gamma$ , we sought to further examine the effects of IFN $\gamma$  on downstream HSC function. We isolated and transplanted 200 Tom+ HSCs or GFP+ drHSCs into lethally irradiated primary recipients along with  $5 \times 10^5$  WBM cells. We assessed PB output in primary and secondary recipients every four weeks for 16 weeks. Prenatal

administration of IFN $\gamma$  did not affect the ratio of recipients with long-term multi-lineage reconstitution for either Tom $^{+}$  HSCs or GFP $^{+}$  drHSCs in primary recipients (**Fig. 5A**), while secondary recipients had a lower ratio of recipients with with LTMR (**Fig. 5J**). IFN $\gamma$  exposure increased PB chimerism in primary recipients of both Tom $^{+}$  HSC and GFP $^{+}$  drHSC for GM, platelets, and B-cell lineages, but not T-cells (**Fig 5B-I**). Compared to saline-treated controls, primary recipients of IFN $\gamma$ -exposed GFP $^{+}$  drHSCs also exhibited significantly increased BM chimerism across all HSPC populations at 18 weeks (**SFig. 4A-F**). In contrast, primary recipients of Tom $^{+}$  HSCs only exhibited increased BM chimerism in LT-HSCs (**SFig. 4B**), MPP3s (**SFig. 4E**), GMPs (**SFig. 4G**), and MkPs (**SFig. 4H**), indicating myeloid bias at the progenitor level. Surprisingly, recipients of GFP $^{+}$  drHSC also showed increased chimerism in downstream BM myeloid progenitors, including MkPs (**SFig. 4H**) and GMs (**SFig. 4J**), reflecting the increase in myeloid cells observed in the PB (**Fig. 5F-g**). Chimerism of BM progenitors for lymphoid cells, including CLP (**SFig. 4K**) and B- and T-cell progenitors (**SFig. 4L-M**) were unaffected by IFN $\gamma$  exposure across all recipients.

In secondary recipients of Tom $^{+}$  HSCs, chimerism remained unchanged in PB for GM, platelets, and B-cells (**Figure 5K-M**), while T-cell chimerism increased (**Fig. 5N**). PB chimerism was also unchanged overall in secondary recipients of GFP $^{+}$  drHSCs (**Fig. 5O-R**). Analysis of BM cells in secondary recipients of Tom $^{+}$  HSCs revealed that compared to saline controls, chimerism was generally equivalent across all conditions (**SFig. 4N-W, Y**) except for an increase of in CLPs (**Fig. SFig. 4X**) and T-cells (**Fig. 5Z**), in tandem with increased T-cells in PB (**Fig. 5N**). In secondary BM recipients of GFP $^{+}$  HSCs, there was increased chimerism in ST-HSCs (**SFig. 4P**), MPP2s (**SFig. 4Q**), MPP3s (**SFig. 4R**). Under saline conditions, the disparity of chimerism between Tom $^{+}$  HSC and GFP $^{+}$  drHSC recipients in HSPCs was significant, with Tom $^{+}$  HSCs having higher chimerism than

GFP<sup>+</sup> drHSCs. Subsequently, this difference is lost in the IFN $\gamma$  condition, with HSPCs having no difference overall in between Tom<sup>+</sup> HSCs and GFP<sup>+</sup> drHSCs (**SFig. 4N**), except in the LT-HSC (**SFig. 4O**), GMPs, MkPs, Eps (**SFig. 4T-V**), and CLPs (**SFig. 4X**), due to an increase in Tom<sup>+</sup> HSC chimerism driving this difference. Thus, prenatal exposure to IFN $\gamma$  alone *increased* self-renewal capacity, output, and myeloid bias of both Tom<sup>+</sup> HSCs and transient GFP<sup>+</sup> drHSCs upon transplantation.

### **3.3.6 Fetal hematopoietic stem cells (HSCs) respond directly to maternal IFN $\gamma$ through IFN $\gamma$ receptor**

During prenatal inflammation, hematopoietic progenitors can be directly activated by maternal inflammatory mediators that cross the placenta or, alternatively, a separate inflammatory response could be initiated within the fetus that independently evokes changes within HSPCs. We first investigated whether maternal sources of IFN $\gamma$  crossed into the fetal environment. Pregnant IFN $\gamma$  knock out (IFN $\gamma$ <sup>-/-</sup>) dams were injected via intraperitoneal injection at E14.5 with 20  $\mu$ g recombinant IFN $\gamma$ . Cytokine analysis of both fetal AF and FL revealed the presence of IFN $\gamma$  in IFN $\gamma$ KO fetuses (**Fig. 6A**), demonstrating for the first time that maternal IFN $\gamma$  crossed the maternal-fetal barrier. LT-HSCs in FL express the IFN $\gamma$  receptor (IFN $\gamma$ R) (Chambers, Shaw et al. 2007, Baldrige, King et al. 2010) and can therefore directly sense IFN $\gamma$ . To investigate the fetal HSC response via the IFN $\gamma$  receptor, IFN $\gamma$ R <sup>+/</sup>- dams were time mated with IFN $\gamma$ R <sup>-</sup>/<sub>-</sub> males (**Fig. 6B**). At E14.5, pregnant dams were injected with 20  $\mu$ g of IFN $\gamma$  and fetal liver HSPCs were quantified at E15.5. Overall cellularity of both IFN $\gamma$ R <sup>+/</sup>- and IFN $\gamma$ R <sup>-</sup>/<sub>-</sub> FL HSPCs was on average lower under saline conditions (**SFig. 5A**) as compared to the Flkswitch model where all mice are IFN $\gamma$ R <sup>+/</sup>+, likely due the importance of basal IFN $\gamma$  signaling for early HSC specification (Espin-Palazon, Weijts et al. 2018). Surprisingly, prenatal IFN $\gamma$

exposure similarly expanded HSPCs overall in both +/- and -/- fetuses (**Fig. 6C**), despite the absence of the IFN $\gamma$ R in -/- fetuses. Interestingly, deletion of the IFN $\gamma$ R on the fetal side resulted in an accumulation of IFN $\gamma$  in AF, suggesting accumulation of cytokine due to lack of receptor signaling (**SFig. 5C, D**). When further examined across HSPC populations, deletion of the IFN $\gamma$ R resulted in abrogated expansion of both LT-HSCs (**Fig. 6D**) and ST-HSCs (**Fig. 6E**). However, IFN $\gamma$  treatment expanded MPP populations (**Fig. 6F-H**) even in -/- fetuses. These data suggest that while IFN $\gamma$  directly acts upon fetal HSCs, downstream activation, and expansion of other HSPC populations is dissociated from HSC activation and may be driven other cytokines produced from maternal IFN $\gamma$ R signaling.

To determine the dynamics of the fetal HSPC response independent of direct activation by IFN $\gamma$ , we performed the opposite cross, wherein IFN $\gamma$ R -/- dams were time mated with IFN $\gamma$ R +/- males (**Fig. 6I**). Deletion of the maternal IFN $\gamma$ R and thereby the maternal IFN $\gamma$ -signaling response eliminated the cellular response of of LT-HSCs and ST-HSCs in both +/- and -/- fetuses (**Fig. 6K 6L**). In contrast, in fetuses with an intact copy of receptor (+/-), MPPs continued to show a heightened response to maternal injection with IFN $\gamma$ , despite the inability of the dam to mount an IFN $\gamma$ -signaling response. Collectively, the data would suggest that IFN $\gamma$ -signaling is necessary in both fetal and maternal side to elicit an enhanced LT-HSC and ST-HSC response. Moreover, while MPPs are sensitive to IFN $\gamma$ -signaling, it can be bypassed by an IFN $\gamma$ R-induced maternally-derived mediator and implies that the immediate MPP response is distinct compared to fetal HSCs which require both direct IFN $\gamma$ -signaling and a maternal derived IFN $\gamma$ -induced factor. In IFN $\gamma$ R -/- dams, a single injection of IFN $\gamma$  produced increased levels of measurable IFN $\gamma$  cytokine in the serum (**SFig. 5B**). Coincidentally, IFN $\gamma$ R -/- fetuses had higher levels of IFN $\gamma$  in amniotic fluid and fetal liver supernatant in both saline (**SFig. 1C, E**) and IFN $\gamma$

conditions (**SFig. 5D, F**). Detection of IFN $\gamma$  on the fetal side in the absence of IFN $\gamma$ R at the maternal-fetal interface indicates significant passive transport of IFN $\gamma$  across the placenta and therefore independent of receptor-mediated transcytosis. These differences in cytokine levels may also explain the discrepancy in results from different maternal genotypes. The “buildup” of IFN $\gamma$  in the -/- mom compared to +/- could reflect the lack of receptor expression and receptor-mediated endocytosis of IFN $\gamma$  (Marchetti, Monier et al. 2006) within the responding cells, as IFN $\gamma$  has nowhere to bind. Together, these data provide direct evidence that IFN $\gamma$  crosses the placenta and initiates a multifaceted immune response within the fetus. The fetal hematopoietic response therefore coordinates signals across the maternal-fetal interface, and also reflects the dynamic and diverse responses of distinct HSPCs.

### **3.4 Discussion**

Our investigation reveals the multifaceted response of fetal hematopoietic stem and progenitor cells (HSPCs) to maternal infection with *Toxoplasma gondii*. *T. gondii* is a ubiquitous TORCH pathogen, with severe implications for fetal health and development. Congenital infections such as *T. gondii* drive alterations to fetal immunity and shape the postnatal immune response in offspring, but the cellular mechanisms underlying those changes are poorly understood. Here, we are the first to demonstrate that fetal HSPCs are directly affected by congenital infection, and that congenital infection affects the long-term function of fetal HSCs. Maternally-derived IFN $\gamma$  crosses the placenta and drives myeloid-biased output without affecting self-renewal upon transplantation. As observed in adult hematopoiesis, our results suggest that the response of fetal HSCs to infection could have direct implications for postnatal immunity.

*T. gondii* elicits a typical Type II IFN $\gamma$ -mediated host immune response to resolve infection and clear parasites (Sturge and Yarovinsky 2014). This well-characterized immune interplay, along with *T. gondii*'s role as a pregnancy-related infection makes *T. gondii* an ideal model of maternal infection during pregnancy. During gestation, this response has been demonstrated to limit vertical transmission at the expense of fetal growth and survival (Abou-Bacar, Pfaff et al. 2004). In our model, maternal *T. gondii* infection resulted in highly elevated levels of IFN $\gamma$  in maternal serum, although maternal IFN $\gamma$  levels were higher in the less virulent Pru strain as compared to the more virulent RH strain. Both *T. gondii* strains caused significant fetal growth restriction, but the RH strain induced a broader inflammatory response in the fetus, as indicated by high levels of IL-6 and IL-1 $\alpha$  in the amniotic fluid. We did not directly assess vertical transmission; however, given the degree of virulence, it would be expected that the RH strain would be vertically transmitted more frequently than Pru infections. Adoptive transfer experiments confirmed that HSPCs themselves were not directly infected, as transplantation of cells infected with even one RH parasite would have resulted in immediate death (Mordue, Monroy et al. 2001). In this context and given the degree of growth restriction and inflammation induced by congenital RH infection, it is not surprising that we observed more severe depletion of fetal HSPCs in response to congenital RH infection *in situ*.

In contrast to the effect of congenital infection on hematopoiesis *in situ*, adoptive transfer assays revealed that both moderate and severe maternal inflammation induced by either strain of *T. gondii* did not only not impinge upon HSC function but enhanced it. Despite increased proliferation *in situ* in response to congenital infection, Tom<sup>+</sup> HSCs demonstrated increased myeloid output upon primary transplant, and sustained output in a secondary transplant setting, even in response to a highly virulent infection.

This is akin to the response seen in adult HSCs to acute infection (Essers, Offner et al. 2009, Baldrige, King et al. 2010, Matatall, Shen et al. 2014, Haas, Hansson et al. 2015). Congenital infection had a virulence-dependent deleterious effect on function of the GFP+ drHSC. Whereas the less virulent Pru infection increased myeloid output resulting in a loss of lymphoid bias, and significantly increased GM and B-cell output upon secondary transplantation. RH infection impaired LTMR in primary transplantation and resulted in complete exhaustion in secondary transplantation. The disparate response of two fetal HSC populations may reflect the capacity of each to respond directly and differentially to inflammatory mediators induced by congenital infection. We have also previously described the Tom+ HSC as more “adult-like”, as it persists into adulthood and contributes to the adult HSC compartment (Beaudin, Boyer et al. 2016). The response of the Tom+ HSC is more consistent with an adult response, whereas the response of the GFP+ drHSC may be more typical of transient progenitors that may rapidly differentiate to support the immune response to infection.

Previous work has shown that the effects of an actual infection on adult hematopoiesis can differ greatly from the impact of a single cytokine. For example, BM hematopoiesis responds very differently to direct infection with cytomegalovirus and vesicular stomatitis virus, viruses that induce a typical Type-1 interferon response, as compared to direct injection with interferon-inducing reagents, such as poly(I:C) (Hirche, Frenz et al. 2017). Perhaps not surprisingly, despite induction of comparable IFN $\alpha$  levels, viral infections were found to evoke complex inflammatory responses that activated HSCs in a manner independent of IFNAR signaling. To resolve the extent to which the fetal hematopoietic response to congenital *T. gondii* infection was driven by IFN $\gamma$ , the primary cytokine mediating immune clearance in *T. gondii* infection (Suzuki, Orellana et al. 1988). We compared fetal hematopoiesis after prenatal exposure to both IFN $\gamma$  and infection with



two strains of *T. gondii* of increasing virulence. Direct injection of IFN $\gamma$  induced effects on fetal HSCs in vivo and upon transplantation that were comparable to those observed in response to the less virulent Pru infection. Hence, it is plausible that with a less virulent infection, maternally-derived IFN $\gamma$  may be the major driver of the HSC response, whereas with more virulent infections other cytokines, such as IL-6 and IL-1 $\alpha$ , may further impact HSC function (Mirantes, Passequé et al. 2014).

To begin to dissect the requirement for IFN $\gamma$  responsiveness across the maternal-fetal interface, we examined the effect of direct injection of IFN $\gamma$  in crosses of IFN $\gamma$ R  $-/-$  mice. We first confirmed that maternal IFN $\gamma$  can directly cross the placenta by demonstrating the presence of maternally-injected IFN $\gamma$  in fetal tissues in IFN $\gamma$   $-/-$  mice. We also demonstrated that while the fetal IFN $\gamma$ R is required for the HSC response, it is not required for the immediate responsiveness of more differentiated MPPs. These data imply that MPPs respond to distinct inflammatory cues compared to HSCs, perhaps responding directly to downstream cytokines induced by maternal IFN $\gamma$ R signaling, such as IL-6 (Biondillo, Konicek et al. 1994), which suggests a highly orchestrated hematopoietic response to inflammation. Interestingly, it appears that maternal IFN $\gamma$ R expression and maternal IFN $\gamma$ -mediated response regulate the fetal response, as maternal deletion impaired the fetal HSC response even in fetuses with an intact receptor (**SFig. 5A**) further suggesting that IFN $\gamma$ R-receptor signaling induces other inflammatory mediators that regulate fetal HSC function. What these IFN $\gamma$ -induced factors are have yet to be experimentally determined. Another interesting observation was that lack of IFN $\gamma$  receptor on either the fetal or maternal side caused accumulation of IFN $\gamma$  in fetal tissues, likely due to lack of uptake by the receptor (Marchetti, Monier et al. 2006) which could further enhance fetal HSC responses to IFN $\gamma$  in our system. These interactions illustrate the complex interface between the fetal and maternal response

that is mediated not only by the broad and diverse cytokine response of the mother, but also the discrete and independent cytokine response initiated by the fetus.

Our study is the first of its kind to explore the fetal hematopoietic response to congenital infection. By comparing the effects of a multifaceted infection to the effects of a single cytokine injection on fetal HSPCs, our work begins to narrow down the inflammatory mediators of the hematopoietic response to infection. We also leveraged genetic models to determine if maternal signals, such as IFN $\gamma$ , cross the fetal-maternal interface and interact with fetal hematopoietic cells to drive the hematopoietic response. Due to limitations of our model of congenital infection, we were unable to investigate the effects of congenital infection on postnatal hematopoiesis, instead using transplantation as a proxy of the long-term functional impact to HSCs. Still, we demonstrate the maternally-derived IFN $\gamma$  acts directly on fetal HSCs to shape their long-term hematopoietic output without affecting their self-renewal potential. Our data therefore provide a novel mechanism whereby congenital infection might shape postnatal immune responses in offspring by affecting the function and output of developing hematopoietic stem cells.

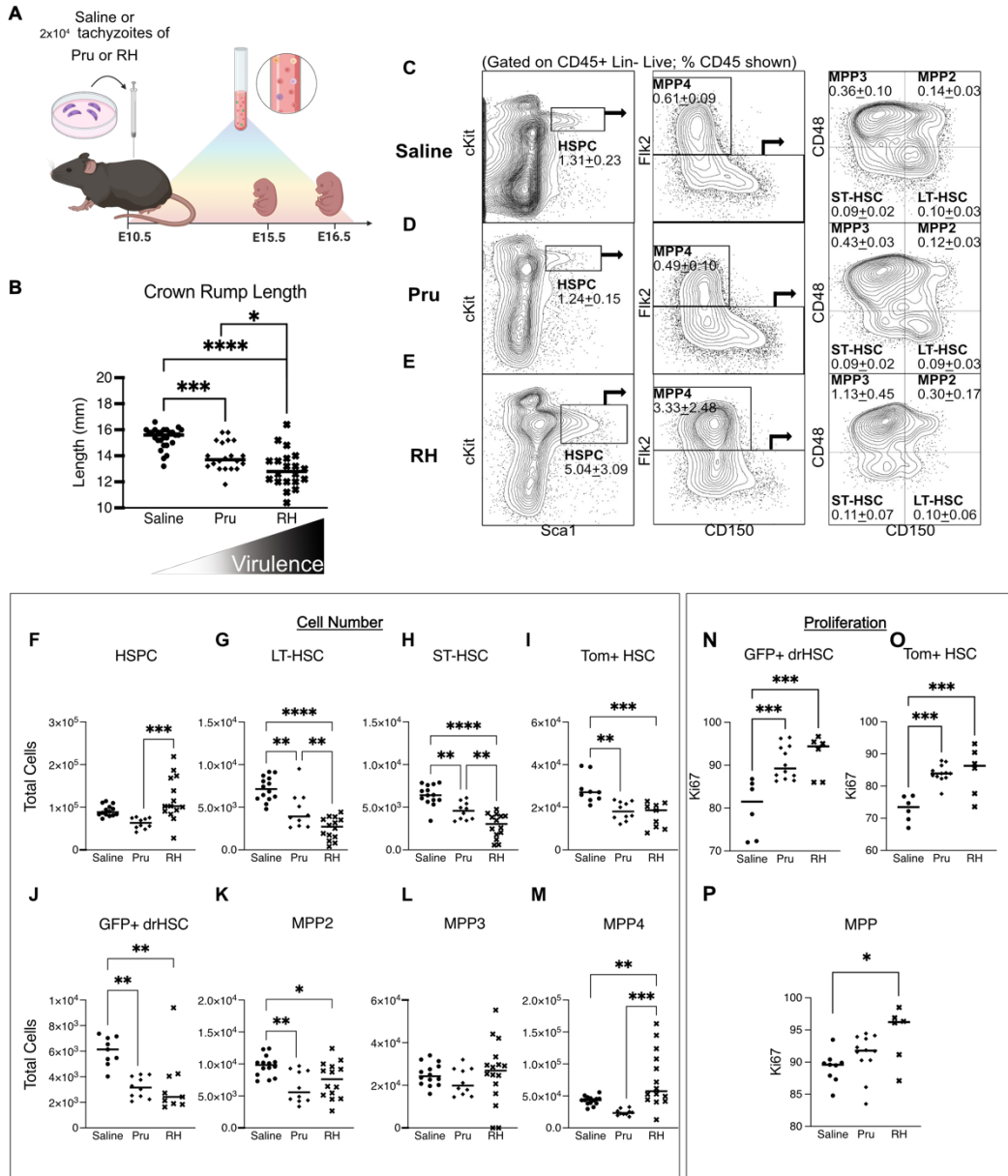
**Table 3-1** *Toxoplasma gondii* strains

<b>Condition</b>	<b>Virulence</b>	<b>Lethal dose (LD)</b>
<i>Pru Δhxgprt</i>	Type "II" Strain. Intermediate virulence	$LD_{50} = 10^2-10^4^*$
<i>RH Δhxgprt Δku80</i>	Type "I" Strain. High virulence.	$LD_{100} = <10^*$

\*(Saeij, Boyle et al. 2005)

### 3.5 Figures

**Figure 1: *In utero* exposure to inflammation from *Toxoplasma gondii* directs fetal hematopoiesis**



**A)** Schematic of model of maternal infection with *Toxoplasma gondii*. At E10.5, pregnant Flkswitch dams were injected with saline or  $2 \times 10^4$  tachyzoite parasites. Fetal outcomes were assessed at E15.5 and E16.5.

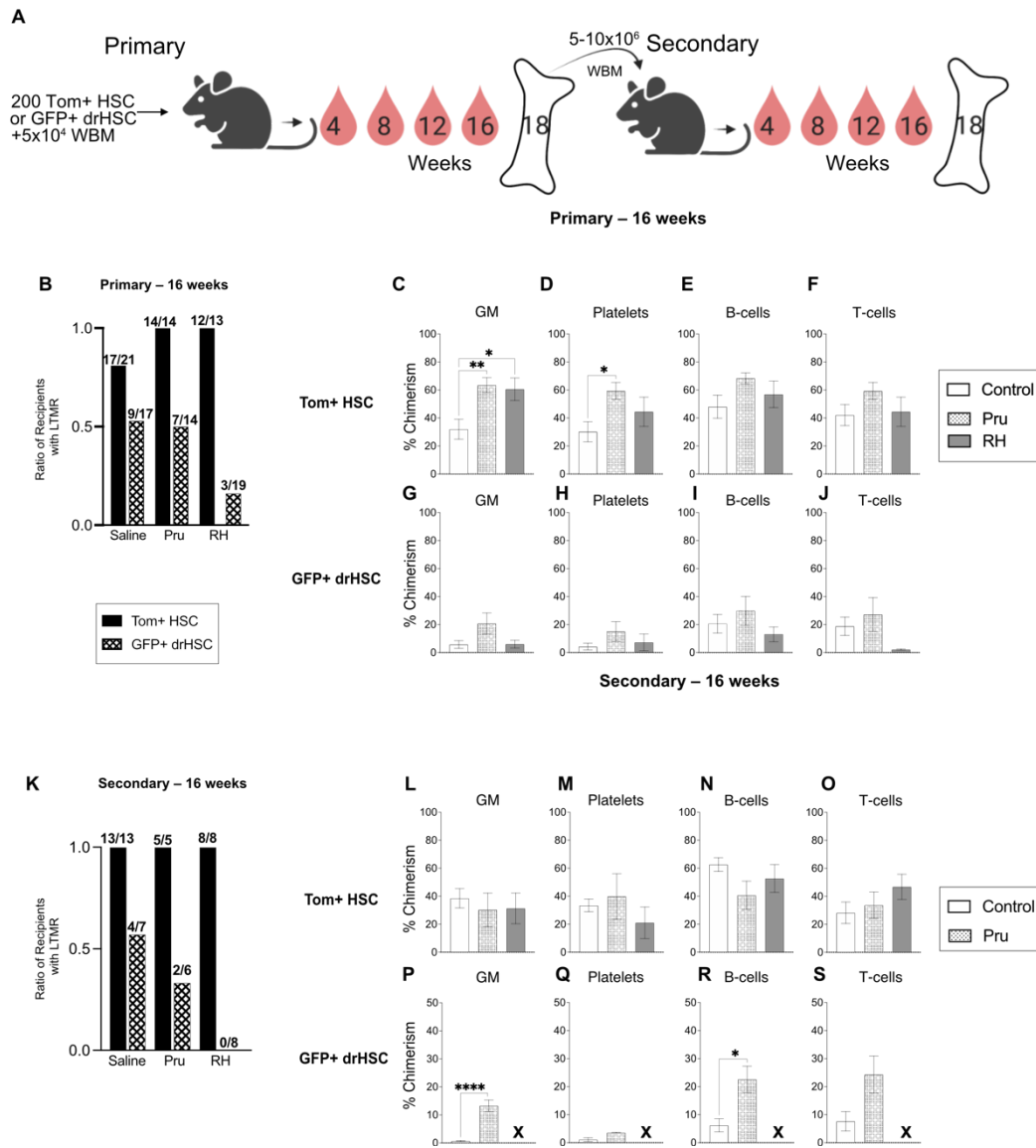
**B)** Crown-rump length (fetal size) was measured in E16.5 fetuses following saline or maternal infection with Pru or RH strains of *Toxoplasma gondii* (**Figure 1A**).

**C-E)** Representative gating strategy and frequencies of various hematopoietic stem and progenitor cell populations in E16.5 fetal liver after **C)** saline, **D)** Pru, or **E)** RH conditions. Frequency  $\pm$  SD as a percentage of total CD45<sup>+</sup>, live, lin<sup>-</sup> cells shown.

**F-M)** Total cellularity of **F)** HSPCs, **G)** LT-HSCs, **H)** ST-HSCs, **I)** Tom<sup>+</sup> HSCs, **J)** GFP<sup>+</sup> drHSCs, **K)** MPP2, **L)** MPP3, **M)** MPP4 in E16.5 fetuses following saline or maternal infection with Pru or RH as shown in **Figure 1A**.

**N-P)** Frequency of **N)** GFP<sup>+</sup> drHSCs **O)** Tom<sup>+</sup> HSCs **P)** MPPs (CD150<sup>-</sup> HSPCs) expressing Ki67 (G1+G2-M-S) at E16.5 following saline or maternal infection with Pru or RH as shown in **Figure 1A**. For all analysis above bars represent mean. One-way ANOVA with Tukey's test. \* $p \leq 0.05$ ; \*\* $p \leq 0.01$ ; \*\*\* $p \leq 0.001$ ; \*\*\*\* $p \leq 0.0001$ .

**Figure 2: *In utero* exposure to inflammation from *Toxoplasma gondii* modulates fetal HSC long-term multi-lineage reconstitution and differentiation**



**A)** Schematic of transplantation experiment. After maternal treatment with saline or maternal infection with Pru or RH as shown in **Figure 1A**, 200 E15.5 FL Tom+ HSCs or GFP+ drHSCs were transplanted into lethally irradiated WT recipients along with  $5 \times 10^4$  WT whole bone marrow (WBM) cells. Transplant recipients were monitored for 16 weeks and assessed for peripheral blood (PB) output of mature blood cell populations every 4 weeks. At 18 weeks, bone marrow chimerism was

assessed.  $1 \times 10^6$  WBM cells from fully reconstituted Tom+HSC recipients or  $2 \times 10^6$  WBM cells from GFP+ drHSC recipients were transplanted into lethally irradiated secondary recipients. Secondary transplant recipients were monitored for 16 weeks and assessed for peripheral blood output of mature blood cell populations every 4 weeks. At 18 weeks, bone marrow chimerism was assessed.

**B)** Ratio of primary recipients from **Figure 2A** with long-term multi-lineage reconstitution (LTMR:  $\geq 1\%$  peripheral blood chimerism) in all 4 lineages (granulocyte/macrophages [GM], Platelets, B- and T-cells), n of mice is shown as the numerator.

**C-F)** Peripheral blood (PB) chimerism of recipient mice with LTMR in **C)** granulocytes and macrophages (GM), **D)** Platelets, **E)** B-cells, and **F)** T-cells in primary Tom+ HSC transplant recipients of mice in **Figure 2A** at week 16 post-transplantation.

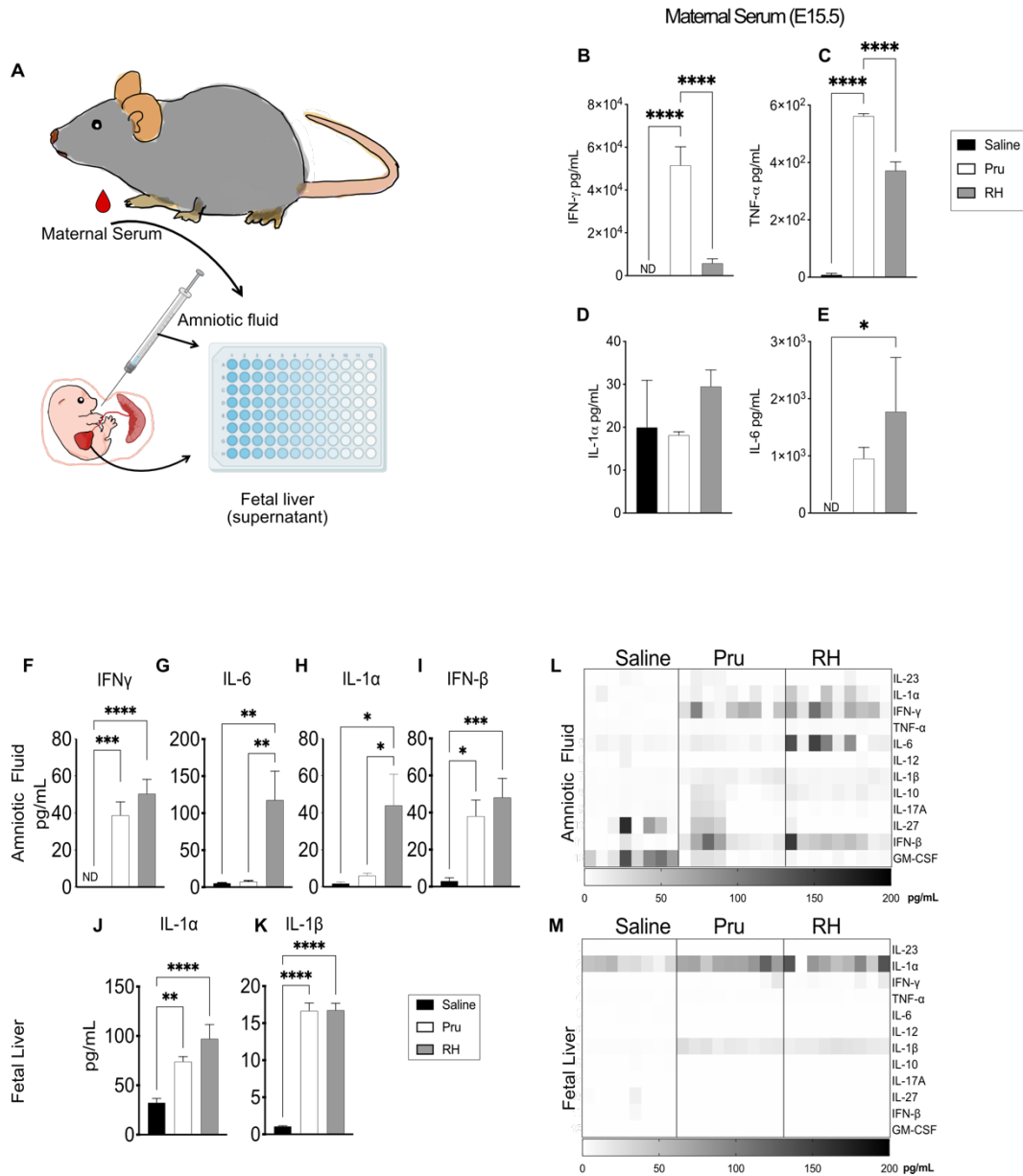
**G-J)** Peripheral blood (PB) chimerism of **G)** granulocytes and macrophages (GM), **H)** Platelets, **I)** B-cells, and **J)** T-cells in primary GFP+ drHSC transplant recipients of mice in **Figure 2A** at week 16 post-transplantation.

**K)** Ratio of secondary recipients from **Figure 2A** with long-term multi-lineage reconstitution ( $\geq 0.1\%$  PB chimerism) in all 4 lineages (GM, Platelets, B- and T-cells), n is shown as the numerator.

**L-S)** Peripheral blood (PB) chimerism of recipient mice with LTMR **L)** granulocytes and macrophages (GM), **M)** Platelets, **N)** B-cells, and **O)** T-Cells in secondary Tom+ HSC transplant recipients of mice in **Figure 2A** at week 16 post-transplantation.

**P-S)** Peripheral blood (PB) chimerism of **P)** granulocytes and macrophages (GM), **Q)** Platelets, **R)** B-cells, and **S)** T-cells in secondary GFP+ drHSC transplant recipients of mice in **Figure 2A** at week 16 post-transplantation. No recipients were reconstituted for GFP+ drHSCs in RH, indicated by "X". For graphs C-F, L-S plotted is the the mean, +/- SD. One-way ANOVA with Tukey's test; \*p  $\leq 0.05$ ; \*\*p  $\leq 0.01$ ; \*\*\*p  $\leq 0.001$ ; \*\*\*\*p  $\leq 0.0001$ .

**Figure 3: *Toxoplasma gondii* virulence from maternal infection modulates inflammation in the fetal environment**



**A)** Schematic of experimental procedure of multiplex inflammation cytokine assay. At E15.5 following maternal infection (**Figure 1A**), maternal serum, fetal amniotic fluid and liver supernatant were collected. A multiplex cytokine assay with Biogen Legendplex (Mouse Inflammation Panel) was performed by flow cytometry.



**B-E)** Cytokine expression of **B)** IFN $\gamma$ , **C)** TNF- $\alpha$ , **D)** IL-1 $\alpha$ , and **E)** IL-6 in E15.5 maternal serum following infection model in **Figure 1A**; n=3 mice/condition.

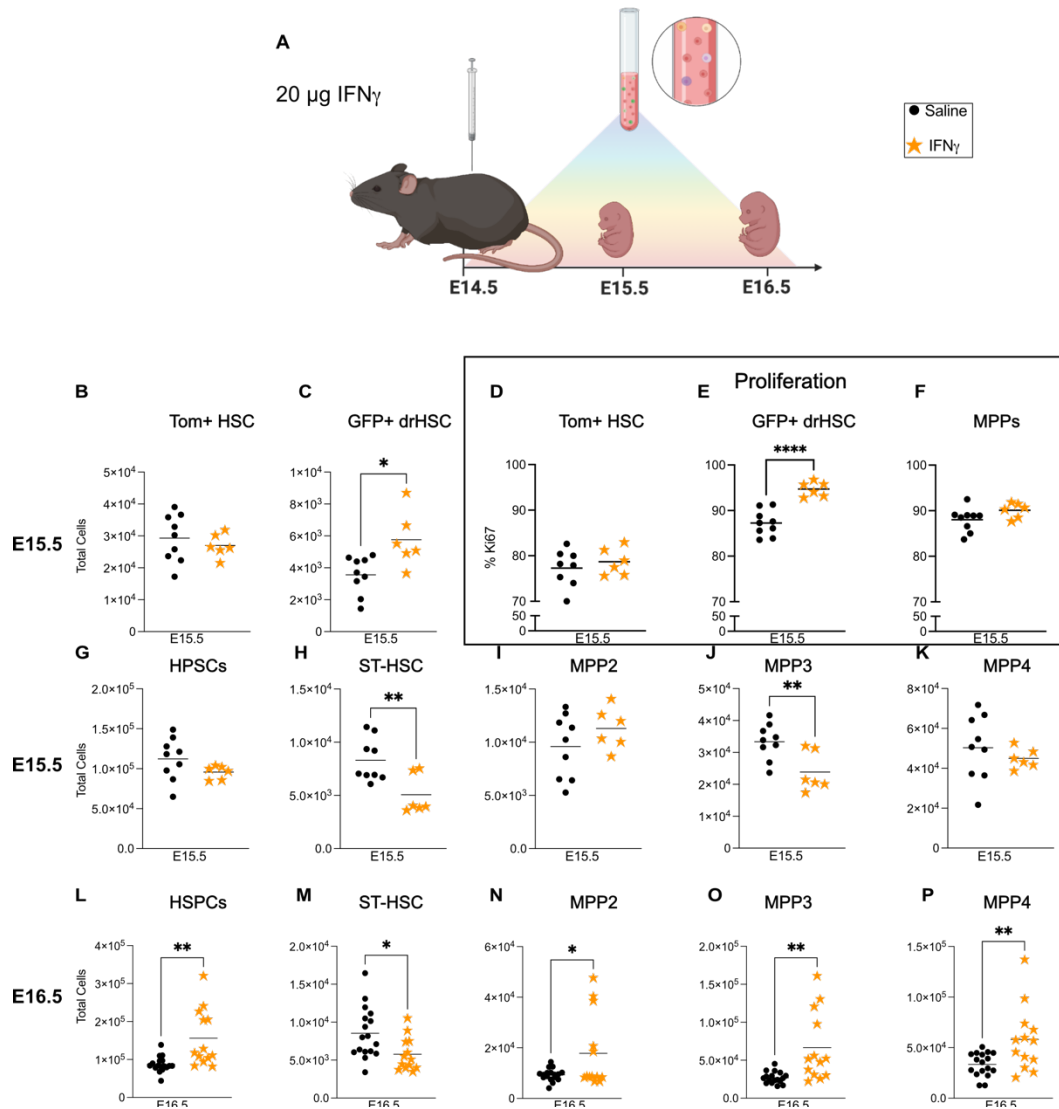
**F-I)** Measure of **F)** IFN $\gamma$ , **G)** IL-6, **H)** IL-1 $\alpha$  and **I)** IFN- $\beta$  cytokine in fetal amniotic fluid at E15.5 following infection model in **Figure 1A**.

**L)** Heatmap of inflammatory cytokines in fetal amniotic fluid at E15.5. Each column represents the result from an individual fetus.

**J-K)** Measure of **J)** IL-1 $\alpha$ , and **K)** IL-1 $\beta$  cytokine in fetal liver supernatant at E15.5 following infection model in **Figure 1A**. For all analysis above bars represent mean, +SD. One-way ANOVA with Tukey's test. \*p  $\leq$  0.05; \*\*p  $\leq$  0.01; \*\*\*p  $\leq$  0.001; \*\*\*\*p  $\leq$  0.0001. n=8-9 fetuses from at least 3 litters/condition.

**M)** Heatmap of inflammatory cytokines in fetal liver at E15.5, each column represents the result from an individual fetus.

**Figure 4: *In utero* exposure to IFN $\gamma$  directs fetal hematopoiesis**



**A)** Schematic of model of maternal inflammation with IFN $\gamma$ . At E14.5 pregnant Flk1<sup>Cre</sup> dams were injected with either saline or 20  $\mu\text{g}$  of recombinant murine IFN $\gamma$ . Fetal cells were analyzed by flow cytometry at E15.5 and E16.5.

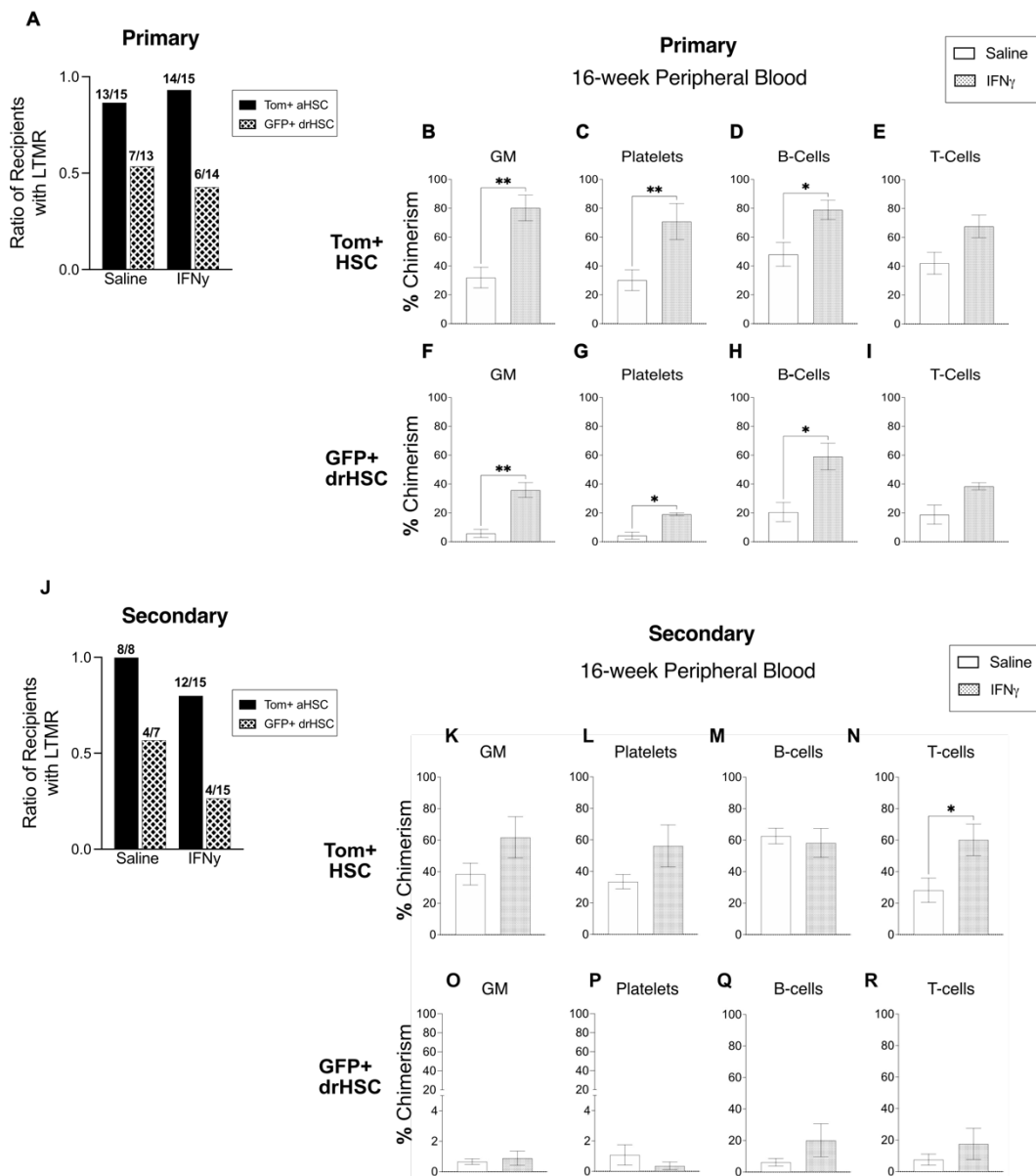
**B-C)** Total cellularity of **B)** Tom+ HSCs and **C)** GFP+ drHSCs at E15.5.

**D-F)** Frequency of **D)** Tom+ HSCs, **E)** GFP+ drHSCs, and **F)** Multipotent Progenitors (“MPP” CD150<sup>-</sup> HSPCs) expressing Ki67 (G1+G2-M-S) at E15.5.

**G-K)** Total cellularity of **G)** HSPCs, **H)** ST-HSCs, **I)** MPP2, **J)** MPP3, and **K)** MPP4 at E15.5.

**L-P)** Total cellularity of **L)** HSPCs, **M)** ST-HSCs, **N)** MPP2, **O)** MPP3, and **P)** MPP4 at E16.5. For all analysis above bars represent mean, and cumulative results of 4 experiments/condition are plotted. Unpaired student's t-test. \* $p \leq 0.05$ ; \*\* $p \leq 0.01$ ; \*\*\* $p \leq 0.001$ ; \*\*\*\* $p \leq 0.0001$ .

**Figure 5: *In utero* exposure to IFN $\gamma$  directs fetal hematopoietic stem cell differentiation**



**A)** Ratio of recipients with long-term multi-lineage reconstitution (LTMR:  $\geq 1\%$  PB chimerism) in all 4 lineages (GM, Platelets, B- and T-cells). Transplant schematic follows **Figure 2A**, for mice shown in **Figure 4A**, n of mice is shown as the numerator.

**B-E)** Peripheral blood (PB) chimerism of **B)** granulocytes and macrophages (GM), **C)** Platelets, **D)** B-cells, and **E)** T-cells in Tom+ HSC transplant recipients of mice in **Figure 2A** at week 16 post-transplantation.

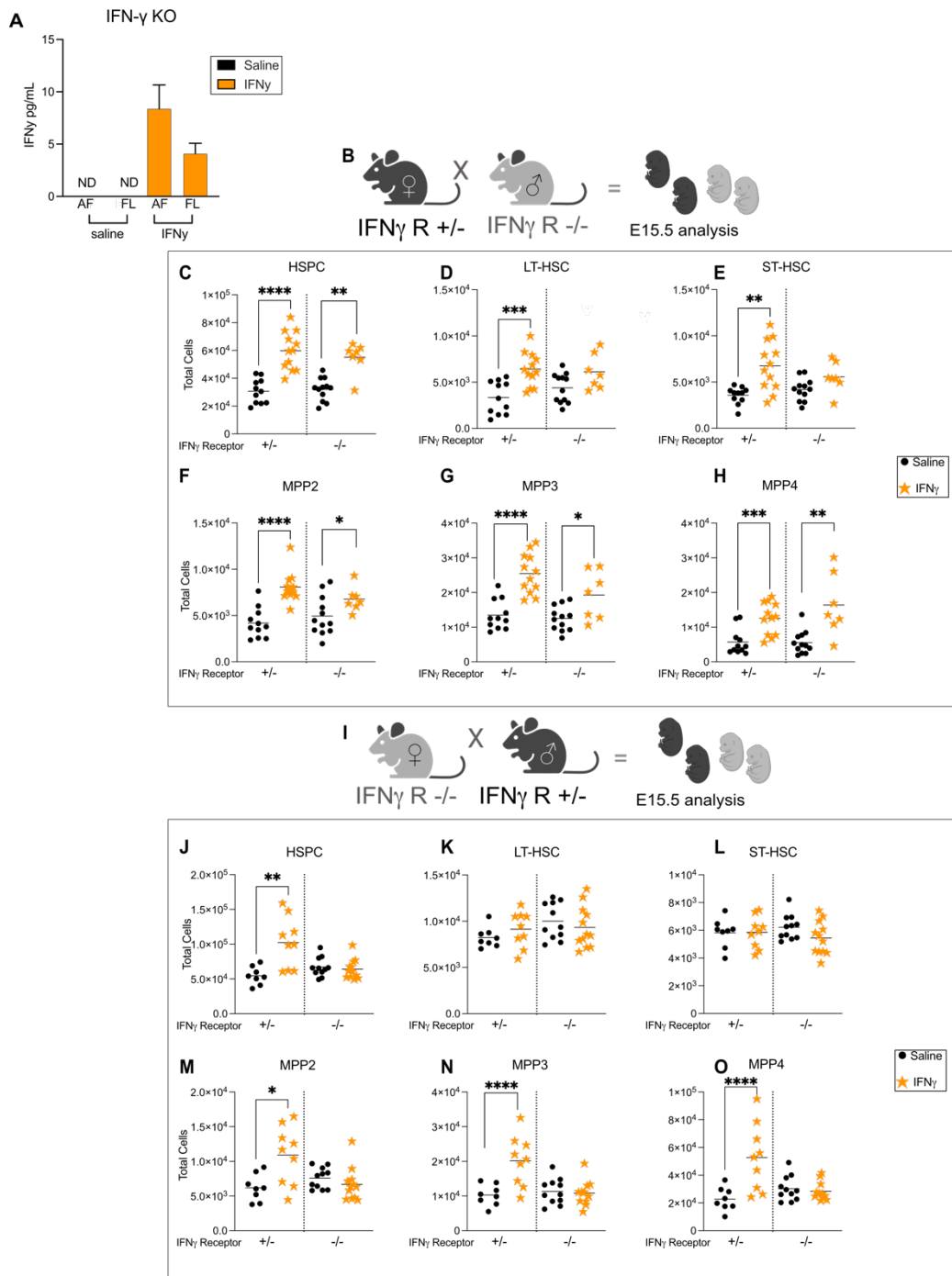
**F-I)** Peripheral blood (PB) chimerism of **F)** granulocytes and macrophages (GM), **G)** Platelets, **H)** B-cells, and **I)** T-cells in GFP<sup>+</sup> HSC transplant recipients of mice in **Figure 2A** at week 16 post-transplantation.

**J)** Ratio of secondary transplants recipients with long-term multi-lineage reconstitution ( $\geq 1\%$  PB chimerism) in all 4 lineages (GM, Platelets, B- and T-cells). Transplant schematic follows **Figure 2A**, for mice shown in **Figure 4A**, n of mice is shown as the numerator

**K-N)** Peripheral blood (PB) chimerism of **K)** granulocytes and macrophages (GM), **L)** Platelets, **M)** B-cells, and **N)** T-cells in secondary Tom<sup>+</sup> HSC transplant recipients of mice in **Figure 2A** at week 16 post-transplantation.

**O-R)** Peripheral blood (PB) chimerism of **Q)** granulocytes and macrophages (GM), **R)** Platelets, **S)** B-cells, and **T)** T-cells in secondary transplant recipients of GFP<sup>+</sup> drHSC in **Figure 2A** at week 16 post-transplantation. For all % chimerism experiments, mice not showing LTMR were not included in analysis and bars represent mean. Unpaired student's t-test. \* $p \leq 0.05$ ; \*\* $p \leq 0.01$ ; \*\*\* $p \leq 0.001$ ; \*\*\*\* $p \leq 0.0001$ .

**Figure 6: Fetal HSCs respond directly to maternal IFN $\gamma$  through IFN $\gamma$  receptor**



**A)** IFN $\gamma$  cytokine measured in the amniotic fluid (AF) and fetal liver supernatant (FL) of 'IFN $\gamma$ KO' (IFN $\gamma$  -/-) mice following injection of cytokine on E14.5 as shown

in **Figure 4A**. ND = not detectable. Plotted is the mean of 3 fetuses/condition and error bars represent +/- SD.

**B)** Schematic of IFN $\gamma$ R  $-/-$  timed matings. IFN $\gamma$ R  $+/-$  dams were time mated to IFN $\gamma$ R  $-/-$  males and injected with saline or 20  $\mu$ g IFN $\gamma$  at E14.5. Fetal liver HSPCs were analyzed at E15.5.

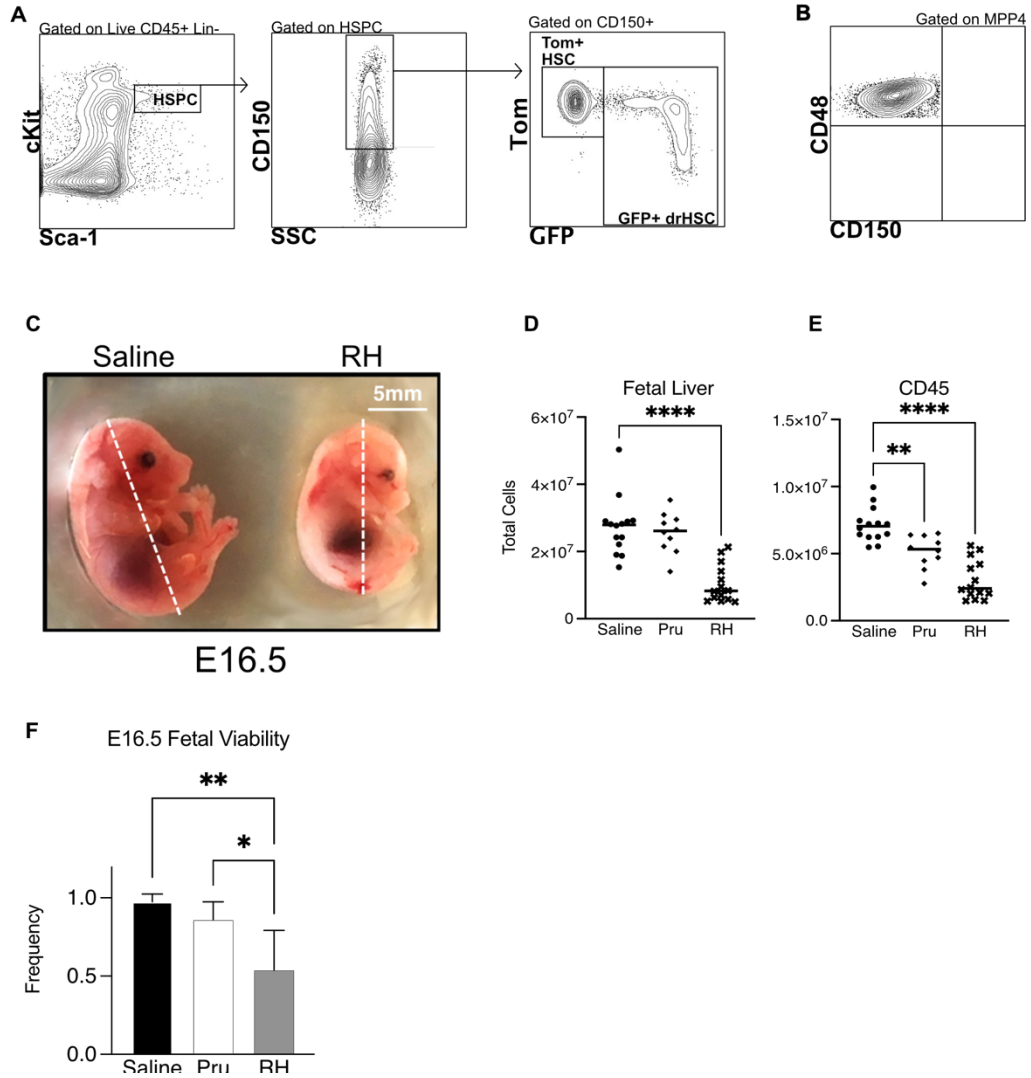
**C-H)** Total cellularity of **C)** HSPCs, **D)** LT-HSCs, **E)** ST-HSCs, **F)** MPP2, **G)** MPP3 and **H)** MPP4 in saline or IFN $\gamma$  exposed littermates of each genotype ( $+/-$  or  $-/-$ ), as derived from the cross as shown in **B** (IFN $\gamma$ R  $+/-$  dam).

**I)** Schematic of IFN $\gamma$ RKO timed matings. IFN $\gamma$ R  $-/-$  dams were time mated to IFN $\gamma$ R  $+/-$  males and injected with saline or 20  $\mu$ g IFN $\gamma$  (as in **Figure 4A**).

**J-O)** Total cellularity of **J)** HSPCs, **K)** LT-HSCs, **L)** ST-HSCs, **M)** MPP2, **N)** MPP3 and **O)** MPP4 in saline or IFN $\gamma$  exposed littermates of each genotype ( $+/-$  or  $-/-$ ), as shown in **I** (IFN $\gamma$ R  $-/-$  dam). For all analysis bars represent mean. Unpaired student's t-test. \* $p \leq 0.05$ ; \*\* $p \leq 0.01$ ; \*\*\* $p \leq 0.001$ ; \*\*\*\* $p \leq 0.0001$ .

## Supplemental Figures

**SFigure 1: Inflammation from maternal infection with *Toxoplasma gondii* modulates fetal growth and hematopoietic development**



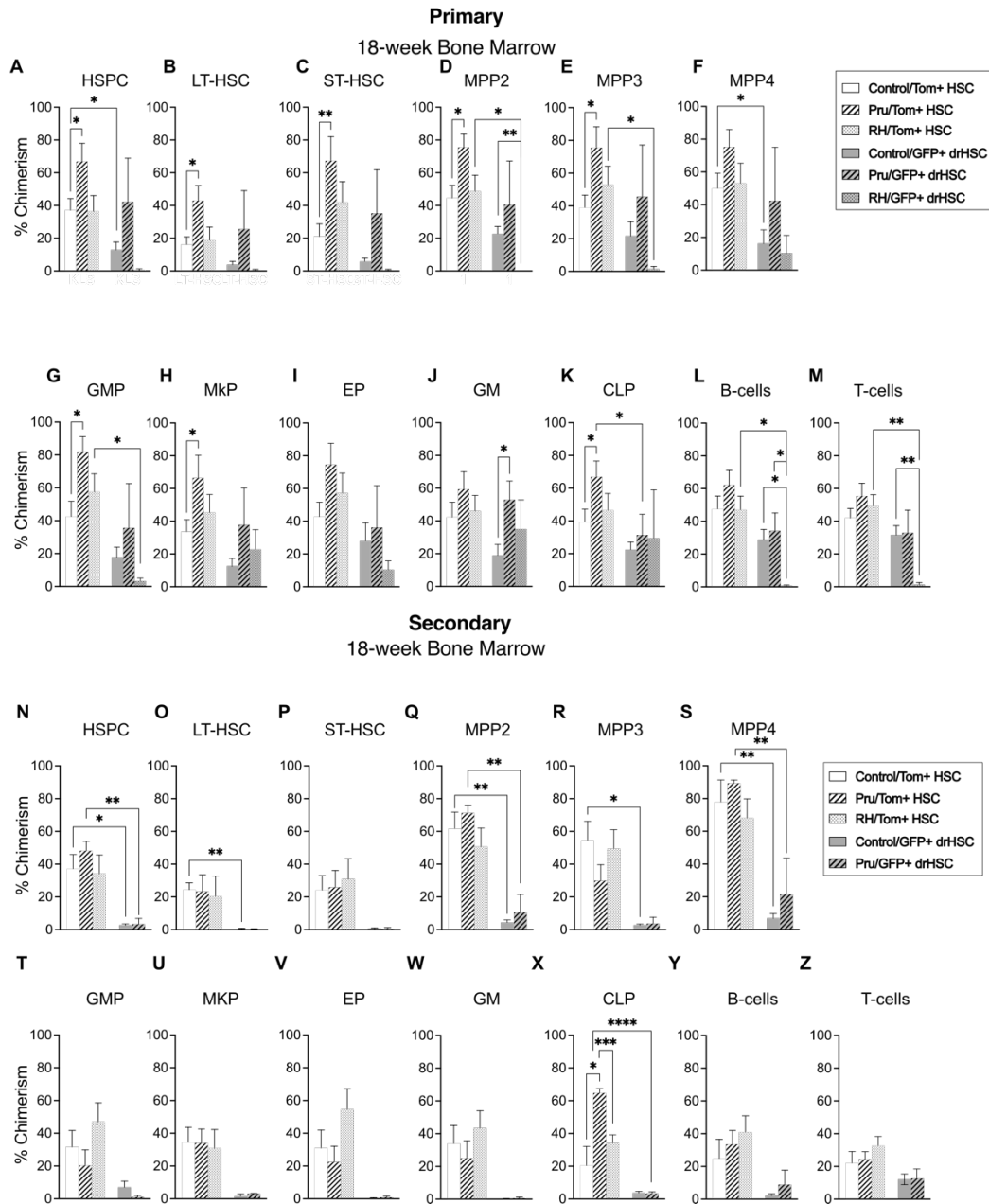
**A)** Representative gating strategy for fetal liver Tom+ HSCs and GFP+ drHSCs at E15.5.

**B)** Representative gating strategy for MPP4+ cells.



- C)** Visual comparison of crown rump length from E16.5 fetuses from saline and RH infected mothers, as in **Figure 1A**.
- D)** Total cellularity of E16.5 fetal liver cells.
- E)** Total cellularity of CD45+ cells in fetal liver at E16.5. For D and E, each dot represents results from an individual fetus, 4 litters were analyzed per each condition.
- F)** Frequency of fetal viability observed in E16.5 litters following saline or infection with Pru or RH; n=4 litters/condition.

**Figure 2: Maternal infection with *Toxoplasma gondii* leads to lasting changes in BM reconstitution of fetal HSCs**

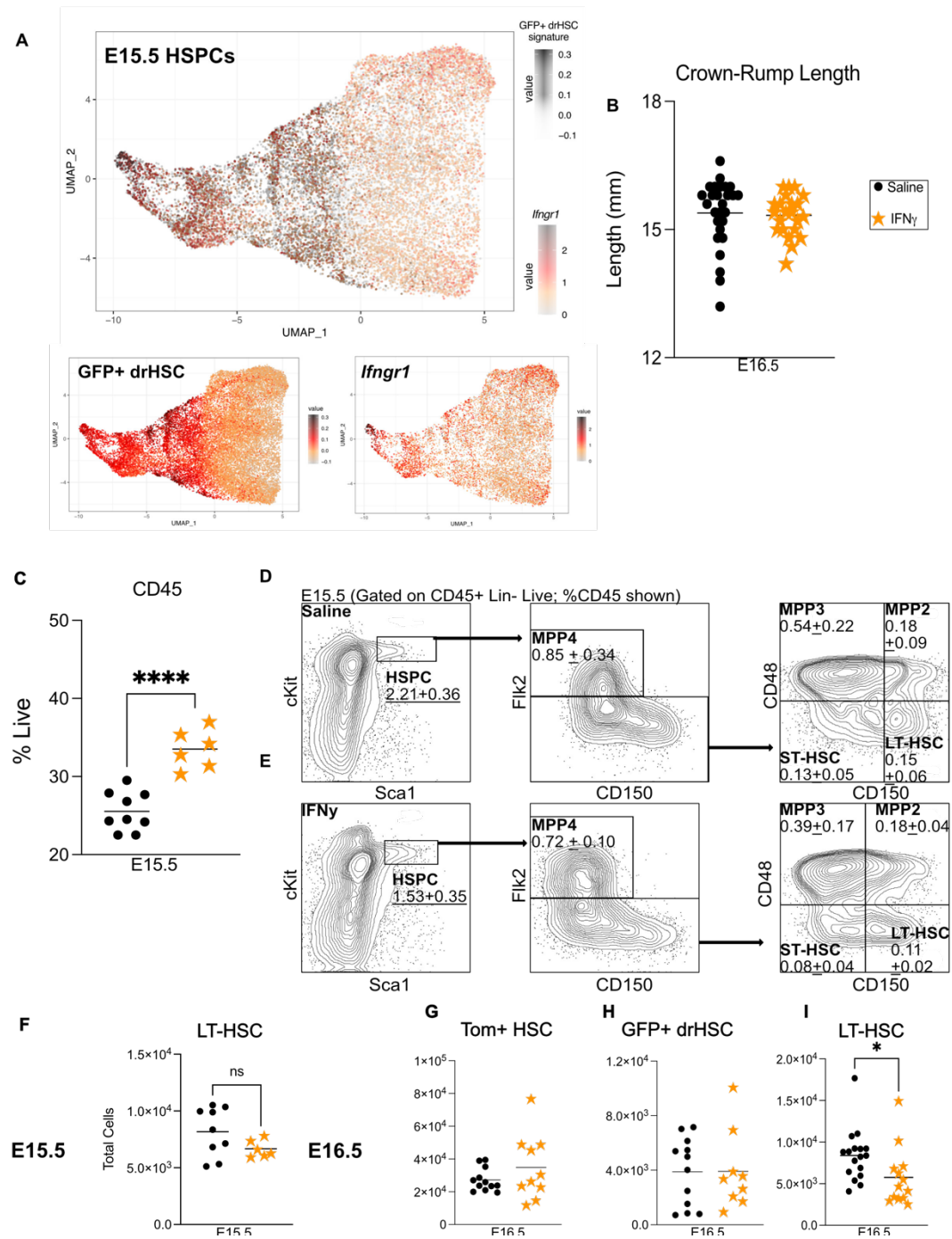


**A-M)** Bone Marrow (BM) chimerism of **A)** HSPCs, **B)** LT-HSCs, **C)** ST-HSCs, **D)** MPP2, **E)** MPP3, **F)** MPP4, **G)** granulocyte macrophage progenitors (GMP), **H)** megakaryocyte progenitors (MkP), **I)** erythroid progenitors (EP), **J)** granulocyte/macrophages (GM), **K)** common lymphoid progenitors (CLP), **L)** B-

cells, and **M**) T-cells in primary Tom<sup>+</sup> HSC and GFP<sup>+</sup> drHSC transplant recipients at 18-weeks post-transplant. Bars represent mean  $\pm$  SD. \*p  $\leq$  0.05; \*\*p  $\leq$  0.01.

**N-Z**) Bone Marrow (BM) chimerism of **N**) HSPCs, **O**) LT-HSCs, **P**) ST-HSCs, **Q**) MPP2, **R**) MPP3, **S**) MPP4, **T**) granulocyte macrophage progenitors (GMP), **U**) megakaryocyte progenitors (MkP), **V**) erythroid progenitors (EP), **W**) granulocyte/macrophages (GM), **X**) common lymphoid progenitors (CLP), **Y**) B-cells, and **Z**) T-cells in secondary Tom<sup>+</sup> HSC and GFP<sup>+</sup> drHSC transplant recipients at 18-weeks post-transplant. For all analyses above, bar represents mean. 2-way ANOVA. \*p  $\leq$  0.05; \*\*p  $\leq$  0.01; \*\*\*p  $\leq$  0.001; \*\*\*\*p  $\leq$  0.0001. No reconstitution was present for the secondary recipients of the GFP<sup>+</sup> drHSC.

**SFigure 3: *In utero* exposure to IFN $\gamma$  directly impacts fetal HSPCs**



**A)** UMAP showing overlap between enrichment GFP+ drHSC gene signature to *Ifngr1* expression in E15.5 HSPCs. Color bars indicate enrichment scoring assessed by the AddModuleScore function.

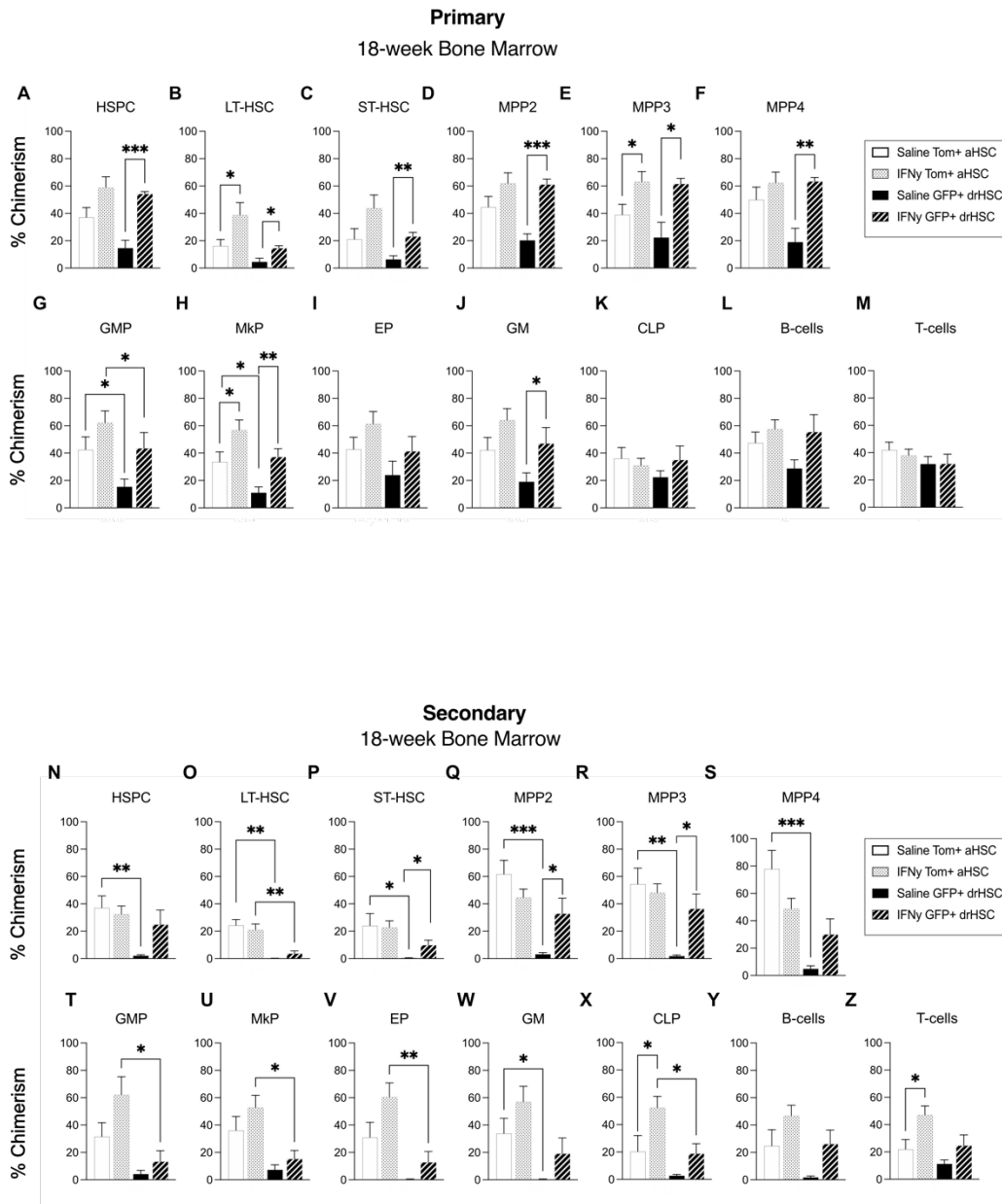
**B)** Crown-rump length of E16.5 fetuses following maternal IFN $\gamma$  injection at E14.5. Bars represent mean.

**C)** CD45+ +/- SD cell frequency of live fetal liver cells at E15.5.

**D-E)** Representative gating strategy and frequency of various hematopoietic stem and progenitor cells (HSPCs) in E15.5 fetal liver after **D)** saline or **E)** IFN $\gamma$  treatment. Frequency  $\pm$  SD as a percentage of CD45 cells shown.

**F-H)** Total cellularity of **F)** LT-HSCs in E15.5 FL and **G)** Tom+ HSCs, **H)** GFP+ drHSCs, and **I)** LT-HSCs in E16.5 FL. Bar represents the mean. Unpaired student's t-test; \*p  $\leq$  0.05; \*\*p  $\leq$  0.01; \*\*\*p  $\leq$  0.001; \*\*\*\*p  $\leq$  0.0001.

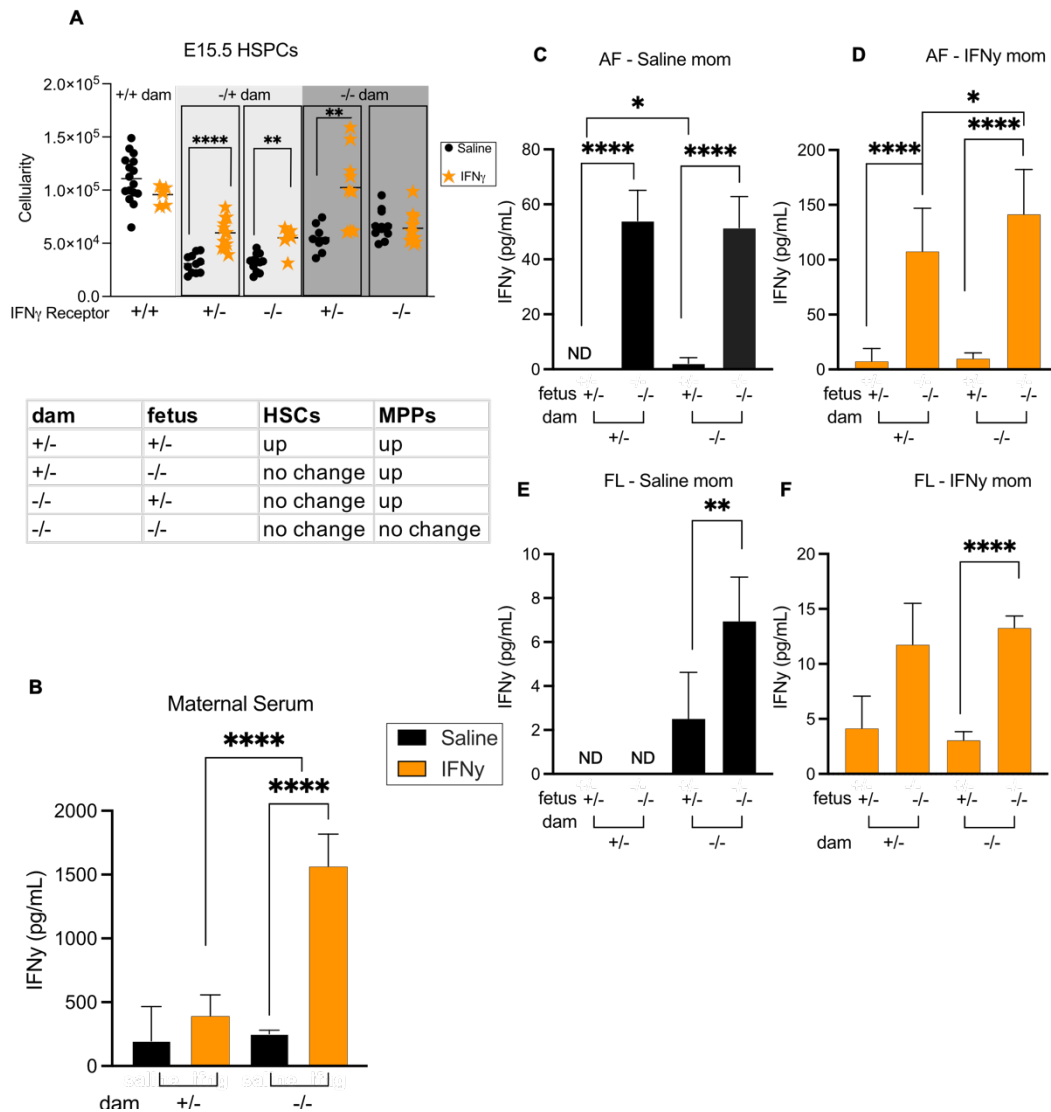
**Figure 4. Bone marrow chimerism from IFN $\gamma$  exposed fetal HSCs following transplantation**



**A-M) Bone Marrow (BM) chimerism of A) HSPCs, B) LT-HSCs, C) ST-HSCs, D) MPP2, E) MPP3, F) MPP4, G) granulocyte macrophage progenitors (GMP), H) Megakaryocyte progenitors (MkP), I) erythroid progenitors (EP), J) granulocyte/macrophages (GM), K) common lymphoid progenitors (CLP), L) B-cells, and M) T-cells in primary Tom+HSC and GFP+drHSC transplant recipients at 18-weeks post-transplant.**

**N-Z)** Bone Marrow (BM) chimerism of **N)** HSPCs, **O)** LT-HSCs, **P)** ST-HSCs, **Q)** MPP2, **R)** MPP3, **S)** MPP4, **T)** granulocyte macrophage progenitors (GMP), **U)** Megakaryocyte progenitors (MkP), **V)** erythroid progenitors (EP), **W)** granulocyte/macrophages (GM), **X)** common lymphoid progenitors (CLP), **Y)** B-cells, and **Z)** T-cells in secondary Tom+HSC and GFP+drHSC transplant recipients at 18-weeks post-transplant. For all experiments above, bars represent mean  $\pm$  SD. \* $p \leq 0.05$ ; \*\* $p \leq 0.01$ ; \*\*\* $p \leq 0.001$ . 2-way ANOVA with Tukey's test.

**SFigure 5 : The role of IFN $\gamma$  and IFN $\gamma$ R in fetal response**



**A)** Cellularity of HSPCs in fetal liver from E15.5 IFN $\gamma$ R crosses from mice in **Figures 4A**, and **6B, I**.

**B)** Comparison of IFN $\gamma$  cytokine in E15.5 maternal serum between IFN $\gamma$ R +/- and -/- dams following saline or IFN $\gamma$  injection.

**C)** Comparison of IFN $\gamma$  cytokine in E15.5 fetal amniotic fluid between IFN $\gamma$ R +/- and -/- pups from either IFN $\gamma$ R +/- or -/- dams following saline injection.

**D)** Comparison of IFN $\gamma$  cytokine in E15.5 fetal amniotic fluid between IFN $\gamma$ R +/- and -/- pups from either IFN $\gamma$ R +/- or -/- dams following IFN $\gamma$  injection.



**E)** Comparison of IFN $\gamma$  cytokine in E15.5 fetal liver supernatant between IFN $\gamma$ R +/- and -/- pups from either IFN $\gamma$ R +/- or -/- dams following saline injection.

**F)** Comparison of IFN $\gamma$  cytokine in fetal liver supernatant between between IFN $\gamma$ R +/- and -/- pups from either IFN $\gamma$ R +/- or -/- dams following IFN $\gamma$  injection. For all

experiments above, bars represent mean  $\pm$  SD. \*p  $\leq$  0.05; \*\*p  $\leq$  0.01; \*\*\*p  $\leq$  0.001;

\*\*\*\*p  $\leq$  0.0001. 2-way ANOVA. N=10-14 fetuses from at least 3 litters/condition.

## Chapter 4: Conclusions

### 4.1 Contributions to the field

#### 4.1.1 Exploring the link between hematopoiesis and immunity *in utero*

The work presented in this dissertation expands knowledge in two parallel fields: hematopoiesis and immunity. The field of early hematopoietic development is defined by studies unraveling the origin and development of both stem and progenitor cells while the fetal immune response to inflammation has rarely been considered. Despite growing interest in the the impact of inflammation and infection on adult hematopoiesis, very little is known about how these perturbations influence fetal hematopoiesis and development. Adult HSCs can respond to inflammation directly through the circulation, but the fetal-maternal barrier and its permeability to specific signals is understudied and adds a layer of complexity to studies of the fetal hematopoietic response (Apostol, Jensen et al. 2020). Recent work has shown that “training” of hematopoietic cells can occur through epigenetic mechanisms that allow heightened response to subsequent immune insult of the progeny of HSCs. However, this work has only been explored in the context of adult hematopoiesis and immune function. Conversely, current studies of fetal HSC development rarely look at immediate differences in functional outcomes due to aberrant signaling. While there is an obvious link to hematopoietic development, function, and ultimately, immunity, our studies are the first to demonstrate that collectively, the maternal immune response and fetal hematopoietic function are unequivocally linked through interactions that occur at both the HSC and progenitor level in the fetus. We explore, for the first time, the specific impact of maternal inflammation through indirect stimulation with IFN $\alpha$  by poly (I:C), direct stimulation by

maternal injection of IFN $\gamma$ , and finally a novel maternal infection model with two strains of *Toxoplasma gondii*. Through these models we observed both immediate and long-term changes to fetal HSC function due to inflammation. In addition, we were able to link maternal inflammation via cytokine stimulation with changes to the cytokine milieu of the fetal environment and ultimately, changes to fetal HSC function through gene expression, proliferation and transplantation. Our findings are the first to link prenatal inflammation with direct effects on fetal HSC development and hematopoietic function in a mouse model of prenatal inflammation and infection.

#### **4.1.2 Experimental models of the effects of prenatal inflammation on fetal hematopoiesis**

While modeling maternal immune activation with pIC has previously been employed as a model of perturbation in studies of neural development (Meyer, Feldon et al. 2009), we are the first to utilize it as an acute inflammation event to study hematopoiesis and immune development during pregnancy. In combination with our Flkswitch lineage tracing model, in which we have previously identified two distinct subsets of fetal HSCs with distinct functional properties, we were able to track the immediate response of the entire HSPC compartment across ontogeny. Additionally, through transplantation, we were also able to assess the long-term consequences of maternal immune activation on HSC function in a primary and secondary transplant setting. After successfully modeling maternal immune activation with pIC, we next decided to test our model in the context of an actual infection with *Toxoplasma gondii*, the first maternal infection model to study fetal hematopoiesis. We chose *T. gondii* for several reasons, including its adaptability in modulating virulence by choosing the appropriate parasite strain and host combination, its relevance to

pregnancy as a vertically transmitted pathogen, and its well-characterized host immune response that we leveraged to discover potential inflammatory drivers to the fetal HSC response. We postulated that because *Toxoplasma gondii* elicited an IFN $\gamma$  based response from the host (in this case the pregnant dam), that the specific IFN $\gamma$  response could be teased apart from infection. Like previous studies of hematopoiesis comparing acute cytokine signaling to infection models (Baldrige, King et al. 2010, Matatall, Jeong et al. 2016), our work showcased the divergent response between cytokine and infection.

#### **4.1.3 Generation of a novel single cell sequencing dataset for fetal HSPCs**

One of the challenges we faced when trying to characterize the heterogenous HSPC population in the Flkswitch fetal liver was that there were no previous datasets that explored the entire HSPC compartment in the fetal liver. Sequencing of over 24,000 cells isolated from saline- and MIA-treated fetal liver identified 14 unique clusters in HSPCs. We leveraged bulk sequencing profiles of the Tom+HSC and GFP+ drHSC to identify clusters that overlapped with each cell type. By utilizing several databases where gene expression was generated for unique adult hematopoietic populations based on canonical markers for hematopoietic stem and progenitor (MPP) populations and by using databases with known markers for cell bias (such as lymphoid and myeloid genes), we were able to characterize general trends within the fetal HSPC compartment at steady state and following maternal immune activation to generate a novel dataset that encompasses gene expression profiles of the heterogenous HSC and HSPC compartment. Another factor we explored when generating this dataset was to capture fetal HSPCs under both steady-state and following maternal immune activation with pIC. The divergent gene expression

profiles between the two conditions showcased a distinct shift in population density following MIA that matched our trends in the *in vivo* data (**Chapter 2, Figure 3B-C**). Additionally, the discovery of clusters closely associated with both the GFP+ drHSC and Tom+ HSC identities marked the first time that these specific populations, identified through lineage tracing, were mapped onto the heterogeneous HSPC compartment. While this data was the first of its kind to explore HSPCs in the fetal liver in both steady state and under inflammatory conditions, we merely touched the surface with the breadth of this analysis. Future studies can further utilize this resource by mapping back gene expression profiles of fetal-derived cell types. Additionally, downstream HSPC progenitors such as multi potent progenitors can be further characterized within the context of this dataset to reveal functional differences between phenotypically identified MPPs. As MPPs are responsible for most of the steady-state hematopoietic output in later life (Sun, Ramos et al. 2014), the study of their gene expression and subsequent function in early life are of utmost importance.

#### **4.1.4 Characterizing cytokines present in the fetal hematopoietic environment**

While certain cytokines like IL-6 are constitutively expressed under homeostatic conditions during fetal development (Omere, Richardson et al. 2020) and have been shown to cross the fetal-maternal interface (Dahlgren, Samuelsson et al. 2006), the mechanisms underlying and regulating cytokine transfer from maternal to fetal environments have not yet been elucidated. Interferon signaling is vital to proper fetal development and is necessary for proper HSC emergence in the developing embryo (Espin-Palazon, Weijts et al. 2018). During homeostatic embryonic development, the endothelial to hemogenic transition necessary to generate definitive HSCs is a carefully orchestrated process dependent on proper signals

within space and time. While previous work as shown that bone marrow HSCs have IFN $\gamma$  receptor (Chambers, Shaw et al. 2007), it was unknown if HSCs in the fetal liver were permeable to maternal sources of cytokine. As evidenced by our IFN $\gamma$  receptor crosses, tonic signaling is important for proper HSPC development, as age-matched fetuses in IFN $\gamma$   $-/+$  and  $-/-$  conditions had fewer HSPCs at baseline compared to their WT (IFN $\gamma$  receptor  $+/+$ ) counterparts. We first explored the role of IFN $\gamma$  at the fetal-maternal interface by injecting IFN $\gamma$  cytokine in an IFN $\gamma$  knockout mouse and found that maternal sources of IFN $\gamma$  were found in fetal liver supernatant and amniotic fluid after 24 hours. Our finding also demonstrated that in IFN $\gamma$  receptor  $-/-$  mice, which had no IFN $\gamma$  receptor but could make IFN $\gamma$  cytokine, both adult and fetal tissues accumulated IFN $\gamma$  at steady state and after maternal injection, highlighting that IFN $\gamma$  can passively transfer between the fetal and maternal environment, particularly when it is not utilized to signal at the IFN $\gamma$  receptor. These data provide important and novel information on cytokine transfer at the maternal-fetal interface.

Another important aspect of this work has been to fully characterize the inflammatory repertoire of both the fetal amniotic and liver supernatants at steady-state, following IFN- $\alpha$  induction by pIC, IFN $\gamma$  injection, and finally between two Types of *T. gondii* infection. As compared to maternal serum, there is both overlap (i.e., Type I or II interferon expression) in the signals upregulated in those environments as well as many novel differences found in the fetal tissues following infection and inflammation. Interleukin alpha was the most consistently upregulated cytokine in the fetal tissues following all inflammation or infection conditions. Most interesting were the notable differences in response between the two strains of *T. gondii*, RH and Pru. Instead, it appeared that IL-6 distinguished the RH from Pru cytokine response in the fetus while both infections elicited similar fetal levels of

IFN $\gamma$ . Defining the specific cytokine response within the fetal liver and amniotic fluid during inflammation may help explain what the fetal HSC “sees” during a particular inflammation or infection event. In combination with our IFN $\gamma$ R -/- experiments, these results help dissect the contrast we see between the heterogeneous responses of the fetal HSPC compartment. In the absence of fetal IFN $\gamma$ R, MPPs continue to respond to other signals independent of IFN $\gamma$ . While our primary focus has been on IFN $\gamma$ , specifically in Chapter 3, other cytokines evoked by infection or by IFN $\gamma$ -receptor signaling and passed onto the fetal side may explain the observed differences in the GFP $^+$  HSC trajectory after transplantation between Pru and RH, as the heterogeneous HSPC compartment may have different responsiveness to specific cytokines.

Certain challenges arose that complicated comparative analysis of cytokines across different sources. Namely, liver supernatant may generate levels of inflammatory cytokines that we could not capture due to the limitations of our *ex vivo* assays that required more dilution of raw material for analysis. In order to circumvent this, more sensitive assays or pooling of supernatant in the future may be required. Nevertheless, these novel findings illuminate the complex dynamic between fetal and maternal cytokine signaling and serve as an excellent resource for future studies of the fetal cytokine milieu.

#### **4.1.5 Fetal hematopoiesis exhibits a unique response to maternal inflammation**

In stark contrast with observations in adult bone marrow HSC response to inflammation and infection, our findings revealed a divergent, response of fetal liver hematopoiesis to maternal inflammation. Whereas in adult BM, HSCs respond to inflammation with myeloid biased cellular output and

proliferation that leads to HSC exhaustion, the fetal HSC response is markedly different. Our findings showed that in the MIA model that elicited a Type I IFN $\alpha$  cytokine response in both the fetus and the dam, the Tom<sup>+</sup> HSCs exhausted while GFP<sup>+</sup> drHSCs had no loss in function following secondary transplantation. In contrast, our IFN $\gamma$  injection and *T. gondii* infection models showed a different response. Regardless of inflammation source (IFN $\gamma$  or *T. gondii*) the Tom<sup>+</sup> HSCs either maintained or improved LTMR capability even into secondary transplantation while the GFP<sup>+</sup> drHSCs lost LTMR capability in the virulence-dependent manner. Our single-cell sequencing data, combined with our cytokine analysis may yield some insight into these divergent responses: the GFP<sup>+</sup> drHSC identity corresponds with cells expressing higher levels of interferon responsive genes compared to their Tom<sup>+</sup> HSC counterparts and are thus likely more receptive to inflammatory signals. Indeed, this signal receptor gradient between the two fetal HSC populations can potentially serve to preserve proper hematopoietic output in early development – despite increased responsiveness of GFP<sup>+</sup> drHSCs, they fail to lose LTMR unless exposed to detrimental levels of inflammation as is the case with RH infection. What is unknown is why the Tom<sup>+</sup> HSC, responds differently to Type I vs Type II interferons. Additional functional testing in response to Type I interferons and viral infection is necessary to parse out other divergent functional outcomes between these two fetal HSC subsets (**Figure 1**).

## **4.2 Future directions**

### **4.2.1 Exploring the impact of maternal IFN $\gamma$ exposure on long-term hematopoietic outcomes**

In order to fully appreciate the impact of prenatal inflammation on fetal HSC development, we must also begin to track fate of fetal HSCs across



ontogeny. While the Flkswitch model coupled with maternal immune activation allowed us to gain insight into fetal environmental cues following maternal inflammation, further investigation of the long-term effects on hematopoietic and immune function is warranted. Preliminary findings from our lab indicate that the crosstalk that occurs between maternal immune signals and fetal hematopoietic stem cells has a lasting correlation to immune outcomes in later life (Apostol, et al 2022). GFP+ drHSCs, which generate B1b cells in early life (Beaudin, Boyer et al. 2016) have been shown to be expanded and abnormally persistent in both neonatal and adult bone marrow. Following MIA during gestation, peritoneal B1b cells in the neonate were expanded and shown to generate more IgM, IgG3 and IL-10 on a per cell basis by ELISA (Apostol, López et al. 2022). While these studies highlight a relationship between early life exposure of hematopoietic stem cells and subsequent immune outcomes in later life, further functional studies are warranted. For example, testing functional output of GFP+ B1b cells from GFP+ drHSC transplant recipients can be tested for a more direct correlation between fetal cells and immune outcomes. These types of outcomes can include B1 functional assays such as cytokine and Ig output. Additionally, *ex vivo* analysis of fetal HSC differentiation can link observations from transplantation assays and *in vivo* data to gain further insight into the effect of prenatal inflammation on lineage differentiation. Finally, differential immune outcomes can be elucidated by utilizing control and maternal-exposed mice with subsequent immune challenges such as a viral or parasitic immune challenge in later life. The work presented in this dissertation is the first of its kind to test functional outcomes of fetal HSCs following maternal immune activation and lays the foundation for further study of early life perturbations to immune outcomes.

### 4.2.2 Exploring other infection models

Our preliminary work using both IFN $\gamma$  and *Toxoplasma gondii* of two different virulence Types forms the foundation of subsequent studies comparing infection to cytokine stimulation. *Toxoplasma gondii*, along with other vertically transmitted TORCH (Megli and Coyne 2021) pathogens are relevant models for studying infection during pregnancy. As such, a natural continuation of this research would be to use viral infection in pregnancy on our model of maternal immune activation. Viruses such Cytomegalovirus (CMV) are included in the TORCH nomenclature and are pertinent in the study of fetal and maternal health. Our work in the Type 1 interferon stimulating maternal immune activation model paves the way to use our model of maternal infection with viral models such as MCMV (mouse CMV) and VSV which have previously been used to study hematopoiesis in the adult environment (Hirche, Frenz et al. 2017). Like our IFN $\gamma$  model, we can utilize our pIC data alongside data of IFN $\alpha$  alone to further disentangle the specific impact of cytokine signaling compared to the dynamic cytokine milieu induced by infection and translated into the fetal environment.

## 4.3 Summary

This dissertation summarizes and expands on a growing body of literature that indicates how maternal microbial exposure can shape fetal immune development by highlighting possible mechanisms of fetal hematopoietic training, including the direct passage of maternal cytokines into the fetal environment, which we explore at great length. In tandem we explore work that highlights important findings that the bone marrow hematopoietic stem cell is a direct sensor of inflammation through direct interaction with cytokines in the circulation. Finally, we conclude the first chapter by tying together these two distinct concepts to explain how fetal HSCs develop

during early life, how their heterogeneity plays an important role in early hematopoietic development, and the distinct functional differences between fetal HSCs and their adult counterparts. These concepts allow the proper foundation for exploration of the distinct cellular mechanisms that drive the fetal HSC response to maternal inflammatory signals.

An added layer of complexity in fetal hematopoiesis is the heterogeneity of multiple groups of fetal HSCs coexisting during early development. We model this heterogeneous compartment by utilizing the Flkswitch lineage tracing model as our primary mouse model during pregnancy. Chapters 2 and 3 explore the impact different maternal inflammatory and infection events on two distinct populations of fetal HSCs. From this model, we learn that unlike bone marrow HSCs in the adult, which respond to inflammation and infection by temporarily increasing proliferation at the expense of the loss of LTMR, fetal HSCs, which at baseline are already more proliferative than adult counterparts, respond by increased proliferation without loss of LTMR, with a few exceptions which are summarized in **Figure 2**. These findings are the first of their kind to explore functional changes to the diverse fetal HSC repertoire. Further testing will need to be done to elucidate the differences between Type I and Type II interferon between Tom+ HSCs and GFP+ drHSCs. Nevertheless, these observations along with the novel single cell database we generated using E15.5 HSPCs, our profiling of cytokines in the fetal environment, as well as the work specifically with IFN $\gamma$  and infection, which establishes *Toxoplasma gondii* as a viable model of maternal infection in the field of fetal hematopoiesis in total have formed the necessary foundation for further studies in this field.

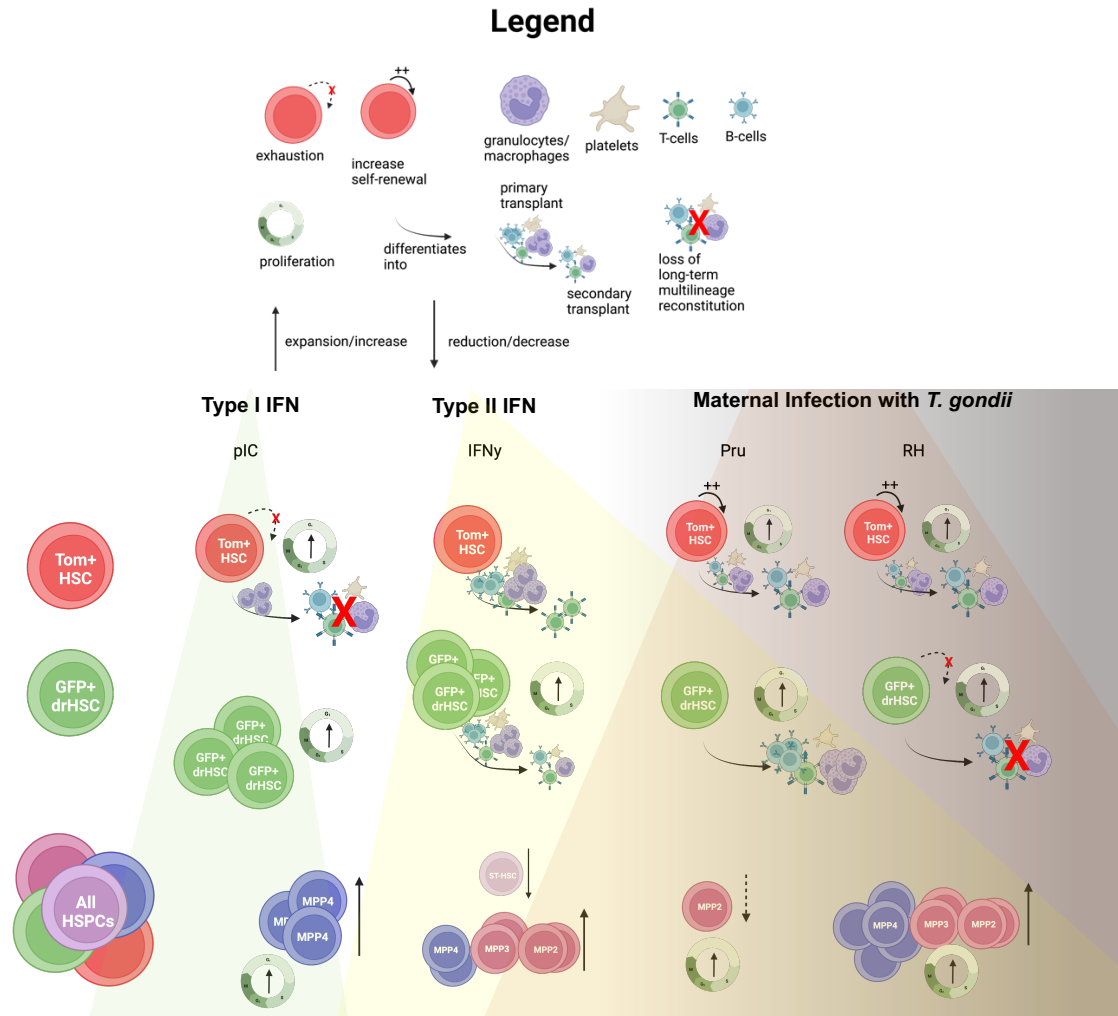


**Figure 1. A summary of the impact to fetal Tom+ HSCs, GFP+ drHSCs, and HSPCs following maternal inflammation induced by pIC, IFN $\gamma$ , Pru and RH infections.**

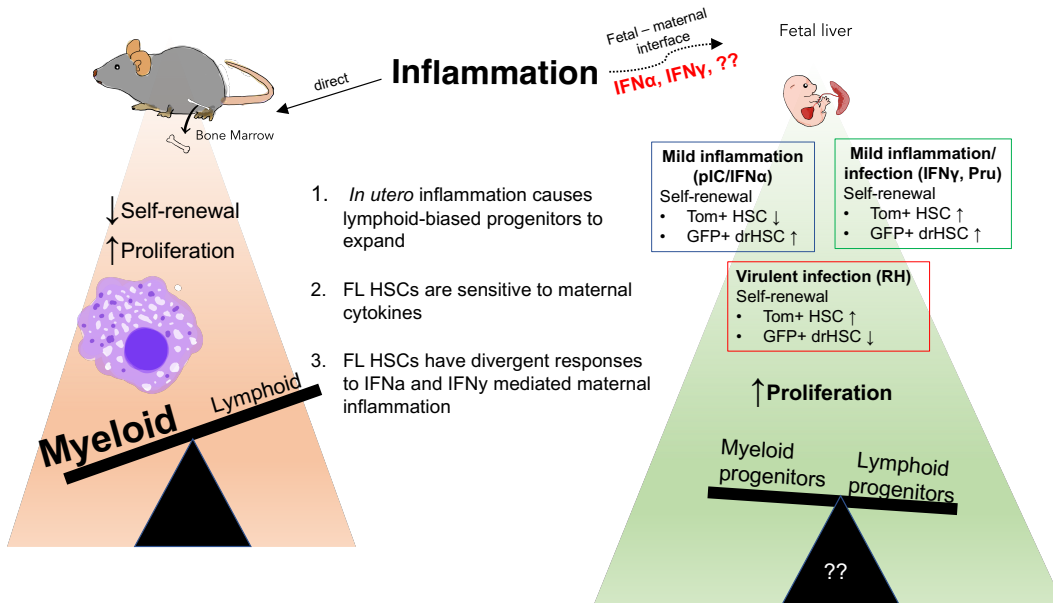


**Figure 2. An overview of the differences between the adult bone marrow fetal liver hematopoietic responses to inflammation.**

## References

- Aaltonen, R., et al. (2005). "Transfer of proinflammatory cytokines across term placenta." Obstet Gynecol **106**(4): 802-807.
- Abou-Bacar, A., et al. (2004). "Role of gamma interferon and T cells in congenital Toxoplasma transmission." Parasite immunology **26**(8-9).
- Abu-Raya, B., et al. (2016). "Transfer of Maternal Antimicrobial Immunity to HIV-Exposed Uninfected Newborns." Front Immunol **7**: 338.
- Adams Waldorf, K. M., et al. (2011). "Choriodecidual group B streptococcal inoculation induces fetal lung injury without intra-amniotic infection and preterm labor in Macaca nemestrina." PLoS One **6**(12): e28972.
- Ander, S. E., et al. (2019). "Immune responses at the maternal-fetal interface." Sci Immunol **4**(31).
- Apostol, A. C., et al. (2020). "Training the Fetal Immune System Through Maternal Inflammation-A Layered Hygiene Hypothesis." Front Immunol **11**: 123.
- Apostol, A. C., et al. (2022). "Prenatal inflammation perturbs fetal hematopoietic development and causes persistent changes to postnatal immunity."
- Baldrige, M. T., et al. (2010). "Quiescent haematopoietic stem cells are activated by IFN-gamma in response to chronic infection." Nature **465**(7299): 793-797.
- Baldrige, M. T., et al. (2011). "Inflammatory signals regulate hematopoietic stem cells." Trends Immunol **32**(2): 57-65.
- Barboza, R., et al. (2019). "Fetal-Derived MyD88 Signaling Contributes to Poor Pregnancy Outcomes During Gestational Malaria." Front Microbiol **10**: 68.
- Beaudin, A. E., et al. (2016). "A Transient Developmental Hematopoietic Stem Cell Gives Rise to Innate-like B and T Cells." Cell Stem Cell **19**(6): 768-783.
- Beaudin, A. E. and E. C. Forsberg (2016). "To B1a or not to B1a: do hematopoietic stem cells contribute to tissue-resident immune cells?" Blood **128**(24): 2765-2769.

- Beerman, I., et al. (2010). "Functionally distinct hematopoietic stem cells modulate hematopoietic lineage potential during aging by a mechanism of clonal expansion." Proceedings of the National Academy of Sciences of the United States of America **107**(12): 5465-5470.
- Benz, C., et al. (2012). "Hematopoietic stem cell subTypes expand differentially during development and display distinct lymphopoietic programs." Cell Stem Cell **10**(3): 273-283.
- Bigna, J. J., et al. (2020). "Global, regional, and country seroprevalence of *Toxoplasma gondii* in pregnant women: a systematic review, modelling and meta-analysis." Scientific Reports **10**(1): 1-10.
- Biondillo, D., et al. (1994). "Interferon-gamma regulation of interleukin 6 in monocytic cells." The American journal of physiology **267**(5 Pt 1).
- Bowie, M. B., et al. (2006). "Hematopoietic stem cells proliferate until after birth and show a reversible phase-specific engraftment defect." J Clin Invest **116**(10): 2808-2816.
- Boyer, S. W., et al. (2012). "Mapping stem cell differentiation pathways from hematopoietic stem cells using Flk2/Flt3L lineage tracing." Cell Cycle **11**(17): 3180-3188.
- Boyer, S. W., et al. (2011). "All hematopoietic cells develop from hematopoietic stem cells through Flk2/Flt3-positive progenitor cells." Cell Stem Cell **9**(1): 64-73.
- Busch, K., et al. (2015). "Fundamental properties of unperturbed haematopoiesis from stem cells in vivo." Nature **518**(7540): 542-546.
- Böiers, C., et al. (2013). "Lymphomyeloid contribution of an immune-restricted progenitor emerging prior to definitive hematopoietic stem cells." Cell Stem Cell **13**(5): 535-548.
- Cabezas-Wallscheid, N., et al. (2014). "Identification of regulatory networks in HSCs and their immediate progeny via integrated proteome, transcriptome, and DNA methylome analysis." Cell Stem Cell **15**(4): 507-522.
- Cardenas, I., et al. (2010). "Viral infection of the placenta leads to fetal inflammation and sensitization to bacterial products predisposing to preterm labor." J Immunol **185**(2): 1248-1257.

Chambers, S., et al. (2007). "Aging hematopoietic stem cells decline in function and exhibit epigenetic dysregulation." PLoS biology **5**(8).

Christensen, J. L. and I. L. Weissman (2001). "Flk-2 is a marker in hematopoietic stem cell differentiation: a simple method to isolate long-term stem cells." Proceedings of the National Academy of Sciences of the United States of America **98**(25): 14541-14546.

Crisan, M., et al. (2016). "BMP and Hedgehog Regulate Distinct AGM Hematopoietic Stem Cells Ex Vivo." Stem Cell Reports **6**(3): 383-395.

Dahlgren, J., et al. (2006). "Interleukin-6 in the maternal circulation reaches the rat fetus in mid-gestation." Pediatr Res **60**(2): 147-151.

Dauby, N., et al. (2012). "Uninfected but not unaffected: chronic maternal infections during pregnancy, fetal immunity, and susceptibility to postnatal infections." Lancet Infect Dis **12**(4): 330-340.

de Bruijn, M. F., et al. (2000). "Definitive hematopoietic stem cells first develop within the major arterial regions of the mouse embryo." Embo J **19**(11): 2465-2474.

Dzierzak, E. and N. A. Speck (2008). "Of lineage and legacy: the development of mammalian hematopoietic stem cells." Nat Immunol **9**(2): 129-136.

Ema, H. and H. Nakauchi (2000). "Expansion of hematopoietic stem cells in the developing liver of a mouse embryo." Blood **95**(7).

Espin-Palazon, R., et al. (2018). "Proinflammatory Signals as Fuel for the Fire of Hematopoietic Stem Cell Emergence." Trends Cell Biol **28**(1): 58-66.

Esplin, B. L., et al. (2011). "Chronic exposure to a TLR ligand injures hematopoietic stem cells." J Immunol **186**(9): 5367-5375.

Essers, M. A., et al. (2009). "IFNalpha activates dormant haematopoietic stem cells in vivo." Nature **458**(7240): 904-908.

Ficara, F., et al. (2008). "Pbx1 regulates self-renewal of long-term hematopoietic stem cells by maintaining their quiescence." Cell Stem Cell **2**(5): 484-496.



- Frame, J. M., et al. (2013). "Erythro-myeloid progenitors: "definitive" hematopoiesis in the conceptus prior to the emergence of hematopoietic stem cells." Blood Cells Mol Dis **51**(4): 220-225.
- Frascoli, M., et al. (2018). "Alloreactive fetal T cells promote uterine contractility in preterm labor via IFN- $\gamma$  and TNF- $\alpha$ ." Sci Transl Med **10**(438).
- Furusawa, J., et al. (2016). "Promotion of Expansion and Differentiation of Hematopoietic Stem Cells by Interleukin-27 into Myeloid Progenitors to Control Infection in Emergency Myelopoiesis." PLoS Pathog **12**(3): e1005507.
- Gao, X., et al. (2018). "The hematopoietic stem cell niche: from embryo to adult." Development (Cambridge, England) **145**(2).
- Gazit, R., et al. (2013). "Transcriptome analysis identifies regulators of hematopoietic stem and progenitor cells." Stem Cell Reports **1**(3): 266-280.
- Gbédandé, K., et al. (2013). "Malaria modifies neonatal and early-life toll-like receptor cytokine responses." Infect Immun **81**(8): 2686-2696.
- Gekas, C. and T. Graf (2013). "CD41 expression marks myeloid-biased adult hematopoietic stem cells and increases with age." Blood **121**(22): 4463-4472.
- Gentek, R., et al. (2018). "Epidermal  $\gamma\delta$  T cells originate from yolk sac hematopoiesis and clonally self-renew in the adult." J Exp Med **215**(12): 2994-3005.
- Georgios, P., et al. (2009). "Toxoplasmosis snapshots: global status of *Toxoplasma gondii* seroprevalence and implications for pregnancy and congenital toxoplasmosis." International journal for parasitology **39**(12).
- Ginhoux, F. and M. Guillems (2016). "Tissue-Resident Macrophage Ontogeny and Homeostasis." Immunity **44**(3): 439-449.
- Haas, J. D., et al. (2012). "Development of interleukin-17-producing gammadelta T cells is restricted to a functional embryonic wave." Immunity **37**(1): 48-59.
- Haas, S., et al. (2015). "Inflammation-Induced Emergency Megakaryopoiesis Driven by Hematopoietic Stem Cell-like Megakaryocyte Progenitors." Cell Stem Cell **17**(4): 422-434.

Haas, S., et al. (2018). "Causes and Consequences of Hematopoietic Stem Cell Heterogeneity." Cell Stem Cell **22**(5): 627-638.

He, Q., et al. (2015). "Inflammatory signaling regulates hematopoietic stem and progenitor cell emergence in vertebrates." Blood **125**(7): 1098-1106.

Hirche, C., et al. (2017). "Systemic Virus Infections Differentially Modulate Cell Cycle State and Functionality of Long-Term Hematopoietic Stem Cells In Vivo." Cell Rep **19**(11): 2345-2356.

Hong, M., et al. (2015). "Trained immunity in newborn infants of HBV-infected mothers." Nat Commun **6**: 6588.

Humann, J., et al. (2016). "Bacterial Peptidoglycan Traverses the Placenta to Induce Fetal Neuroproliferation and Aberrant Postnatal Behavior." Cell Host Microbe **19**(6): 901.

Kallapur, S. G., et al. (2014). "Fetal immune response to chorioamnionitis." Semin Reprod Med **32**(1): 56-67.

Kaufmann, E., et al. (2018). "BCG Educates Hematopoietic Stem Cells to Generate Protective Innate Immunity against Tuberculosis." Cell **172**(1-2): 176-190.e119.

Khan, J., et al. (2016). "Fetal liver hematopoietic stem cell niches associate with portal vessels." Science (New York, N.Y.) **351**(6269).

Kim, I., et al. (2006). "Enhanced purification of fetal liver hematopoietic stem cells using SLAM family receptors." Blood **108**(2): 737-744.

King, K. Y. and M. A. Goodell (2011). "Inflammatory modulation of HSCs: viewing the HSC as a foundation for the immune response." Nat Rev Immunol **11**(10): 685-692.

Kongsomboonvech, A., et al. (2020). "Naïve CD8 T cell IFN $\gamma$  responses to a vacuolar antigen are regulated by an inflammasome-independent NLRP3 pathway and *Toxoplasma gondii* ROP5." PLoS pathogens **16**(8).

Host resistance to *Toxoplasma gondii* relies on CD8 T cell IFN $\gamma$  responses, which if modulated by the host or parasite could influence chronic infection and parasite transmission between hosts. Since host-parasite interactions that govern this response are not fully elucidated, we investigated require ...

Kovacs, A. A. Z. and C. Maternal, and Adolescent Center for Infectious Diseases and Virology, Division of Pediatric Infectious Diseases, Keck

Medicine of the University of Southern California, Los Angeles (2022). "Zika, the Newest TORCH Infectious Disease in the Americas." Clinical Infectious Diseases **70**(12): 2673-2674.

Kuhn, L., et al. (2005). "Does severity of HIV disease in HIV-infected mothers affect mortality and morbidity among their uninfected infants?" Clin Infect Dis **41**(11): 1654-1661.

Levy, O. and J. L. Wynn (2014). "A prime time for trained immunity: innate immune memory in newborns and infants." Neonatology **105**(2): 136-141.

Li, Y., et al. (2014). "Inflammatory signaling regulates embryonic hematopoietic stem and progenitor cell production." Genes & development **28**(23).

Luckey, C. J., et al. (2006). "Memory T and memory B cells share a transcriptional program of self-renewal with long-term hematopoietic stem cells." Proceedings of the National Academy of Sciences of the United States of America **103**(9): 3304-3309.

Malek, A., et al. (1997). "Protein transport across the in vitro perfused human placenta." Am J Reprod Immunol **38**(4): 263-271.

Malek, A., et al. (1998). "Transport of proteins across the human placenta." Am J Reprod Immunol **40**(5): 347-351.

Mann, M., et al. (2018). "Heterogeneous Responses of Hematopoietic Stem Cells to Inflammatory Stimuli Are Altered with Age." Cell Rep **25**(11): 2992-3005.e2995.

Marchetti, M., et al. (2006). "Stat-mediated signaling induced by Type I and Type II interferons (IFNs) is differentially controlled through lipid microdomain association and clathrin-dependent endocytosis of IFN receptors." Molecular biology of the cell **17**(7).

Mariani, S. A., et al. (2019). "Pro-inflammatory Aorta-Associated Macrophages Are Involved in Embryonic Development of Hematopoietic Stem Cells." Immunity **50**(6): 1439-1452.e1435.

Matatall, K. A., et al. (2016). "Chronic Infection Depletes Hematopoietic Stem Cells through Stress-Induced Terminal Differentiation." Cell Rep **17**(10): 2584-2595.

Matatall, K. A., et al. (2014). "Type II interferon promotes differentiation of myeloid-biased hematopoietic stem cells." Stem cells **32**(11): 3023-3030.

- Mawa, P. A., et al. (2017). "Maternal BCG scar is associated with increased infant proinflammatory immune responses." Vaccine **35**(2): 273-282.
- May, K., et al. (2009). "Antibody-dependent transplacental transfer of malaria blood-stage antigen using a human ex vivo placental perfusion model." PLoS One **4**(11): e7986.
- Medlock, E. S., et al. (1993). "Granulocyte colony-stimulating factor crosses the placenta and stimulates fetal rat granulopoiesis." Blood **81**(4): 916-922.
- Medvinsky, A. and E. Dzierzak (1996). "Definitive hematopoiesis is autonomously initiated by the AGM region." Cell **86**(6): 897-906.
- Megli, C. J. and C. B. Coyne (2021). "Infections at the maternal–fetal interface: an overview of pathogenesis and defence." Nature Reviews Microbiology: 1-16.
- Meyer, U., et al. (2009). "In-vivo rodent models for the experimental investigation of prenatal immune activation effects in neurodevelopmental brain disorders." Neurosci Biobehav Rev **33**(7): 1061-1079.
- Mirantes, C., et al. (2014). "Pro-inflammatory cytokines: emerging players regulating HSC function in normal and diseased hematopoiesis." Experimental cell research **329**(2).
- Mitroulis, I., et al. (2020). "Regulation of the Bone Marrow Niche by Inflammation." Front Immunol **11**: 1540.
- Mitroulis, I., et al. (2018). "Modulation of Myelopoiesis Progenitors Is an Integral Component of Trained Immunity." Cell **172**(1-2): 147-161.e112.
- Moore, M. A. and D. Metcalf (1970). "Ontogeny of the haemopoietic system: yolk sac origin of in vivo and in vitro colony forming cells in the developing mouse embryo." Br J Haematol **18**(3): 279-296.
- Moran-Crusio, K., et al. (2011). "Tet2 loss leads to increased hematopoietic stem cell self-renewal and myeloid transformation." Cancer Cell **20**(1): 11-24.
- Mordue, D. G., et al. (2001). "Acute Toxoplasmosis Leads to Lethal Overproduction of Th1 Cytokines."
- Muller, A. M., et al. (1994). "Development of hematopoietic stem cell activity in the mouse embryo." Immunity **1**(4): 291-301.

- Nagai, Y., et al. (2006). "Toll-like receptors on hematopoietic progenitor cells stimulate innate immune system replenishment." Immunity **24**(6): 801-812.
- Natama, H. M., et al. (2018). "Modulation of innate immune responses at birth by prenatal malaria exposure and association with malaria risk during the first year of life." BMC Med **16**(1): 198.
- Netea, M. G., et al. (2016). "Trained immunity: A program of innate immune memory in health and disease." Science **352**(6284): aaf1098.
- North, T. E., et al. (2002). "Runx1 expression marks long-term repopulating hematopoietic stem cells in the midgestation mouse embryo." Immunity **16**(5): 661-672.
- Novales, J. S., et al. (1993). "Maternal administration of granulocyte colony-stimulating factor improves neonatal rat survival after a lethal group B streptococcal infection." Blood **81**(4): 923-927.
- Omere, C., et al. (2020). "Interleukin (IL)-6: A Friend or Foe of Pregnancy and Parturition? Evidence From Functional Studies in Fetal Membrane Cells." Frontiers in physiology **11**.
- Pietras, E. M. (2017). "Inflammation: a key regulator of hematopoietic stem cell fate in health and disease." Blood.
- Pietras, E. M., et al. (2016). "Chronic interleukin-1 exposure drives haematopoietic stem cells towards precocious myeloid differentiation at the expense of self-renewal." Nat Cell Biol **18**(6): 607-618.
- Pietras, E. M., et al. (2015). "Functionally Distinct Subsets of Lineage-Biased Multipotent Progenitors Control Blood Production in Normal and Regenerative Conditions." Cell Stem Cell **17**(1): 35-46.
- Rebel, V., et al. (1996). "The repopulation potential of fetal liver hematopoietic stem cells in mice exceeds that of their liver adult bone marrow counterparts." Blood **87**(8).
- Reikie, B. A., et al. (2014). "Altered innate immune development in HIV-exposed uninfected infants." J Acquir Immune Defic Syndr **66**(3): 245-255.
- Robbins, J., et al. (2012). "Tissue barriers of the human placenta to infection with *Toxoplasma gondii*." Infection and immunity **80**(1).

Roopenian, D. C. and S. Akilesh (2007). "FcRn: the neonatal Fc receptor comes of age." Nat Rev Immunol **7**(9): 715-725.

Saeij, J., et al. (2005). "Differences among the three major strains of *Toxoplasma gondii* and their specific interactions with the infected host." Trends in parasitology **21**(10).

Sawamiphak, S., et al. (2014). "Interferon gamma signaling positively regulates hematopoietic stem cell emergence." Developmental cell **31**(5).

Schneider, C., et al. (2019). "Tissue-Resident Group 2 Innate Lymphoid Cells Differentiate by Layered Ontogeny and In Situ Perinatal Priming." Immunity **50**(6): 1425-1438.e1425.

Schuettpeitz, L. G. and D. C. Link (2013). "Regulation of hematopoietic stem cell activity by inflammation." Front Immunol **4**: 204.

Scott, N. M., et al. (2017). "Protection against maternal infection-associated fetal growth restriction: proof-of-concept with a microbial-derived immunomodulator." Mucosal Immunol **10**(3): 789-801.

Senegas, A., et al. (2009). "Toxoplasma gondii-induced foetal resorption in mice involves interferon-gamma-induced apoptosis and spiral artery dilation at the maternofetal interface." International journal for parasitology **39**(4).

Shiono, Y., et al. (2007). "Maternal-fetal transmission of *Toxoplasma gondii* in interferon-gamma deficient pregnant mice." Parasitol Int **56**(2): 141-148.

Staber, P. B., et al. (2013). "Sustained PU.1 levels balance cell-cycle regulators to prevent exhaustion of adult hematopoietic stem cells." Mol Cell **49**(5): 934-946.

Stegmann, B. J. and J. C. Carey (2002). "TORCH Infections. Toxoplasmosis, Other (syphilis, varicella-zoster, parvovirus B19), Rubella, Cytomegalovirus (CMV), and Herpes infections." Current women's health reports **2**(4).

Sturge, C. and F. Yarovinsky (2014). "Complex immune cell interplay in the gamma interferon response during *Toxoplasma gondii* infection." Infection and immunity **82**(8).

Sun, J., et al. (2014). "Clonal dynamics of native haematopoiesis." Nature **514**(7522): 322-327.

Suzuki, Y., et al. (1988). "Interferon-gamma: the major mediator of resistance against *Toxoplasma gondii*." Science (New York, N.Y.) **240**(4851).

Takizawa, H., et al. (2017). "Pathogen-Induced TLR4-TRIF Innate Immune Signaling in Hematopoietic Stem Cells Promotes Proliferation but Reduces Competitive Fitness." Cell Stem Cell **21**(2): 225-240.e225.

Wilcox, C. R. and C. E. Jones (2018). "Beyond Passive Immunity: Is There Priming of the Fetal Immune System Following Vaccination in Pregnancy and What Are the Potential Clinical Implications?" Front Immunol **9**: 1548.

Yamashita, M. and E. Passegué (2019). "TNF- $\alpha$  Coordinates Hematopoietic Stem Cell Survival and Myeloid Regeneration." Cell Stem Cell **25**(3): 357-372.e357.

Yilmaz, O. H., et al. (2006). "SLAM family markers are conserved among hematopoietic stem cells from old and reconstituted mice and markedly increase their purity." Blood **107**(3): 924-930.

Yockey, L. J. and A. Iwasaki (2018). "Role of Interferons and Cytokines in Pregnancy and Fetal Development." Immunity **49**(3).

Zaretsky, M. V., et al. (2004). "Transfer of inflammatory cytokines across the placenta." Obstet Gynecol **103**(3): 546-550.